R-10-10

# Models for transport and fate of carbon, nutrients and radionuclides in the aquatic ecosystem at Öregrundsgrepen

Anders Christian Erichsen, Flemming Møhlenberg,
Rikke Margrethe Closter, Johannes Sandberg
DHI

June 2010

**Svensk Kärnbränslehantering AB**
Swedish Nuclear Fuel
and Waste Management Co

Box 250, SE-101 24 Stockholm
Phone +46 8 459 84 00

ISSN 1402-3091
SKB R-10-10

# Models for transport and fate of carbon, nutrients and radionuclides in the aquatic ecosystem at Öregrundsgrepen

Anders Christian Erichsen, Flemming Møhlenberg,
Rikke Margrethe Closter, Johannes Sandberg
DHI

June 2010

*Keywords:* SKBdoc 1260359.

# Summary

The aim of the work was to provide supplementary input to the risk assessment of a planned final nuclear waste repository at Forsmark. The main deliverable was a computed water exchange between basins in the Forsmark marine area for the period 6500 BC to 9000 AD – based on the hydrodynamic modelling – to be used as input to the landscape dose model. In addition and what is described in this report, a second deliverable was development and application of high-resolution models for the marine ecosystem and radionuclide processes. The purpose of this deliverable was to illustrate the spatial and temporal variation in important processes and parameters, while constituting a complement to previous modelling approaches and providing supporting information to discussions of the marine ecosystem, parameters and variation (see Chapter 4 and 6).To this end, a hydrodynamic model of high temporal and spatial resolution was constructed and calibrated for the Forsmark area. An ecosystem model was then developed and coupled to the hydrodynamic model. In turn, a detailed radionuclide model was coupled to the ecosystem model to provide detailed predictions of radionuclide transport and accumulation in the coastal ecosystem.

The ecosystem and radionuclide models were developed in the equation solver MIKE ECOLab that links seamless to the MIKE3 FM hydrodynamic model. The 'standard' ECOLab ecosystem model was extended with six biological state variables, perennial macroalgae, benthic herbivors, detritus-feeders, planktivorus fish and, benthic predators representing the relict isopod *Saduria* and cod. In contrast to the ecosystem model, the radionuclide model was developed from scratch but building on the structure of the ecosystem model and using the output (process rates linking state variables) from the ecosystem model as input to the radionuclide model. Both the ecosystem model and the radionuclide model were run for several years (5–8 years) to bring state variables into quasi-stationary equilibrium within the model area.

The coupled ecosystem and radionuclide models were used to simulate present conditions, i.e. 2020 AD. Six radionuclides were modelled explicitly in addition to C-14. They represent a wide range of accumulation potentials and partition coefficients ($K_d$, distribution of radionuclides between water, sediment and biota).

The ecosystem and associated radionuclide model include a detailed sediment module where radionuclides can be bound by adsorption to the organic and inorganic fractions, be precipitated, be transported by resuspension and later deposited at larger depths. With the exception of radionuclides with very low particle affinity, such as Cl-35, the majority of radionuclides released in basins where they were introduced via groundwater flow remained in the sediments even after a simulation period of eight years. The spread of radionuclides with high partition coefficients for sediments from areas with groundwater flow takes place by sediment resuspension and subsequent transport and sedimentation. In the case of radionuclides with lower partition coefficients, release from the sediments to the water column followed by transport of dissolved radionuclides by currents plays a larger role.

A significant result of the modelling was the quantification of the seasonal and spatial variation in radionuclide accumulation and in bioconcentration factors (BCFs) with spatial variation of BCFs often ranging 2 to 3 orders of magnitude. This variation was dominated by spatial differences in concentrations of radionuclides in water. In basins where radionuclides were introduced by groundwater flow, BCFs were typically 2–3 orders of magnitude lower than in deep basins without radionuclide release in the groundwater.

In phytoplankton and grazers, bioconcentration factors (BCFs) scaled linearly to partition coefficients (Kd), underlining the fact that adsorption is an important process for radionuclide accumulation in the lower parts of the food web, and also underlining the important role of Kd in the model. In contrast, BCFs were much higher in benthic fauna such as detritus feeders, and although Kd did influence BCFs the larger part of the variation was influenced by other processes including accumulation of radionuclides via food.

# Contents

# 1 Introduction and background

The main scope of this report is to provide the background information and documentation for a coupled hydrodynamic-ecological-radionuclide model developed for the Öregrundsgrepen. The coupled model is applied to predict the spread of radionuclides and subsequent accumulation in sediments and biota following a hypothetical loss of radionuclides from a depository. The results from the hydrodynamic model provide inputs to the coupled ecosystem and the results from the ecological model provide inputs to the radionuclide models. The ecosystem model is used to illustrate the spatial and temporal variation in important processes and parameters, as well as constituting a complement to previous modelling approaches. The radionuclide model further illustrates a possible alternative to the radionuclide transport modelling in SR-Site.

The report first presents an overview of the modelling framework in Chapter 2, followed by a detailed presentation of the ecological model set-up for Öregrundsgrepen, including new developments to encompass important biological features of the coastal system of Öregrundsgrepen (Chapter 3). Results from calibration and simulation of the ecological model are shown in Chapter 4. The radionuclide model is presented in detail in Chapter 5, and modelled distribution of radionuclides in water, sediment and the different biological components are presented in Chapter 6.

Besides the general scope detailed objectives of the work were to construct a comprehensive but yet flexible and user-friendly radionuclide model which allowed concentrations of radionuclides in sediments, plants, benthic invertebrates and fish to be modelled with a high spatial and temporal resolution.

# 2 Modelling framework

The model area that encompasses the marine environment at Forsmark is defined as the semi-enclosed area that exists today between the mainland and the island of Gräsö. This area is called Öregrundsgrepen (see Figure 2-1). The extent of this area varies significantly over geological time scales, primarily due to land uplift. Thus, the area now identified as Öregrundsgrepen was part of an open coastal sea at 6500 BC and will probably disappear completely due to land uplift at about 9000 AD.

To estimate water exchange a hydrodynamic model was developed using MIKE by DHI software MIKE 3 FM. Resolution of the model varies from less than 20 m (near coast) to > 100 m in the open part. A detailed description of the hydrodynamics model is found in /Karlsson et al. 2010/.

The ecosystem and radionuclide food web models for the present-day situation have been implemented in MIKE by DHI software ECOLab, based mainly on data collected during a single year (2004). Conceptually, the ecosystem model and the radionuclide model have been developed based on the general food web structure developed in earlier modelling studies within the area, see e.g. Chapters 4 and 6 in /Kumblad and Kautsky 2004/, but the present high-resolution analysis considers only six selected radionuclides.

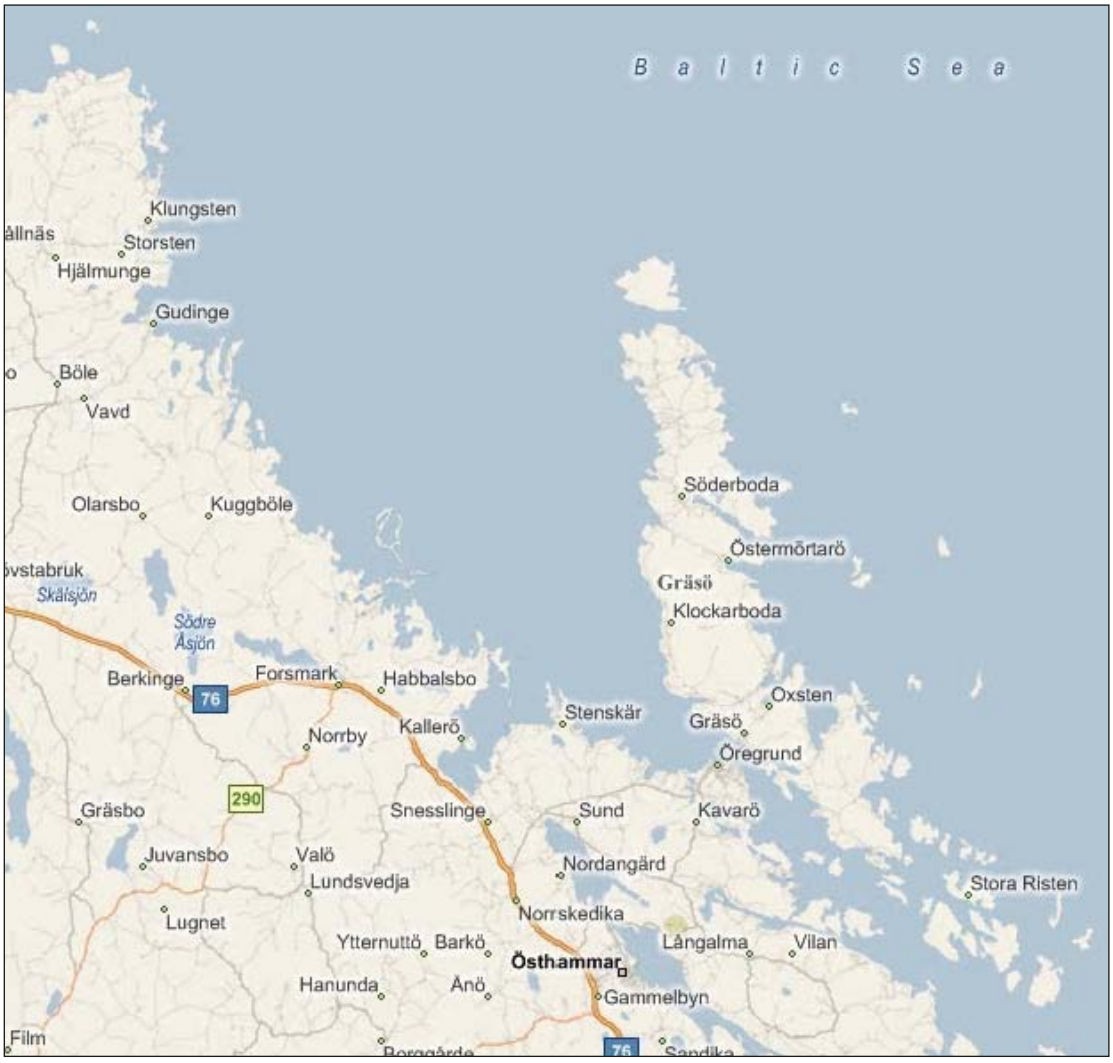


***Figure 2-1.*** *Map showing the location of Öregrundsgrepen, a funnel-shaped coastal embayment between the island of Gräsö and the mainland.*

## 2.1 Overview of ECOLab

ECOLab is a numerical simulation software for ecological modelling. It is an open and generic tool for customising aquatic ecosystem models to simulate for instance water quality, eutrophication, heavy metals and ecology. It is a Windows application that allows the user to adjust existing ecosystem models or generate new models to target the specific area and the specific problem.

ECOLab uses a so-called ECOLab COM[1] object to perform the ECOLab calculations. The ECOLab object is generic and can be shared with any flow model system. It consists of an interpreter that first translates the equation expressions in the ECOLab template[2] to lists of instructions, which enable the object to evaluate all the expressions in the template. During simulation the model system integrates one time step by simulating the transport of advective state variables (SV) based on hydrodynamics. Initial concentrations, updated AD concentrations (i.e. after advection and dispersion processes), coefficients and updated forcing functions are then loaded into the ECOLab object. The ECOLab object then evaluates all the expressions, integrates one time step, and returns updated concentration values to the general flow model system, which advances one time step. An illustration of the data flow is shown in Figure 2-2.

The advection-dispersion terms of the general flow models (in this case MIKE 3 /DHI 2007a/) utilises the state variables and the mathematical ecosystem description defined in ECOLab and transform the different state variables according to the sum of processes specified in ECOLab;

$$P_c = \frac{dc}{dt} = \sum_{i=1}^{n} process_i \qquad 2\text{-}1$$

where c is the concentration of the ECOLab state variables and n is the number of processes involved for the specific state variable.

Hence, ECOLab functions as a module in the MIKE simulation software (MIKE 11, MIKE 21 and MIKE 3) and ECOLab is linked to the advection-dispersion term of the hydrodynamic flow models, so that transport mechanisms based on advection-dispersion is integrated in the ECOLab simulation.

The ECOLab model tool is fully integrated with the MIKE 11, 21 and 3 hydrodynamic models and is used extensively by commercial MIKE by DHI software users as well as researchers. Recent peer-reviewed studies where ECOLab was instrumental include /Arndt and Regnier 2007, Lessin and Raudsepp 2006, Vanderborght et al. 2007, Rasmussen et al. 2009/.

## 2.2 Detailed description of ECOLab

The description of the ecosystem state variables (SV) in ECOLab is formulated as a set of first order, ordinary coupled differential equations describing the rate of change for each SV based on processes taking place in the ecosystem. All information about ECOLab SV's, processes and their interaction are stored in a so-called generic ECOLab template. The processes contain mathematical expressions with constants, and forcings, that the user must specify and ECOLab sums up the rate of change as specified in Equation 2-1.

The dynamics of advective ECO Lab SVs can be expressed by a set of transport equations, which in non-conservative form can be written as

$$\frac{\partial c}{\partial t} + u\frac{\partial c}{\partial x} + v\frac{\partial c}{\partial y} + w\frac{\partial c}{\partial z} = D_x\frac{\partial^2 c}{\partial z^2} + D_y\frac{\partial^2 c}{\partial z^2} + D_z\frac{\partial^2 c}{\partial z^2} + S_c + P_c \qquad 2\text{-}2$$

where c is the concentration of the ECOLab SV, u, v and w are flow velocity components, $D_x$, $D_y$ and $D_z$ are dispersion coefficients, $S_c$ is a term for source and sinks, including atmospheric depositions, and $P_c$ is a term for ECOLab processes.

[1] Microsoft COM standard.

[2] An ECOLab template contains the mathematical definition of an ECOLab model. It contains information about the included state variables, constants, forcings, processes and the state variables rate-of-change differential equations.

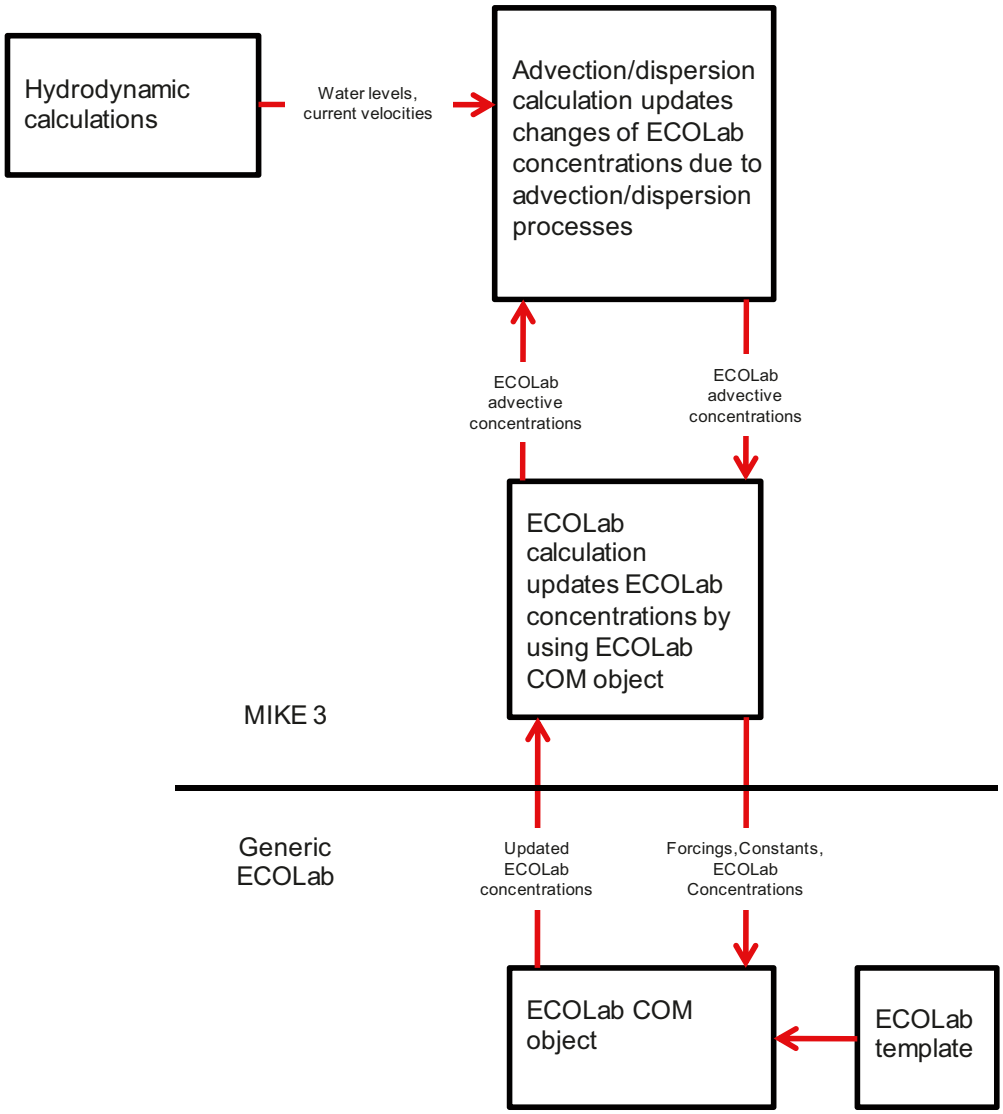


***Figure 2-2.*** *Data flow between the hydrodynamic flow model (in this case MIKE 3) and ECOLab.*

The SV's may be coupled linearly or non-linearly to each other through the ECOLab source term $P_c$. The transport equation can be rewritten as

$$\frac{\partial c}{\partial t} = AD_c + P_c \qquad 2\text{-}3$$

where the term $AD_c$ represents the rate of change in concentration due to advection and dispersion (including sources and sinks).

The ECOLab numerical equation solver makes an explicit time-integration of the above transport equations, when calculating the concentrations to the next time step. An approximate solution is obtained in ECOLab by treating the advection-dispersion term as $AD_c$ as constant in each time step.

The coupled set of ordinary differential equations defined in ECOLab is solved by integrating the rate of change due to both the ECOLab processes themselves and the advection-dispersion processes.

$$c(t+\Delta t) = \int_{t}^{t+\Delta t} (P_c(t) + AD_c)\partial t \qquad 2\text{-}4$$

The advection-dispersion contribution is approximated by

$$AD_c = \frac{c\cdot(t+\Delta t) - c\cdot(t)}{\Delta t} \qquad 2\text{-}5$$

where the intermediate concentration c· is found by transporting the ECO Lab SV as a conservative substance over the time period Δt using the AD module.

The main advantage of this approach is that the explicit approach resolves the coupling and non-linearity problems resulting from complex source ECOLab terms $P_c$, and therefore the ECOLab and the advection-dispersion part can be treated separately.

An implicit approach of solving the transport equations is not possible yet in ECOLab. Two different integration methods are available in ECOLab: Euler and Runge Kutta 4th order. Compared to the above description some processes such as light penetration, sedimentation, buoyancy caused movements need information from the layer above or below and are therefore treated somewhat differently.

In a one-layered model grid the sedimentation of a SV is calculated as if it was any other process. The sedimentation expression is subtracted in the differential equation. However, in a multi-layered system, the solution in each layer is different, because a contribution to the SVs is received from the layer above (if not top layer), see Figure 2-3, and the vertical discretization must be considered when calculating the rate of change for each layer:

$$\frac{dC_n}{dt} = \frac{SEDI\cdot C_{n-1}\cdot dz_{n-1} - SEDI\cdot C_n\cdot dz_n}{dz_n} \qquad 2\text{-}6$$

where SEDI is the sedimentation rate [$d^{-1}$], $C_{n-1}$ is the concentration of particulate matter in the layer n–1 [$g\cdot m^{-3}$], $C_n$ is the concentration of particulate matter in layer n [$g\cdot m^{-3}$], $dz_n$ is the thickness of layer n [m] and $dz_{n-1}$ is the thickness of layer n–1 [m].

Light penetration in the water column is solved using the Lambert-Beer law. In multi-layered systems with vertical varying extinction coefficients, the Lambert-Beer law must be calculated for each layer, and therefore the Lambert-Beer law as argument uses the result of the Lambert-Beer law in the layer above:

$$I_n = I_{n-1}\cdot e^{\eta_n\cdot dz_n} \qquad 2\text{-}7$$

where $I_n$ is the light available for primary production in the actual layer n, $I_{n-1}$ is the irradiance in the layer above, $\eta_n$ is the extinction coefficient and $dz_n$ layer thickness.

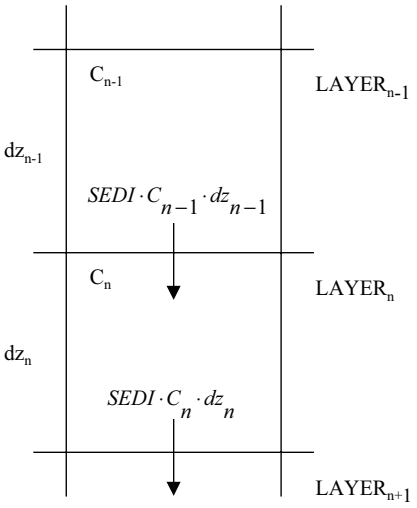


***Figure 2-3.*** *Schematic description of sedimentation (or other buoyancy-caused movements).*

Temperature or other external factors affect most ecological parameters and processes. Some external factors are calculated in the hydrodynamic model, and they are directly coupled to the ECOLab template, so that they can be used as arguments in ECOLab expressions. Additional external factors, such as photosynthetic active light (PAR) can be specified and applied as time series or time varying maps.

Some processes only take place in specific layers of the water column, and such processes are handled by calculating the process at the relevant layer where the process takes place and setting the process to zero in other layers. Examples of this could be processes related to the sediment or re-aeration in the upper water layer.

## 2.3 Test of integration routine in MikeZero ECOLab

The accuracy of numerical models depends strongly on the time step and on the integration rutine used in the model. To test the accuracy of the two different integration routines available in ECOLab, the model results for a simple test case were compared with the exact analytical solution.

The test setup consists of a simple bathymetry of one calculation point, no sources and no evaporation/precipitation. In a simple model setup like this, any hydrodynamic or advection/dispersion transport components do not appear in the model, as there are no other cells to move matter to or receive matter from. Any difference in the concentration of any component in the model will then be due to ECOLab processes or errors in the models computational scheme.

In this set-up a function of exponential growth with a rate of 0.1 per day was programmed in ECOLab and run for one year with an ECOLab time step of 30 minutes, which is the same time step as used in the setup for the ecosystem model Öregrundsgrepen. The model result after one year simulation was then compared with the exact analytical value: $F = \exp(0.1 \text{ per day} \times \text{time}) = \exp(365 \text{ d} \times 0.1/\text{d})$

As mentioned above ECOLab has two optional integration methods, Euler or 4th order Runge-Kutta (RK-4). Euler is a simple linear extrapolation of the difference in value between the last two time steps, where RK-4 uses the results from the value of the last four time steps to extrapolate the next value.

After one year of simulation (17,520 time steps) the accumulated error of the Eulerean integration differed by 3.75% from the analytical solution, while the deviation of the RK-4 result was much lower at $1.1 \times 10^{-5}$%. Hence, with RK-4 the difference between the true result and the model estimate is about one hundred thousand of a percent. The RK-4 method was used in the ECOLab application for the Öregrundsgrepen models.

## 2.4 Linking of models

Three different MIKE models are applied to quantify transports, chemical-biological processes and spread of radionuclides in the Öregrundsgrepen ecosystem. The individual models MIKE3-FM (hydrodynamic), ECOLab (ecosystem) and ECOLab (radionuclide) are applied sequentially where outputs from one model are used as inputs in the subsequent model (Figure 2-4). The argument for such partly uncoupling of models is to minimize simulation time, e.g. the hydrodynamic model operates with a dynamically variable time step of seconds-minutes. If such short time steps are used in the ecological and radionuclide models with numerous state variables simulation time for one year would exceed 1–2 months. Instead, results from the hydrodynamic are stored at 30 min intervals, and these data (current speed, bottom sheer stress etc) are used to transport pelagic state variables between model grid cells and to erode bottom sediments.

In the ECOLab ecosystem model state variables are updated every 30 min (= model time step) determined by the various processes, e.g. primary production, predation, respiration. The ecosystem model is run for 5 consecutive years using the same 2004 year forcings and inputs from the hydrodynamic model. Five years simulation was needed to bring certain state variables such as planktivorus fish and sediment organic content into a quasi-stationary state. During this process the ECOLab model was calibrated against measured data for 2004.

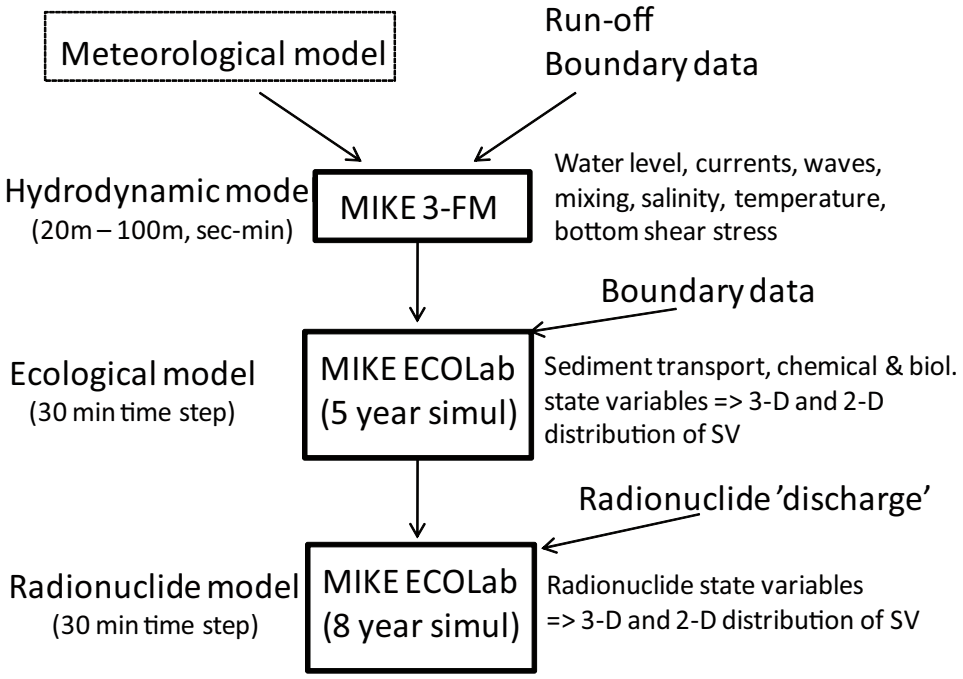


***Figure 2-4.*** *Conceptual diagram showing how MIKE models are linked, forcing data and boundary data needed to 'drive' models.*

After the ecosystem model was calibrated the 5th model year's data was used as input to the ECOLab radionuclide model. Radionuclides were introduced into the model with ground water flow and 8 years' consecutive modelling using the 2004 year forcings and inputs from the hydrodynamic and ecosystem models. Eight years' modeling was found to be sufficient for radionuclides to reach quasi-stationary states (i.e. near-stable concentrations of radionuclides in sediments).

# 3 Implementation of general ECOLab ecosystem model for the Forsmark area

The general models applied for this project are the DHI models entailed in the MIKE Software suite. The driving hydrodynamic model is the MIKE 3 FM /Karlsson et al. 2010/, whereas the ecological model is developed in the ECOLab model system. The basic ECOLab model describes algal and zooplankton growth and the cycling of nutrients (called the "eutrophication module" or EU model). In the application for the Forsmark ecosystem this model is extended to include sedimentation and re-suspension of fine sediments or mud (called the "mud-transport module" or MT model), a detailed description of sediment diagenesis, and explicit formulations to describe 'new' state variables such as benthic deposit-feeders, planktivorus fish, and benthic predators.

Detailed descriptions of model formulations in the standard EU ECOLab template are thoroughly described in the EU-template manual /DHI 2007b, 2008/ and will not be discussed in detail here. In contrast, formulations related to a) additional state variables, b) sediment processes and, c) spread of radionuclides will be described in detail below in this and the following chapter.

The ECOLab model operates using a MIKE hydrodynamic model as a basement to provide transport, dispersion etc of ECOLab state variables (SV). The explicit implementation of MIKE 3 FM for the Forsmark area is described in more details in /Karlsson et al. 2010/.

## 3.1 Overview of ecosystem model

The ecosystem model consists of two major sub-modules: pelagic system and benthic system. They are connected by advective processes leading to exchange of particulate and soluble state variables by processes such as sedimentation, benthic filtration and release of mineralized nutrients from sediment to the water column. For the sake of clarity though, the pelagic system and the benthic system are described separately.

### 3.1.1 Pelagic system

The pelagic cycling of carbon (C), nitrogen (N) and phosphorous (P) is illustrated in Figure 3-1. The most important element in the model is the growth of phytoplankton. The growth of phytoplankton is mainly controlled by nutrient availability, sedimentation, turbidity, temperature and solar radiation. Bacterial degradation of organic matter in the water phase and in the sediment releases inorganic nutrients which then become available for new primary production in the photic zone.

Grazing on phytoplankton by zooplankton (also including benthic filter-feeders) can have a regulating effect on the phytoplankton biomass; hence, grazing on algae is modelled explicitly. The original model does not include secondary producers at a higher trophic level than zooplankton. An additional state variable is planktivorus fish that predate on zooplankton. Grazing and decomposition transforms phytoplankton to zooplankton and detritus respectively. The processes involved do however also transform a small part of the phytoplankton N and P directly into inorganic N and P, the latter accounting for some kind of internal microbial loop.

The organic material produced in the surface (or subsurface waters) will settle with time. The bacterial degradation of this material in the sediment and in the water column utilizes oxygen and can depending, among other things, on the strength of the pycnocline, result in anoxic conditions. The model does not specifically include bacteria biomass, but the effects of bacteria are parameterized (through mineralization) mainly based on temperature.

In the biochemical model the dependency of nutrients on growth of phytoplankton is de-scribed in a two-step process. Firstly, the inorganic nutrients are taken up into an internal pool in the algal cells. Secondly, nutrients from this pool are utilized in production of organic matter. This approach has proven to be very strong in modelling growth of phytoplankton.

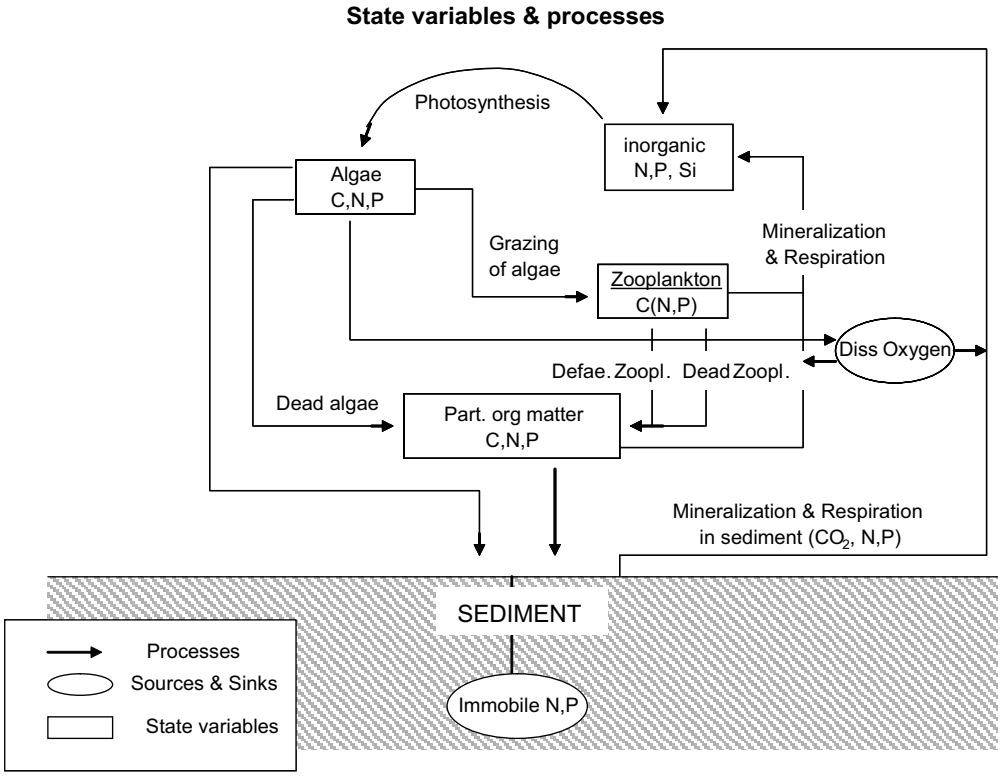


***Figure 3-1.*** *Simplified structure of pelagic ecological module.*

Parts of the Baltic Sea today are at times dominated by nitrogen fixating cyano-bacteria. This N-fixation is regarded an important source of N to the Baltic Sea and estimates suggests that N fixation is comparable to the land-based N load to the Baltic Sea as a total /Larsson et al. 2001/. The model applied for the Forsmark area does not include cyano-bacteria and a potential additional load of N is not accounted for. The basic module and the different governing processes included are described in more detail in /DHI 2007b, 2008/.

In the Baltic Sea substantial amounts of dissolved organic matter (DOC and DON) are present. The original ecological model does not include either of the above mentioned parameters as true SV's. However, some of the effects of both DOC and DON are taken into account: DOC is included indirectly as contribution to the background shading effect, whereas DON is neglected by removing the bio-unavailable N, and modelling only the bio-available N.

In this model also effects from the filter-feeding benthic community are included. Here the filtration capacity is proportional to the shell (gill)-area. The shell-area is described as an area-specific parameter in the model and is regarded as a biological forcing.

### *Reasons for a simple pelagic ecosystem*

Ever since the "discovery" of the "microbial loop" in the early 1980-ies, e.g. /Azam et al. 1983/ there has been a continuous debate on how to incorporate dissolved organic matter, bacteria, heterotrophic flagellates, ciliates, phytoplankton (several groups) and mesozooplankton in planktonic food web models. Microbiologists have tended to take a reductionistic approach trying to promote representation of all known (and unknown) organism groups and their inter-linking processes in their (small scale) models while ecosystem modellers working at larger physical and temporal scales have tried to incorporate the features of the "microbial loop" in more simple (nutrient-phytoplankton-zooplankton-detritus) planktonic models /Steele 1998, Denman 2003/.

We have taken the latter approach also recognising that in the major part of the Forsmark area pelagic production is much less important relative to benthic production. Therefore the pelagic state variables in the model are the simplest possible including phytoplankton, zooplankton, planktivorus fish and detritus in addition to nutrients nitrogen and phosphorus. Figure 3-1 shows a simplified diagram of pelagic pools (state variables) and processes (arrows) interlinking state variables in the model.

In summary, the ecosystem model computes the concentration of phytoplankton, chlorophyll-a, zooplankton, plankton eating fish, dead organic particulate material as well as the nutrients N and P in the water phase. The pelagic system includes the following state variables:

- Phytoplankton (C, N, P)
- Chlorophyll-a
- Zooplankton (C)
- Planktivorus fish (C)
- Detritus (C, N, P)
- Ammonia ($NH_4$)
- Nitrate and Nitrite (NOx)
- Inorganic P ($PO_4$)
- Dissolved Oxygen
- Dissolved inorganic C (DIC)
- Suspended inorganic solids

where state variables only is described by their carbon content (C) a fixed C:N:P ratio is assumed to ensure mass conservation.

### 3.1.2 Benthic system

In the present model set-up the epibenthic autotrophic module represents three functional groups of attached macrophytes: perennial macroalgae (brown algae such as *Fucus*), annual macroalgae (*Ulva*, *Pilayella*), which both take up nutrients from the water column, and "seagrass" (eelgrass) but also including the rooted algae *Chara*, which take up nutrients both from the sediment pore water and from water. Other autotrophic components are epibenthic microphytes and epiphytes growing on macrophytes. The heterotrophic sediment processes include traditional diagenetic sediment processes but also benthic filter-feeders (e.g. *Cardium*), epibenthic grazers (snails), deposit-feeders (e.g. *Macoma* and various amphipods) and a predator (*Saduria*) predating on all other epi- and infauna. In Figure 3-2 and Figure 3-3 are depicted in greater detail how benthic vegetation, sediment diagenesis and benthic heterotrophs link to water column processes.

In summary the benthic system includes:

- Perennial macroalgae (C, N, P)
- Rooted vegetation (C and number of shoots)
- Benthic microalgae and annual algae (C)
- Sediment organic material (C, N, P)
- Sediment inorganic nutrients ($NH_4$, $NO_x$, $PO_4$)
- Iron bound P
- Reduced substances (e.g. $H_2S$)
- Sediment inorganic material

All state variables are defined in terms of carbon (C), nitrogen (N) and phosphorus (P), but silicon can be included if concentration of silicate is thought to limit primary production. As mentioned above the model also includes the transport of fine organic and inorganic material with a size below 63 μm, which encompass sediment silt, and clay fraction and organic matter. In the following the cycling of nutrients and carbon in the water phase and in the sediment is described in more details.

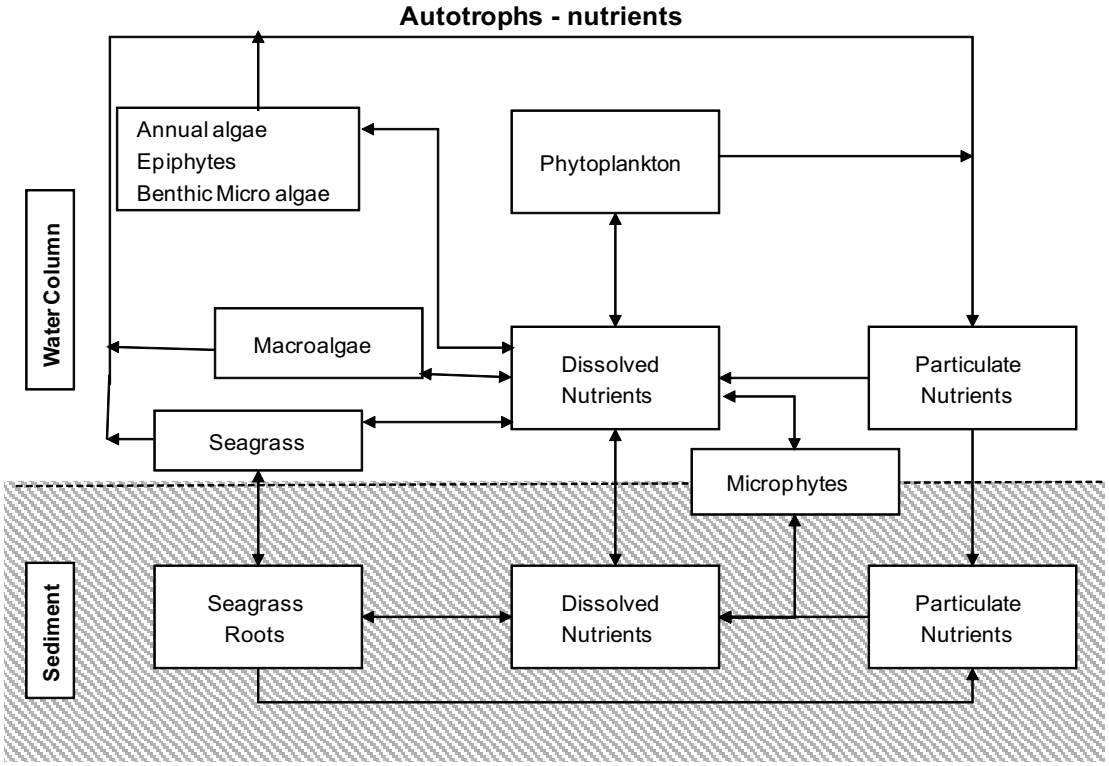


***Figure 3-2.*** *Schematic representation of autotrophs and nutrients in the autotrophic module.*

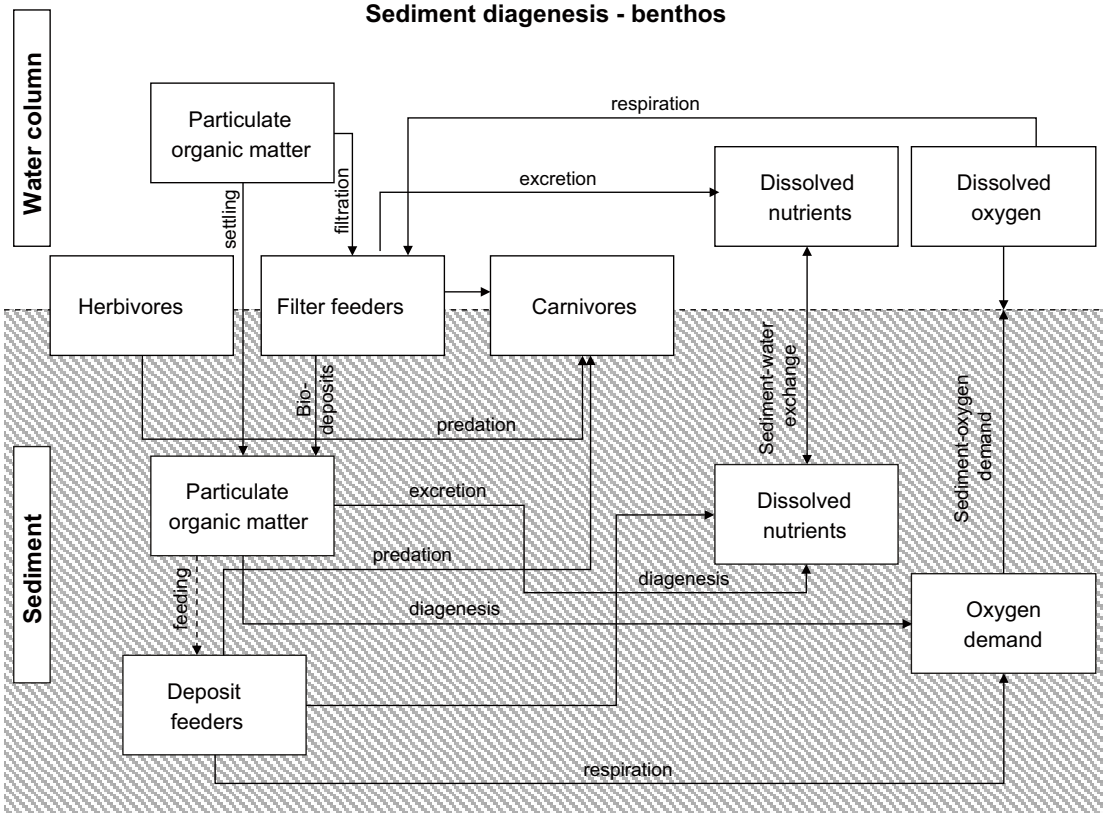


***Figure 3-3.*** *Schematic representation of sediment diagenesis and linkages to water column state variables in ECOLab model. Three heterotrophic functional groups: herbivores (e.g. Hydrobia), deposit-feeders (e.g. Pontoporeia) and benthic carnivors (Saduria/demersal fish) are modelled explicitly, while the influence of filter-feeders (Cardium/Mytilus) on phytoplankton/detritus is included by forcing scaled to their average biomass.*

## 3.2 Detailed description of model state variables

Pelagic state variables such as phytoplankton and dissolved nutrients in a 3-D model invariable can be transported between model grid cells with currents and as such have the ability to occur over the entire model area without any restrictions. However, the realized distribution of biomass in the model is the effect of internal processes (growth, loss, grazing/predation) within a grid cell and physical exchange between grid cells and between water column and sediments. In contrast to pelagic state variables, benthic variables that are fixed on bottom such as fucoid algae that require hard substrate for attachment can only occur in certain grid cells, while non-sessile benthic organisms such as predators can be found in several habitats and growth and loss processes determine if their biomass can be sustained in the individual grid cells.

### 3.2.1 Phytoplankton state variable

Phytoplankton in pelagic models represents a wide suite of photoautotrophic algal species and a few specialized ciliates which houses symbiotic algae or their chloroplasts to carry out primary production. A common feature defining the group is their ability to fix inorganic carbon using solar radiation as energy source (i.e. primary production).

#### *Phytoplankton monitoring in the Forsmark area*

The phytoplankton communities in the Forsmark area (Öregrundsgrepen, Asphällsfjärden, Tixelfjärden) have been monitored in 1972–73 /Eriksson et al. 1977 cited in Wijnbladh et al. 2008/ in 1977–78 /Lindahl and Wallström 1980 cited in Wijnbladh et al. 2008/ and during 2002–2005 /Huononen and Borgiel 2005 cited in Wijnbladh et al. 2008/. Depending on years and area sampled both diatoms and dinoflagellates dominated the spring bloom (March–April) and at coastal stations the phytosynthetic ciliate *Mesodinium rubrum* dominated summer blooms.

In Öregrundsgrepen the yearly mean biomass in 1972–73 was estimated to 0.43 g ww $m^{-2}$ (≈ 10–20 µg C $l^{-1}$), max biomass during spring bloom in 1977–78 amounted to 50 g ww $m^{-2}$, and 20 µg Chl-a $l^{-1}$ (≈ 1,100 µg C $l^{-1}$) and max primary production to 600 mg C $m^{-2}$ $d^{-1}$. In Tixelfjärden monthly means of Chl-a varied between 1.5–3.2 µg Chl-a $l^{-1}$ during March through November. Only one phytoplankton state variable is included in the model, but forced changes in temperature optima will enable a reasonable temporal variation in growth and biomass development.

#### *Growth regulation in model*

The growth of phytoplankton in the applied model is described mechanistic being dependent on light availability, availability of inorganic nitrogen (DIN) and phosphate ($PO_4$) for uptake from water to internal nutrient pools, and temperature. Sub-optimal conditions in any of these factor groups invariable will result in growth rates below the maximum.

Effect of light on primary production and growth rate is described by a saturation function, where the light saturation parameter (Ek) can be used for calibration (see Figure 3-4). Effect of nutrients on growth rate is described by a Droop equation /Droop 1983/, where the cellular nutrient contents (quota) determine growth rather than the dissolved nutrients in the water surrounding the algae. The internal nutrient pools are replenished continuously by uptake from the surrounding water at rates depending on the gradients across the cell walls. The use of Droop kinetics allows some degree of temporal uncoupling between nutrient uptake and growth.

The temperature-dependence of growth rate is described by an Arrhenius equation (Teta = 1.08), but with changing temperature-optimum through seasons. Prior to mid spring (e.g. 20th March) the optimum temperature is set to 5–10°C, later to 20°C and after mid October again to 5°C. The exact dates where optimal temperatures are changed can be regulated during calibration so that a cold water spring bloom of diatoms or dinoflagellates can be simulated and summer blooms of warm-water adapted algae also be reproduced using only one state variable. Likewise the max growth rates can be set to different values for "spring" and "summer" algae (see Figure 3-4).

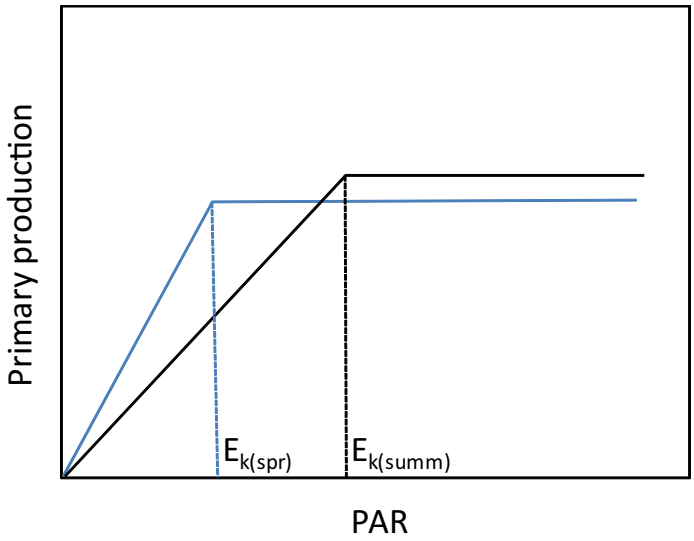


***Figure 3-4.*** *Schematic representation of influence of photosynthetically available radiation (PAR) on primary production. Lower light requirements of spring algae are implemented in the model by a lower Ek-value compared to summer algae.*

### *Growth rate of phytoplankton in the Forsmark area*

Based on literature reviews /Banse 1982, Sarthou et al. 2005/ and extensive experimental studies /Dixon and Syrett 1988**,** Skovgaard and Menden-Deuer 2003, Hansen and Fenchel 2006/, the growth rate of nutrient replete plankton algae under saturating light conditions is found to vary between 0.3 to 2.5 per day, where high growth rates are characteristic for diatoms and much lower rates are characteristic for dinoflagellates and *Mesodinium rubrum* (0.4–0.5 $d^{-1}$). Within the taxonomic groups the maximum growth rate generally increase with demising cell size, e.g. with a doubling of growth rate with a 3–4 fold decrease in cell volume. The max growth rate of bloom-forming *Skeletonema costatum* with a typical volume of 500 $\mu m^3$ is around 2.2 $d^{-1}$ while a large *Rhizosolenia* with a cell volume > $10^5$ $\mu m^3$ has a max growth rate of 0.7–0.8 $d^{-1}$.

Without knowing the full list of phytoplankton species and their concentration through seasons it is likely that 10–30 species occurs in significant amounts at one time at one location in the Forsmark area. Knowing that each phytoplankton species have their characteristic maximum growth rate and nutrient dependency on growth the use of a single set of parameter values to represent a wide variety of algae always will be a compromise. However, years of experience have demonstrated that use of max growth rates of 1.4–1.6 $d^{-1}$ works in most situations. The simulated growth rate in the model is however, much lower than the maximal rates due to light limitation (seasonal: winter, spring and autumn; temporal: overcast, resuspension) and nutrient limitation during summer.

In the current implementation direct uptake of $N_2$ due to activity of cyano-bacteria is not included in the model as we have no indication of presence of these algae in the area. However, this activity can be included by imposing an external N-source over the entire area regulated by temperature and N:P ratios in phytoplankton.

### *Fate of phytoplankton in the model*

The fate pelagic primary production in the model includes:

- Sedimentation to sediment surface where the sedimentation rate is influenced by the nutritional status, i.e. the inner C, N, P-quotas.
- Deaths (e.g. cell lysis) where half of nutrient content is returned directly to inorganic pools in the water column and half to the detritus pools bound in organics (C, N, P).
- Grazing by zooplankton.
- Grazing by benthic filter-feeders such as mussels and cockles. These grazers take their ration from the near-bed layer only and accordingly their impact is greatest at shallower depths or where vertical mixing intensity is high.

### 3.2.2 Zooplankton state variable

Zooplankton in pelagic models usually represents organisms that graze on and ingest phytoplankton. They include members from a variety of taxonomic groups, including heterotrophic flagellates (plants), ciliates, invertebrate larvae (meroplankton) and crustaceans (copepods and cladocerans) among others. In addition to grouping zooplankton into taxonomic groups, they can be grouped according to their size, i.e. microzooplankton (< 200 µm) and mesozooplankton (> 200 µm) or grouped in single cell (protozooplankton) or multi-cell (metazooplankton) organisms.

#### *Zooplankton monitoring in the Forsmark area*

Mesozooplankton has been monitored regularly in Öregrundsgrepen during 1972–73 and in Asphällsfjärden during 2003–04 with mean yearly biomasses between 23 and 35 µg C $l^{-1}$ /Eriksson et al. 1977, Huononen and Borgiel 2005, both cited in Wijnbladh et al. 2008/. In these studies, copepods (primarily *Acartia bifilosa*), meroplankton (seasonal) and the cladoceran *Bosmina* dominated the mesozooplankton community. Other important members of the zooplankton grazer community but not quantified in the above studies are microzooplankton (especially protozooplankton) represented by heterotrophic dinoflagellates and ciliates /Johansson et al. 2004/.

Protozooplankton typically peaks shortly after the phytoplankton spring bloom while mesozooplankton usually peaks in July and August because the developmental rate (from egg to adult) in copepods is strongly influenced by temperature ($Q_{10} \approx 3$ /Kiørboe et al. 1988/). In comparison, population growth in protozooplankton is less temperature dependent, which is probably why these organisms respond quickly to the increasing food availability during the spring phytoplankton bloom. During summer protozooplankton constitute a minor part of the total zooplankton community probably because copepods also take their ration from the ciliates /Kuparinen et al. 1996/, even though another study was less conclusive about the role of copepods controlling ciliates during summer in the Baltic /Samuelsson and Andersson 2003/**.**

#### *Grazing and population growth of zooplankton in model*

In the ECOLab template only one "bulk" zooplankton state variable is included and due to the documented dominance of copepods in the Forsmark area the formulation is primarily based on copepod (*Acartia*) grazing and growth functions, e.g. /Kiørboe et al. 1985/, but the copepod max gross (G/I = 33%) and max net (G/(G+R) = 60%) growth efficiencies have been reduced and the nutrient regeneration in the water column increased to include the predominantly internal role of the microzooplankton in recycling nutrients, i.e. including the role of the "microbial loop" /Steele 1998, Denman 2003/. The primary drawback using this approach is that the post-spring bloom of ciliates is not represented very well and the vertical flux of the spring bloom may be overestimated as algae (and nutrients) are sedimented out and not retained in the water column as if pelagic grazing activity during spring was higher.

For simplicity and in contrast to the phytoplankton state variable the elementary ratios (C:N; C:P; N:P) are kept constant in zooplankton (i.e. only zooplankton C is modelled explicitly) and "surplus" C, N or P compared to the varying ratios in ingested phytoplankton is returned directly to the relevant inorganic nutrient pools in water.

### 3.2.3 Benthic macro- and microphytic state variables

Depending on the coastal slope, wave exposure and gross eutrophication status macrobenthic autotrophs often dominate both biomass and primary production in coastal waters. Dominance of macrophytes is also a characteristic feature of the ecosystem in the Forsmark area /Wijnbladh et al. 2008/. Based on existing knowledge from the area (see below) 3 functionally different autrotrophic benthic state variables are included in the Forsmark model set-up. They include:

- perennial macroalgae (brown algae such as *Fucus* and red algae) that can only occur on hard substrate (bedrock, boulders) and take up nutrients from water,
- rooted macrophytes ("seagrass" and *Potamogeton*) but also including the rooted algae *Chara*, which take up nutrients both from the sediment pore water and from water,
- a lumped group consisting of benthic microphytes, epiphytes growing on macrophytes and the annual macroalgae (*Ulva, Pilayella, Cladophora*). This group has no specific requirements to substrate type.

Emergent macrophytes such as reed, *Phragmites australis* found in the inner parts of Kallrigafjärden are not included in the model.

### *Macrophyte data from the Forsmark Area*

Recognising the important role of macrophytes a large number of diving transects, point samples and in situ rate process studies have been carried out in the Forsmark area /Wijnbladh et al. 2008/. The vegetation in the lower part of the photic zone is dominated by red algae (e.g. *Polysiphonia nigrescens*), at shallower depths brown algae such as the filamentous *Spacelaria arctica* or larger *Fucus vesiculosus* dominate (depending on exposure) and, in the sublittoral green algae, eg. *Cladophora glomerata* can be common.

In sheltered bays such as Kallrigafjärden and Asphällsfjärden soft bottom communities consisting of *Potamogeton pectinatus* and *Chara tomentosa* dominate the macrophytes in shallow areas. A few bays are being more or less secluded from wave exposure and hosts soft bottom. In deeper areas of Tixelfjärden and Kallrigafjärden the Xanthophyceae algae *Vaucheria dichotoma* can be found in high densities.

### *Macrophyte growth and biomass fate in the model*

Benthic macrophytes are associated with the bottom substrate and are quantified in terms of areal densities (e.g. gC $m^{-2}$) rather than volumetric concentrations. In their life stage macrophytes are not subject to hydrodynamic transport but they remain fixed at bottom in grid cells. Instead of settling loss as for phytoplankton macrophyte losses occurs by sloughing of aged leaves (e.g. in *Zostera*), by respiration (C and nutrients returned to inorganic pools) and loss to the detritus pool.

As for phytoplankton the growth of the various benthic vegetation types in the model is dependent on light availability, temperature and nutrient availability. While macroalgae only take up nutrients from the water compartment, phanerogams or rooted macrophytes (e.g. *Potamogeton*, *Zostera*) and *Chara* /Vermeer et al. 2003/ and microphytes growing on sediments also take up nutrients from the upper sediment layer. In addition, the growth of macroalgae and rooted vegetation is also affected by low concentrations of dissolved oxygen.

Furthermore, the growth of rooted macrophytes becomes reduced if oxygenated zone (i.e. the sulfide front) approaches the sediment-water interface. In specific, growth is reduced if the depth where nitrate is present in the sediment is less than 1 cm. Sub-optimal conditions in any of these factor groups invariable will result in growth rates below the maximum. The joint dependence of nutrients, temperature and light is defined by separate growth limiting factors, that range from 0 to 1, where a value of 1 means the factor does not limit growth (i.e. light is at optimum intensity, nutrients are available in excess, etc). The limiting factors are then combined with a maximum growth rate at a reference temperature.

In contrast to phytoplankton description nutrient composition of the macrophytes remains constant (fixed stoichiometric ratios) and growth and nutrient uptake rates are linearly dependent[3]. The effect of light on the growth rate is described by saturation functions where light requirements differ between the three defined groups. Besides light, nutrient requirements, source of nutrients (water, sediment and water) and substrate are the main factors that differentiate the groups in the model. In Table 3-1 are listed the main characteristics of the three groups.

[3] ECOLab macrophyte templates with partial uncoupling of nutrient uptake and growth are available but as this approach will add an additional 6 state variables to the model template with implications for simulation speed it was not applied.

**Table 3-1. Overview of growth characteristics that define the functional benthic vegetation groups in the model. Half-saturation constants for uptake of nitrogen ($K_n$) and phosphorus ($K_p$) differs for sediment and water in rooted vegetation. The constant light requirement for max growth (Ek) was changed during the calibration process.**

| Functional group | Representing | Max growth rate (%/d) | Ek $E/m^2/d$ | $K_n$ / $K_p$ $g/m^3$ |
|---|---|---|---|---|
| Perennial macroalgae | *Fucus,* Red algae | 5 | 18 | not relevant (growth relies on internal conc.) |
| Rooted vegetation | *Zostera* *Potamogeton* *Chara/Vaucheria* | 12 | 15 | Sed: 0.2/0.05 Wat: 0.05/0.01 |
| Micro-epiphytes/ Annual macroalgae | Benthic diatoms Epiphytic algae Annual macroalgae | 120 | 3 | 0.05/0.01 |

### *Previous macrophyte models for Forsmark area*

In the previous model set-up for the Forsmark and the Oskarshamn area /Wijnbladh et al. 2008/ macrophyte growth was calculated from observed and modelled distributions and biomass, e.g. along depth gradients and P/B ratios estimated from production studies carried out in the Forsmark area or from comparable Baltic coastal waters /Wijnbladh et al. 2008, Table 3-18/. Translating the table values into the three macrophyte groups in the ECOLab model daily growth rate of perennial algae range between 3.3–10.4 mgC $(gC)^{-1}$ $(MJ_{PAR})^{-1}$ $d^{-1}$, rooted vegetation 2.4–19.4 mgC $(gC)^{-1}$ $(MJ_{PAR})^{-1}$ $d^{-1}$ while only one value is available for micro-epiphytes (incl. annual macroalgae) at 20.9 mgC $(gC)^{-1}$ $(MJ_{PAR})^{-1}$ $d^{-1}$.

The fate of macrophyte production differs between groups. Overall, macrophytes can be grazed, leaves can be shed as part of aging process and later decayed, such as in *Zostera*, and algal tissue can die because of nutrient or light limitation releasing nutrients directly to the water column or dead tissue fragments can sediment and later eroded and advected. The death rate of rooted vegetation is described as a function of water depth, bottom water oxygen saturation and the sulphide front in the sediment. The water depth is in this respect included to describe the physical stress on leaves due to waves.

### *Rooted macrophytes*

Rooted macrophytes are not grazed in the Forsmark model template as birds are not included in the model. Instead, a slightly larger loss fraction is returned to the detritus pool than if grazers were present. A large number of dynamic models for rooted macrophytes, especially *Zostera* have been published in the literature, e.g. /Verhagen and Niehnuis 1983, Zimmerman et al. 1987, Bocci et al. 1997, Plus et al. 2003/. DHI developed a dynamic eelgrass model in the early 1990's /Bach 1993/ and based on advances published in the literature and numerous modelling studies of estuaries and coastal lagoons the "eelgrass" model has been updated continuously. Besides information on max growth rate, light- and nutrient dependence important characteristics of the rooted macrophyte model include:

1. Only above-ground tissue (leaves) are modelled explicitly but rhizomes and roots are included functionally to mediate nutrient uptake from pore water in the upper sediment layer.
2. Uptake of nutrients takes place from the sediment pore water through roots and from the water through leaves.
3. Accumulated nutrients are retained in the macrophyte patches by returning old leaves to the sediment locally for mineralization.

In the Forsmark model rooted macrophytes are allowed to grow in areas predicted by the statistical model applied in the previous study /Wijnbladh et al. 2008/. In other studies carried out by DHI, distribution and biomass of rooted macrophytes were intrinsic model outputs, i.e. macrophytes were allowed everywhere, but after a model warm-up period they could only sustain where sediment conditions (low $H_2S$ in sediments, rather high nutrient conc. in pore water) and light conditions were appropriate.

#### *Perennial macroalgae*

Besides sufficient light availability perennial macroalgae depend on hard substrate for fixation at a site. Therefore, these algae are only allowed to grow at sites where hard substrate is available. In the Forsmark set-up perennial macroalgae was only allowed to grow at sites predicted by the statistical model applied in the previous study /Wijnbladh et al. 2008/.

The functional algal group encompasses species that can grow under low-light conditions (i.e. red algae) and brown algae such as *Fucus vesiculosus* which require higher light intensities /Markager and Sand-Jensen 1992, Middelboe et al. 2006/. In the Forsmark template perennial macroalgae of the "*Fucus* type" has been prioritized above red algae in the irradiation-production equation, and in effect biomass of perennial macroalgae probably will be underestimated at larger depths.

*Fucus vesiculosus* is considered to be poor food for meso-herbivores /Lotze and Worm 2002/ and high abundance of *Idotea baltica* often found in *Fucus* beds in the Baltic are usually associated with grazing on epiphytes such as *Pilayella littoralis* /Kotta et al. 2006/. In effect, it was chosen that perennial macroalgae are not grazed in the Forsmark model and gradual loss of biomass occurs by tissue die-off when respiration exceeds production, e.g. due to low light or low nutrient availability.

### 3.2.4 Benthic micro- and epiphytes, annual macroalgae

Benthic microalgae can be an important autotrophic component in shallow areas. They can cover large sediment surfaces and take up nutrients partly from the pelagic system and partly from the pore water. As for rooted vegetation the growth is controlled by light availability, nutrients and the oxygen concentration just above the sediment as well as the depth where nitrate is present in the sediment. Benthic micro-algae is regarded fixed and is not transported due to e.g. resuspension.

In contrast to the perennial macorlagae and rooted macrophytes, basic information regarding production and biomass figures for benthic microphytes in the Forsmark areas is much less extensive and estimates of production basically relies on 1–2 irradiation-production relations, an assumption of a uniform biomass distribution within the "niche" defined by substrate and depth and a universal yearly P/B ratio of 12.1.

More information on production and growth rates is available for annual macroalgae (*Pilayella littoralis, Cladophora glomerata* and *Enteromorpha intestinalis*) although this information stem from other coastal areas in the Baltic /Wallentinus 1978, Paalme and Kukk 2003/. Considering the wide range in organism size within this group the growth equation chosen invariable will be a compromise.

In the Forsmark ECOLab template grazing is only important for the **micro-epiphyte group** with key benthic herbivores such as *Hydrobia sp*. (grazing on benthic diatoms), *Macoma baltica* occurring in the photic zone (benthic diatoms), amphipods and the isopod *Idotea baltica* (grazing on annual macroalgae such as *Pilayella littoralis*). The diversity in the micro-epiphyte autotrophic group is also reflected in the associated grazer community (see below). Besides grazing, annual macroalgae can be lost to the detritus pool and mineralised. Degradation rates of *Cladophora glomerata* and *Pilayella littoralis* are available for coastal areas in the Baltic /Paalme et al. 2002/, but as their rates resemble the default degradation rate of detritus (after correcting for temperature) the default detritus degradation rate was applied.

### 3.2.5 Benthic invertebrate state variables and processes

Due to low salinity the species richness of benthic fauna is low in the Baltic, however all major feeding guilds are represented but each group with low member number. Despite the tradition to allocate benthic invertebrates to different feeding guilds, most invertebrates do not ingest or forage on one carbon source only, e.g. filter-feeders ingest suspended detritus along with plankton algae during resuspension events, deposit-feeders may consume microphytes and meiofauna along with detritus and, epibenthic crustaceans (≈ omnivors) may deliberately change diets according to availability of potential food items.

#### *Benthic invertebrate data from the Forsmark area*

A large number of studies on bottom fauna have been carried out in the Forsmark area during the past two decades covering both soft and hard bottom fauna and fauna associated with macro vegetation, see /Wijnbladh et al. 2008/ for a summary of previous studies. Number of taxa was low in the various sampling campaigns, between 2 and 9 except for samplings in vegetation dominated habitats where the maximum taxa number was 19. *Macoma baltica* occurs widespread in the area dominating soft bottom communities in terms of biomass (≈ 5–10 g C $m^{-2}$) at both shallow and at deeper waters.

Other important organisms include the polychaete *Marenzelleria viridis* that attain highest biomass (≈1–3 g C $m^{-2}$) at deeper soft bottom areas. The predator *Saduria entomon* occur widespread in the central Baltic except on hard bottoms, but quantitative data is not readily available for the Forsmark area. Based on a previous review a likely mean biomass of 0.5–1 g C $m^{-2}$ seems likely for the Forsmark area /Haahtela 1990/.

#### *Benthic invertebrate functional groups in model*

For simplicity, only four major functional groups within benthic invertebrates are represented in the Forsmark ECOLab template:

- filter-feeders encompassing amongst others *Mytilus edulis*, *Cardium sp*. and in the most freshwater influenced parts also *Dreissena polymorpha*,
- deposit-feeders/detrivors compassing species such as *Corophium volutator, Monoporeia affinis, Macoma baltica, Marenzelleria viridis,*
- herbivores representing species such as *Macoma baltica, Hydrobia sp.* that ingest microphytes growing on sediment and benthic plants and, *Idothea baltica* primarily ingesting annual macroalgae (e.g. *Pilayella*),
- macrobenthic predators represented by *Saduria entomon* (belonging to the "top-predator" group in the model which also includes larger demersal fish).

Deposit-feeders, herbivores and macrobenthic predators are included as true dynamic state variables, while filter-feeders are included as a forcing function only, where filtration loss on plankton concentration in the near-bed model layer is imposed and scaled according to observed and GAM (General Additive Models) modelled biomass /Wijnbladh et al. 2008/. Hence, opposed to the true state variables biomass of filter-feeders is assumed to be constant through simulation period, but with ingestion capacity varying seasonally with temperature. The exchanges with other state variables besides phytoplankton takes place in the form of distributing the ingested C, N and P from algae between inorganic species ($CO_2$, DIN, $PO_4$) with 50% and detritus 50%.

Deposit-feeder model processes builds on field and experimental data from studies with *Macoma baltica* /Kiørboe and Møhlenberg 1982, Jansen et al. 2009/ and with various polychaetes feeding on detritus /Cammen 1980/. Briefly, assuming an average individual biomass of 15 mgC a max specific ingestion rate of organic carbon of 10% $d^{-1}$ can be expected which translates to a rather low max specific growth rate of 1.5% $d^{-1}$ because of the 'poor' quality of detritus.

## 3.3 Additional model development for the Forsmark application

The above description includes model variables and processes as included in the original ECOLab template applied in different estuaries in Denmark /DHI 2008/ and in Mediterranean lagoons /Rasmussen et al. 2009/. However, to fulfill the needs from SKB several model developments or model extensions have been identified. These developments or adjustments included the following variables:

- Dissolved inorganic carbon (DIC)
- Perennial macroalgae (e.g. *Fucus*)
- Planktivorus fish
- Deposit-feeders
- Benthic filter-feeders
- Benthic predators (including demersal benthic feeding fish)

### 3.3.1 Dissolved Inorganic Carbon (DIC)

An important element, which was not originally included in the model, is dissolved inorganic carbon, DIC. Most processes affecting DIC is already included but only to describe the oxygen cycle and not the DIC system.

Normally, DIC is not included in these kinds of ecosystem models as DIC is not considered as a limiting factor in most open water systems. However, the introduction of DIC was identified as an important element as one element in the radionuclide model will be the modeling of C-14 and hence the uptake of C-14 will depend on the relation between C-14 and C-12.

In this model DIC is described as:

$$\frac{dDIC}{dt} = depc + rezc + redc + reCO2 + remc + denwc\text{-}prbc\text{-}prpc\text{-}prec\text{-}prbd + mSOC + respFCbent + respFCplan + respDFC \quad 3\text{-}1$$

where *depc* is decay of phytoplankton, *rezc* is respiration by zooplankton, *reCO2* is re-aeration of CO2, *redc* is mineralization of dead organic particulate matter, *remc* is respiration by mussels, *denwc* is nitrate respiration of dead organic particulate matter, *prbc* is production of macro algae, *prpc* is production of phytoplankton, *prbd* is production of benthic micro algae, *mSOC* is mineralization of sediment carbon (two layers), *respFCbent* is respiration by benthic feeding fish, *respFCplan* is respiration by plantivoir fish and *respDFC* is respiration by deposit feeders.

All the above processes except *reCO2* are already included in the model. The re-aeration of CO2 is expressed similar to the re-aeration of dissolved oxygen, and is described as follows:

$$reCO2 = 3.93 \cdot \sqrt{u}/dz^{1.5} + (2.07 + (0.215 \cdot U10)^{1.7})/100 \cdot 24 \cdot (co2air\text{-}DIC)/dz \quad 3\text{-}2$$

Where *u* is current speed, *dz* is depth of model surface layer *U10* is wind speed at 10 m above water surface, *co2air* is saturation of $CO_2$ at given salinity. The DIC saturation is based on Buch's relations /Buch 1945/ and is described as follows:

$$co2air = 0.99 \cdot 1.01 \cdot (0.0016 \cdot sali^4 - 0.0254 \cdot sali^3 + 0.1192 \cdot sali^2 + 0.0635 \cdot sali + 0.1846) \cdot 12.01115 \quad 3\text{-}3$$

where *sali* is salinity.

Inorganic N and P released from the sediment are included in the pore-water pool, (see description in the previous section). This is not the case for DIC. When the sediment is mineralized the released DIC is instantaneously included in the pelagic system just above the sediment surface.

### 3.3.2 Perennial macroalgae

The benthic algae described in the previous section include annual macroalgae (e.g. *Ulva*), and benthic microalgae. However, as perennial macroalgae, i.e. *Fucus* dominates the phytobenthos community on hard substrate in shallow waters the ecosystem model was extended with a dedicated state variable representing *Fucus*. The overall functionality of the existing macroalgae formulation (annual macroalgae) in ECOLab was adopted but growth rates and sloughing rates were changed to give a less pronounced seasonal signal and higher survival.

### 3.3.3 Deposit-feeders

Deposit-feeders ingest sediment that ultimately can contain high concentrations of radionuclides that subsequently can lead to high radionuclide concentration in deposit-feeders. Therefore, they are included in the ecosystem model. In the model, deposit feeders acts as food source for the benthic feeding fish, and covers all deposit-feeders included in the sub groups: micro-fauna, meio-fauna and macro-fauna.

Growth of deposit-feeders is only possible where soft bottom is estimated and is described as follows:

$$\frac{dDFC}{dt} = assi\text{-}respDFC\text{-}mortDFC\text{-}predDFC \qquad 3\text{-}4$$

where *DFC* is the concentration of deposit feeders C, *assi* is assimilation, *respDFC* is respiration, *mortDFC* is mortality and *predDFC* is predation by benthic feeding fish.

Here the involved processes are described:

$assi = kassi \cdot SOC1$

$respDFC = krespdfc \cdot DFC$

$mortDFC = kmortdfc \cdot DFC$

$predDFC = kpred \cdot (DFC/dz\text{-}1)/(DFC/dz + KDF\text{-}1) \cdot FCbent \cdot POW(tetapred, temp\text{-}20)$

where *kassi*, *krespdfcm, kmortdfc* and *kpred* are constants describing respiration, mortality and predation at 20°C. *DFC* is the concentration of deposit feeders, *SOC1* is the concentration of unconsolidated carbon in the sediment, *dz* is the depth of the actual model bottom layer, *KDF* is a half-saturation constant, *FCbent* is the concentration of benthic feeding fish/predatory invertebrates and *tetapred* is a temperature function. Moreover, predation on deposit-feeders is only allowed if the concentration of deposit feeders exceeds 1 gC/m$^2$ and the total water depth is larger than 1.5 m.

### 3.3.4 Benthic feeding fish

Fish – either they are benthic feeding fish or predatory invertebrates – behave differently than the standard ecosystem variables. They move differently and they are not diluted (and dissolved) as are the other pelagic parameters. To solve this we have tried to fix the fish in space, resulting in a stationary description. By this approach we have solved the problems of dilution, and we anticipate a positive growth only where the benthic food production is sufficiently high to maintain a fish stock.

The description in the model includes:

$$\frac{dFCbent}{dt} = predDFC\text{-}respFCbent\text{-}mortalityFCbent \qquad 3\text{-}5$$

where *FCbent* is the concentration of benthic feeding fish, *predDFC* is predation on deposit feeders (se equation above), *respFCbent* is respiration and *mortalityFCbent* is mortality.

The last two processes are described as follows:

$respFCbent = kFCBent \cdot predDFC \cdot POW(tetaresp, temp\text{-}20)$

$mortalityFCbent = mort\_FCbent \cdot FCbent \cdot POW(tetamort, temp\text{-}20)$

where *kFCbent* and *mort_FCbent* are constants describing the rate of respiration respectively mortality at 20 degree C, and *tetaresp* and *tetamort* are temperature corrections for respiration respectively mortality.

### 3.3.5 Planktivorus fish

Similar to the benthic feeding fish the planktivorus fish are described as follows:

$$\frac{dFCpla}{dt} = predZC\text{-}respFCplan\text{-}mortalityFCplan \qquad 3\text{-}6$$

where *FCpla* is the concentration of planktivorous fish, *predZC* is predation on zooplankton, *respFCplan* is respiration and *mortalityFCplan* is mortality.

Both respiration and mortality are equal to the respiration and mortality of benthic feeding fish, and the grazing on zooplankton is described as follows:

$$predZC = kzc \cdot (ZC - 0.007) / (ZC + Kz - 0.007) \cdot FCpla \cdot POW(tetapred, temp - 20) \quad 3\text{-}7$$

where *kzc* is the grazing rate at 20 degree C and *Kz* is the half-saturation constant. The model does not allow grazing on zooplankton if the concentration of zooplankton is below 7 µgC/l.

The introduction of planktivorous fish has also altered the mortality description for zooplankton. Instead of a combination of a first-order and density-dependent (i.e. $ZC^2$) mortality, the new formulation include grazing on zooplankton from planktivorous fish and a first-order mortality (i.e. age-related).

### 3.3.6 Benthic filter-feeders

Filter-feeders are not modelled explicitly but the effects of the filter-feeders in the ecosystem are included using abundance and biomass data from monitoring program.

## 3.4 Ecosystem data

Running the ecosystem model requires a number of external data, e.g. forcings, boundaries, etc which will be described shortly in this section. An overview of how models are linked is discussed in Section 2.4.

### 3.4.1 Forcings

The forcings required to perform the ecosystem modeling are:

- Wind (speed and direction) – wind is utilized for e.g. wave generation and re-aereation, and the wind files are included through the hydrodynamic set-up.
- Current (speed) – besides transport through water movements, current speed is utilized for estimation of re-suspension. Current is computed by the hydrodynamic model.
- Salinity – salinity is utilized for e.g. oxygen and DIC saturation, and is computed by the hydrodynamic model.
- Temperature – is utilized in most of the biological processes, and is computed by the hydrodynamic model.
- Deposition of nitrogen – a source of inorganic nitrogen. Here assumed constant at 0.9 kg N/ha.
- Photosynthetic available radiation (PAR) – utilized by algae and benthic flora. PAR is delivered as a time series and is shown in Figure 3-5.

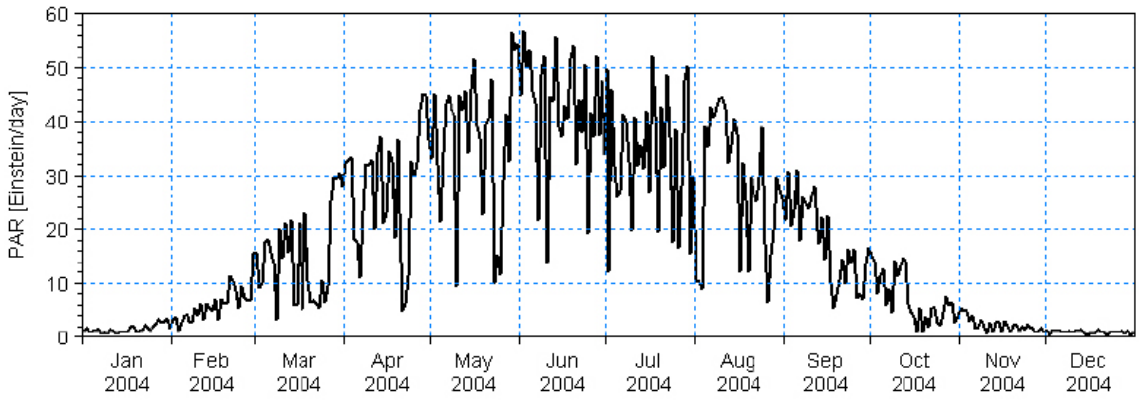


***Figure 3-5.*** *Time series of PAR used for the ecosystem model.*

### 3.4.2 Boundary data

The model requires boundary data on the northern as well as the southern boundary. The most obvious data applied for boundary are output from a regional ecosystem model or measurements from nearby measurement stations.

For this study measured interpolated data have been applied. For now, two measurement stations have been addressed to provide boundary data for the two boundaries:

- Norra Randen – this station is located south of Öregrundsgrepen, see Figure 3-6, and suitable for the southern boundary.
- C14 – this station is the only station available north of Öregrundsgrepen, see Figure 3-6. However, C14 is located far from the area of interest and not suited for boundary conditions.

Evaluating the data available at C14 also revealed that only total N and total P was measured and no information on inorganic fractions or phytoplankton (chlorophyll-a) was included in the measurements. Hence, C14 was discarded as boundary data and Norra Randen applied for both the southern and the northern boundary.

The measurements from Norra Randen covering 2004 with monthly samplings at 4 depth strata /Walve and Larsson 2007/ were transformed into model parameters by multiplication, division or subtractions of measurement data (see Table 3-2). Interpolation of measurement data between samplings and depth was carried out in the MIKE ECOLab routine.

### 3.4.3 Initial data (pelagic system)

The initial values in the pelagic system are flushed relatively quickly why uniform concentrations are applied distributed in the entire model area. Initial values for the pelagic system are estimated based on the same assumptions as listed in Table 3-2, i.e. based on 'Janaury' data from 2004 sampled at Norra Randen. By repeating the model for 5 consecutive years the initial values of pelagic state variables are of less importance, except for benthic and planktivous fish.

With respect to benthic feeding fish and planktivorous fish the initial values were estimated and set to 0.2 g C/m$^3$. The initial values for the benthic feeding fish only applied in the bottom layer of the model. By comparing results from the last time step for each of the years 4 and 5 even the fish data was close to be in a quasi-stationary equilibrium after 5 years.

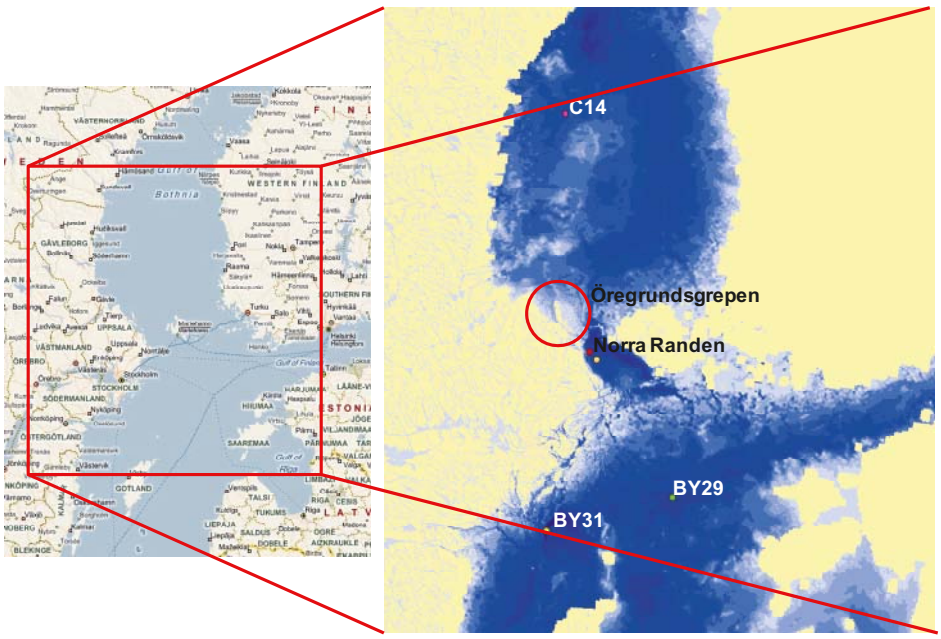


***Figure 3-6.*** *Map showing measurement stations (C14, By29, By31 and Norra Randen) in the Baltic Sea where offshore boundary conditions for the Öregrundsgrepen model are available (red circle). Data from the Baltic Environmental Database /BED 2009/ at the Department of Systems Ecology, Stockholm University.*

**Table 3-2. Transformation of measurements into pelagic model parameters. Measurements were obtained from /Walve and Larsson 2007/.**

| Model parameter | Measurement | Transformation/assumptions |
|---|---|---|
| Phytoplankton C (PC) | | 30 × CH |
| Phytoplankton N (PN) | | PC/6 |
| Phytoplankton P (PP) | | PC/42 |
| Chlorophyll-a (CH) | Chlorophyll-a[1] | |
| Zooplankton C (ZC) | | PC/10 |
| Detritus C (DC) | | 5 × DN |
| Detritus N (DN) | Total N reduced by 170 µg/l | TN – NH – NOx – PN |
| Detritus P (DP) | Total P | TP – $PO_4$ – PP |
| Ammonium (NH) | $NH_4$ | |
| Nitrate (NOx) | $NO_2$+$NO_3$ | |
| Inorganic P (IP) | $PO_4$ | |
| Dissolved Oxygen (DO) | DO | |
| Dissolved inorganic C (DIC) | | 15 mg/l (assumption) |
| Inorganic solids (SSI) | | 5 mg/l (assumption) |

[1] Chlorophyll-a is only available for year 2003 and not year 2004. However, we assume that the levels are identical in the two years and that the spring bloom is initiated more or less equal between the two years, why the 2003 chlorophyll-a data are used for year 2004 as well.

### 3.4.4 Initial data (benthic system)

Every model needs initial values for each state variable, but using the model approach with 5 years' consecutive modelling using repeated forcing data the actual values become less critical, because regulating processes will bring state variables into an equilibrium where growth and loss processes come into balance.

An overriding feature of benthic state variables is their requirements to the character of seabed, e.g. perennial macroalgae can only exist on hard substrate and rooted macrophytes and deposit-feeders can only exist on soft sediment. For initial values we used data from monitoring and previous modelling /Wijnbladh et al. 2008/. Average biomasses were applied uniformly over the appropriate seabed type, and within few years the governing processes in the ecosystem model forced the state variables into a quasi-stationary state.

For initial sediment parameters all were derived from raster GIS data of surface concentration of TOC (SKB GIS-database, GIS request #08_31, 08_33, 08_34 and 08_50), but applying ratios of C:N, C:P from comparable costal sediments. Again it should be stressed that erosion/resuspension and relocation of sediments driven by modelled bottom sheer stress will result in spatial distributions that after 5 years of modeling will differ from initial concentrations. For the benthic system the initial values applied and the origin are listed in Table 3-3.

### 3.4.5 Sources

Two rivers are included in the ecosystem model: Forsmarksån and Olandsån. Nutrient concentrations (and TOC) are only available for Forsmarksån, and we assumed that Olandsån had identical concentrations to Forsmarksån /SLU 2008/. The assumptions/transformations from measurements to model variables are described in Table 3-2. TOC introduced into the model area from river water was entered into the detritus pool.

**Table 3-3. Transformation of available data sets into initial values of benthic state variables.**

| Model parameter | Where in model area/ assumptions | Transformation/assumptions |
|---|---|---|
| Macroalgae C (BC) (perennial) | Only on hard bottom (based on SOC) | 1 g C/$m^2$ and successive modelling. |
| Macroalgae N (BN) | Only on hard bottom (based on SOC) | 0.167 g C/$m^2$ and successive modelling. |
| Macroalgae P (BP) | Only on hard bottom (based on SOC) | 0.024 g C/$m^2$ and successive modelling. |
| Eelgrass C (EC) | Only on soft bottom (based on SOC) | 2 g C/$m^2$ and successive modelling. |
| No. of eelgrass shoots (NNEC) | Only on soft bottom (based on SOC) | 20 shoots/$m^2$ and successive modelling. |
| Benthic micro algae C (BDC) (+annual algae) | Everywhere | 0.02 g C/$m^2$ and successive modeling. |
| O2 penetration into the sediment (KDO2) | Everywhere | 0.005 m and successive modeling. |
| Oxidized layer (KDOX) | Everywhere | 0.05 m and successive modeling. |
| Sediment C, unconsolidated (SOC1) | Total Carbon GIS data (rastert_top10cm1) | 30% of the total C pool 0.05 g P/$m^2$ and successive modelling. |
| Sediment C, consolidated (SOC2) | Total Carbon GIS data (rastert_top10cm1) | 70% of the total C pool 0.05 g P/$m^2$ and successive modelling. |
| Sediment P, unconsolidated (SOP1) | Only on soft bottom (based on SOC) | SOC1/420.05 g P/$m^2$ and successive modelling. |
| Sediment P, consolidated (SOP2) | Only on soft bottom (based on SOC) | SOC2/420.05 g P/m2 and successive modelling. |
| Iron bound P (FESP) | Only on soft bottom (based on SOC) | SOP1 and successive modelling. |
| Pore water P (SIP) | Only on soft bottom (based on SOC) | 0.05 g P/$m^2$ and successive modelling. |
| Sediment N, unconsolidated (SON1) | Only on soft bottom (based on SOC) | SOC1/60.05 g P/$m^2$ and successive modelling. |
| Sediment N, consolidated (SON2) | Only on soft bottom (based on SOC) | SOC2/60.05 g P/$m^2$ and successive modelling. |
| Pore water NH4 (SNH) | Only on soft bottom (based on SOC) | 0.01 g N/$m^2$ and successive modelling. |
| Pore water NOx (SNO) | Only on soft bottom (based on SOC) | 0.05 g N/$m^2$ and successive modelling. |
| Reduced substance (SH2S) | Only on soft bottom (based on SOC) | 1 g $H_2S$/$m^2$ and successive modelling. |
| Sediment inorganic matter, unconsolidated (SIM1) | Only on soft bottom (based on SOC) | 500 g/$m^2$ and successive modelling. |
| Sediment inorganic matter, consolidated (SIM2) | Only on soft bottom (based on SOC) | 10,000 g/$m^2$ and successive modelling. |
| Deposit feeders C | Only on soft bottom (based on SOC) | 10 g C/$m^2$ and successive modelling. |

# 4 Results and validation of ecosystem model

One very important forcing to the ecosystem model is the hydrodynamic model. The hydrodynamic model has been setup and validated and for comments on the hydrodynamic model is referred to /Karlsson et al. 2010/. The ecosystem model has been validated against a number of monitoring stations (SKB database SICADA, Delivery #08_111 and 08_112) within the Öregrundsgrepen area, see Figure 4-1. Except for stations PFM000083 and PFM000084, measurements for the validation year 2004 are available for all stations.

In the following a few examples from the validation are presented. All model results shown below (time series from monitoring stations or 2D-plots of benthic state variables) represent the quasi-stationary conditions obtained after 5 years of consecutive simulation with repeating meteorological forcing data from 2004.

## 4.1 Nutrients (C, N, P)

In Figure 4-2, Figure 4-3 and Figure 4-4 time series of modelled carbon, nitrogen and phosphorous are compared to measurements. In Figure 4-3 measured total N (TN) includes all N-compounds including DON. A large part of dissolved organic nitrogen is non-labile and constitutes a 'stable floor' in the Figure 4-3 for TN, equivalent to 170 µg DON. The model clearly underestimates $NO_x$ and TN at PFM000063 (and at other shallow coastal stations), probably due to local run-off not fully accounted for. Also, the model predicts short-lived increases in POC and PON (resuspension events) occurring on a weekly to monthly basis, while such events were not captured during the nine sampling occasions. Besides, the model generally simulates observations quite well.

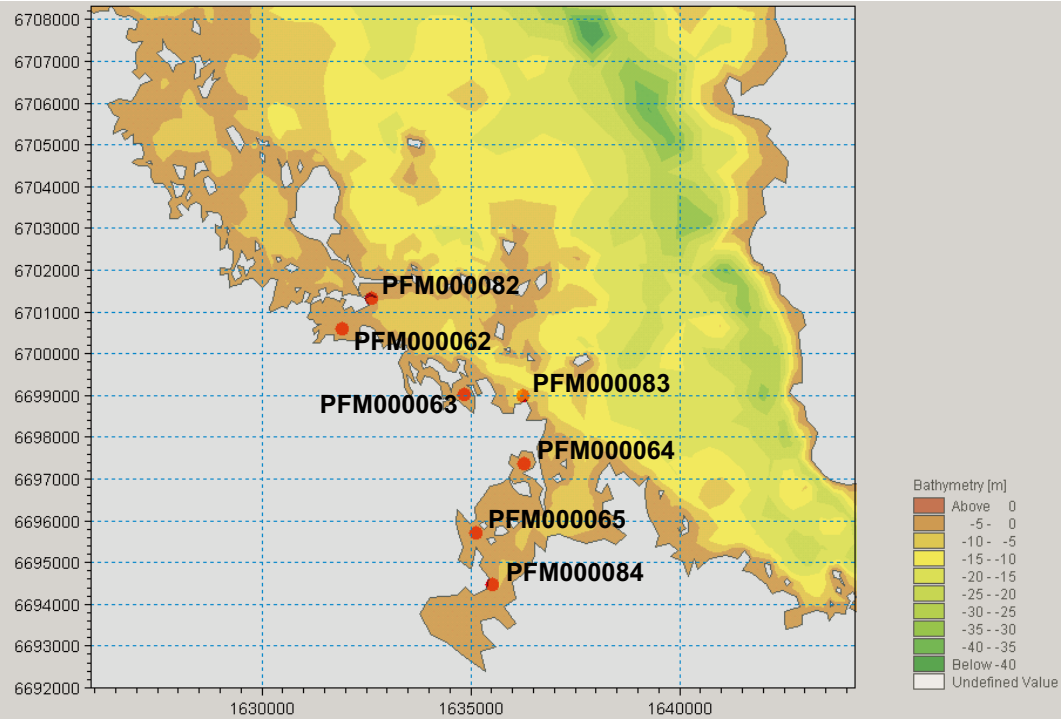


***Figure 4-1.*** *Measurement stations in the site investigations program by SKB used for calibration and validation of the ECOLab ecosystem model.*

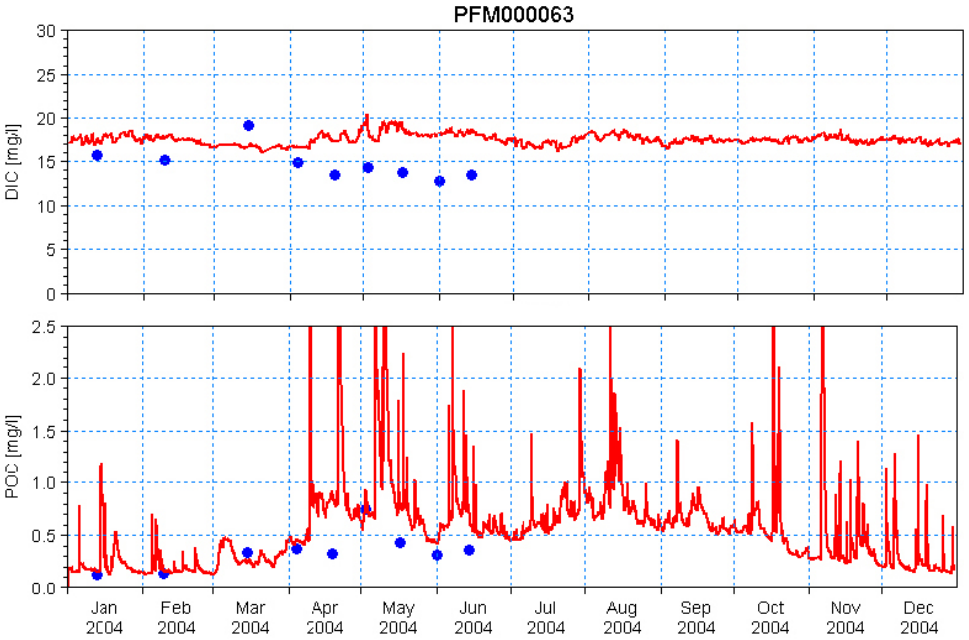


***Figure 4-2.*** *Time series of surface concentrations of DIC (top) and POC (bottom). Blue dots are measurements whereas red lines are model results.*

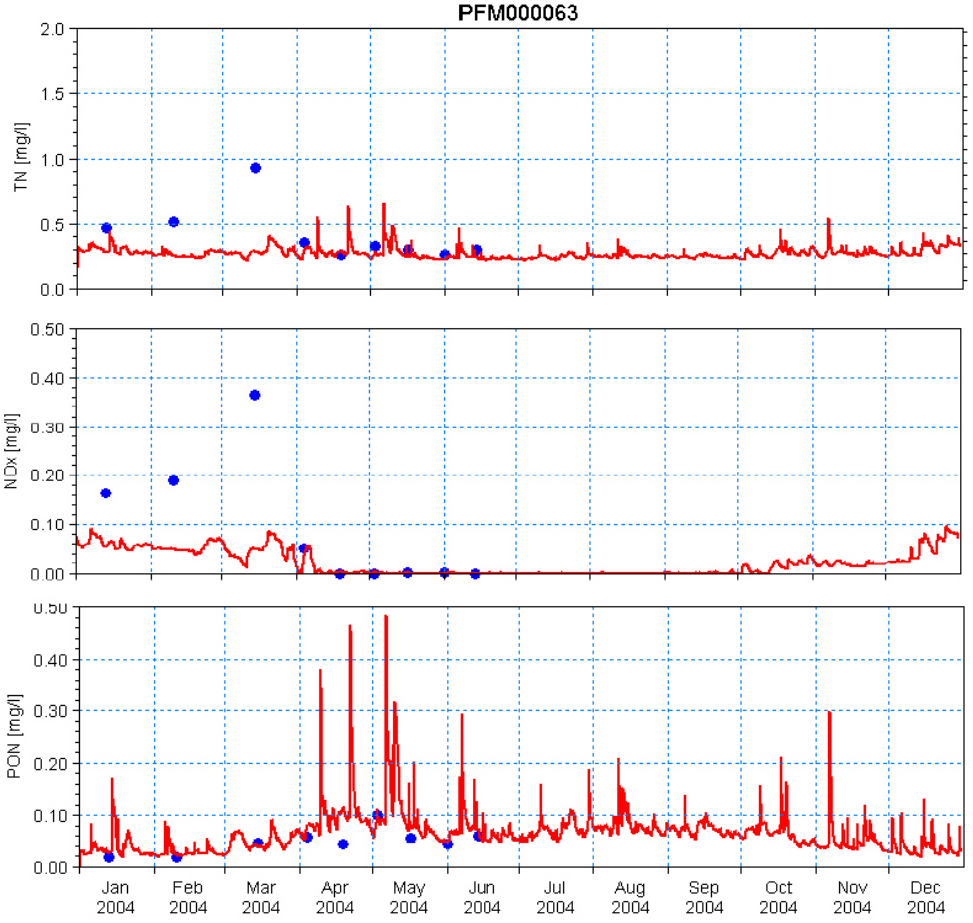


***Figure 4-3.*** *Time series of surface concentrations of TN (top), NOx (middle) and PON (bottom). Blue dots are measurements whereas red lines are model results.*

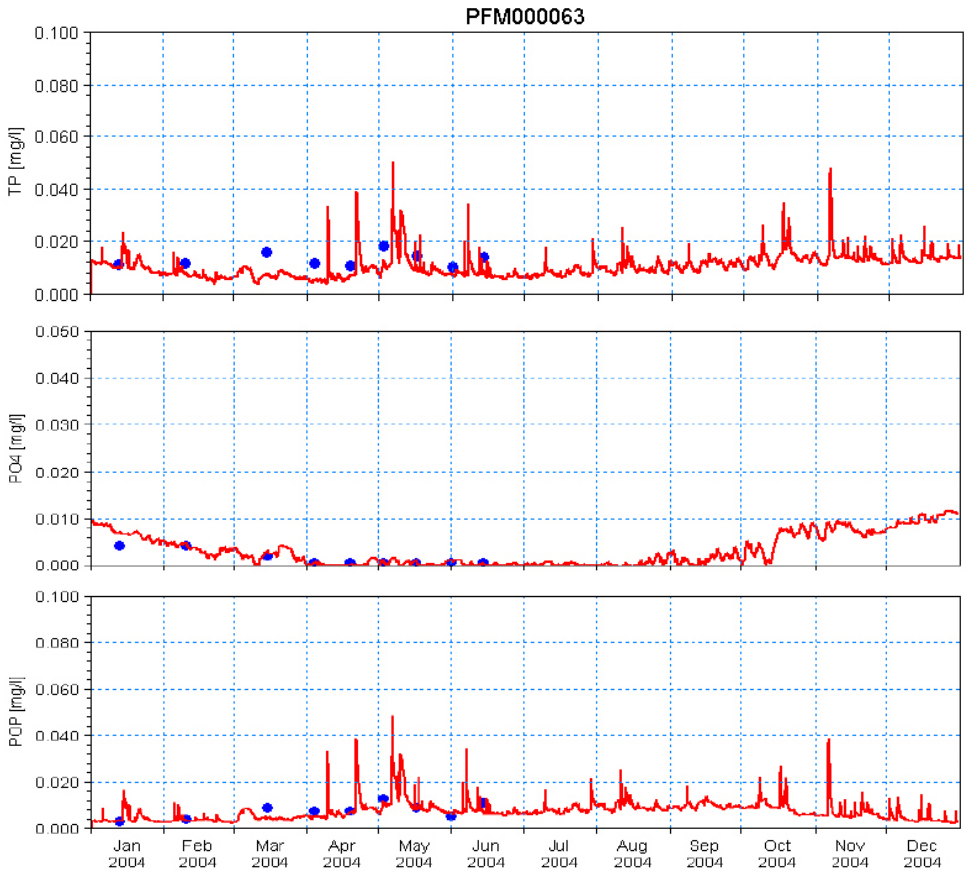


***Figure 4-4.*** *Time series of surface concentrations of TP (top), PO4 (middle) and POP (bottom). Blue dots are measurements whereas red lines are model results.*

## 4.2 Plankton, Secchi depth and oxygen

In Figure 4-5 time series of modeled and measured chlorophyll-a, zooplankton and Secchi depth from PFM000063 are shown. Unfortunately, zooplankton monitoring data from PFM000063 are not available, but for the nearby station PFM000062 zooplankton biomass varied between 0.006 and 0.009 mgC $l^{-1}$ in the autumn of 2003 and was around 0.001 mgC $l^{-1}$ in April–May 2005 /Huononen and Borgiel 2005/. In comparison, the model only slightly overestimates the measured values in the autumn but predicts almost an order of magnitude higher zooplankton concentration in April–May. A likely explanation is that the zooplankton state variable in the ECOLab model includes all grazers on phytoplankton. This means that microzooplankton and heterotrophic flagellates are also included, while the monitoring data only include mesozooplankton, primarily copepods and cladocerans.

Secchi depth (SD) measurements at PFM000063 varied between 1.8 and 4.2 m during January–June 2004, while the modeled SD never exceeded 2 m. This discrepance is due to a lower average depth (1.7 m) in the model bathymetry for the grid cell where PFM000063 is located and a restriction in the ECOLab model that the Secchi depth cannot exceed the actual water depth. At a nearby grid cell where the depth exceeds 10 m (green dashed line in Figure 4-5) the modeled Secchi depth varied between 4 and 9 m.

## 4.3 Rooted vegetation

Rooted vegetation is not a dominating element of the benthic flora in Öregrundsgrepen because of scattered distribution of available soft substrate. However, rooted vegetation has been included in the model in areas with soft bottom.

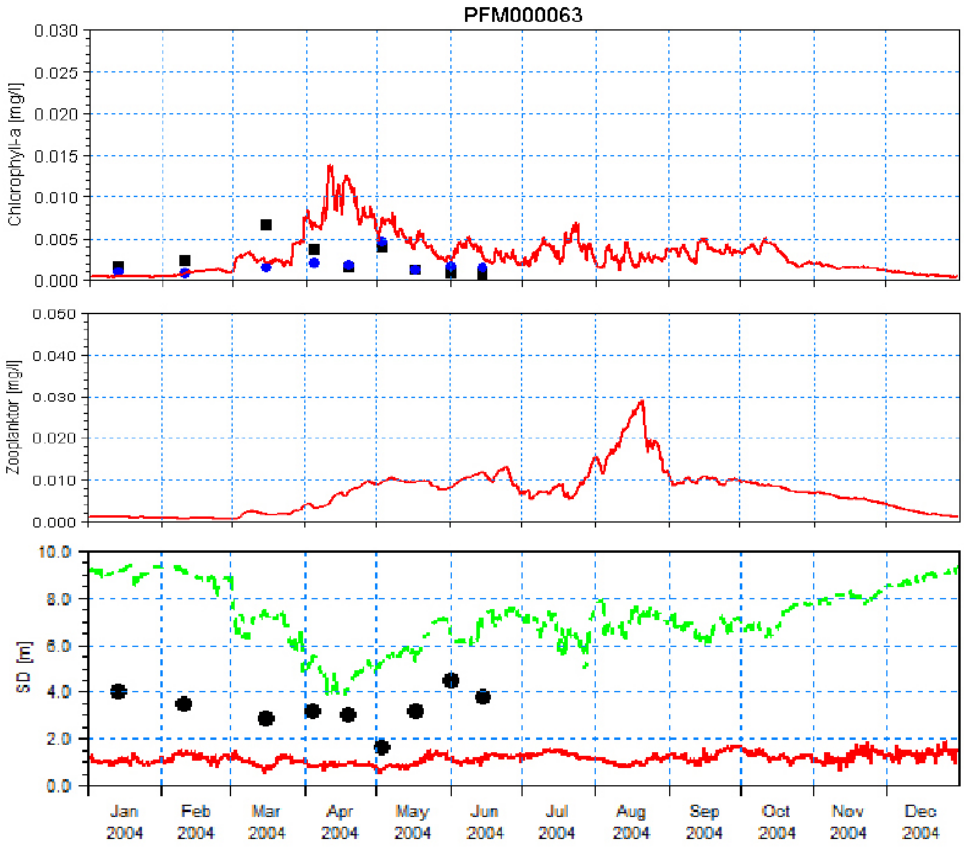


***Figure 4-5.*** *Time series of surface concentrations of chlorophyll-a (top), zooplankton and Secchi depth (bottom). Dots are measurements whereas red lines are model results. The dashed green line in the bottom panel is the modeled Secchi depth in a deeper, nearby grid cell (see text).*

A snapshot of the model results from June 1 is presented in Figure 4-6 and previous estimates based on site investigations and GIS-modelling is shown in Figure 4-7. The two sets of model results are in reasonable agreement on the spatial distribution of rooted vegetation, i.e. the distribution is confined to shallow and wave protected areas with the highest freshwater influence, but the GIS-model predicted biomasses are on average 3–5 times higher than the ECOLab model (based on model extracts from Basins 116, 117, 118, 120, 121, 123, 126, 134). In the ECOLab model biomass of rooted vegetation is primarily limited by nutrient concentrations in sediments and light availability. To impose a much higher growth and biomass of rooted vegetation will lead to violations in other ecosystem state variables.

## 4.4 Perennial macro algae and benthic microalgae

In Figure 4-8 the modelled distribution of perennial macroalgae is shown, and in Figure 4-9 is shown the modelled results of the microalgae (i.e. sum of benthic microalgae and annual macroalgae). Biomass of perennial macroalgae range from 0 to > 75 gC $m^{-2}$, with the highest values and the most extended occurrence along the western coastline.

The values and distribution are in reasonable agreement with the results from the site investigations /Wijnbladh et al. 2008/. In contrast, modelled concentration of microlalgae/annual algae attaining a maximum biomass of ca 3 gC $m^{-2}$, is much lower than the (few) samples taken in connection with the site investigation /Wijnbladh et al. 2008/. A closer examination of model data shows that the low biomass is caused by nutrient limitation of growth rather than a large grazing pressure.

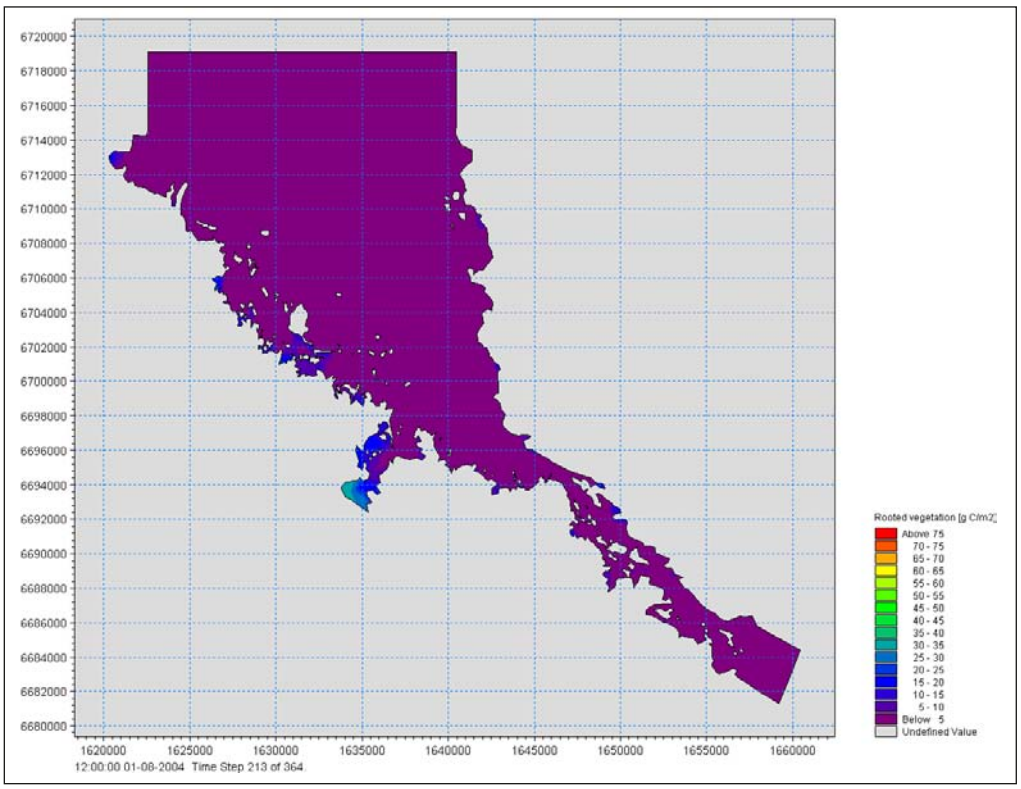


***Figure 4-6.*** *Modeled distribution of rooted vegetation (g C/m²) on 1 August 2004.*

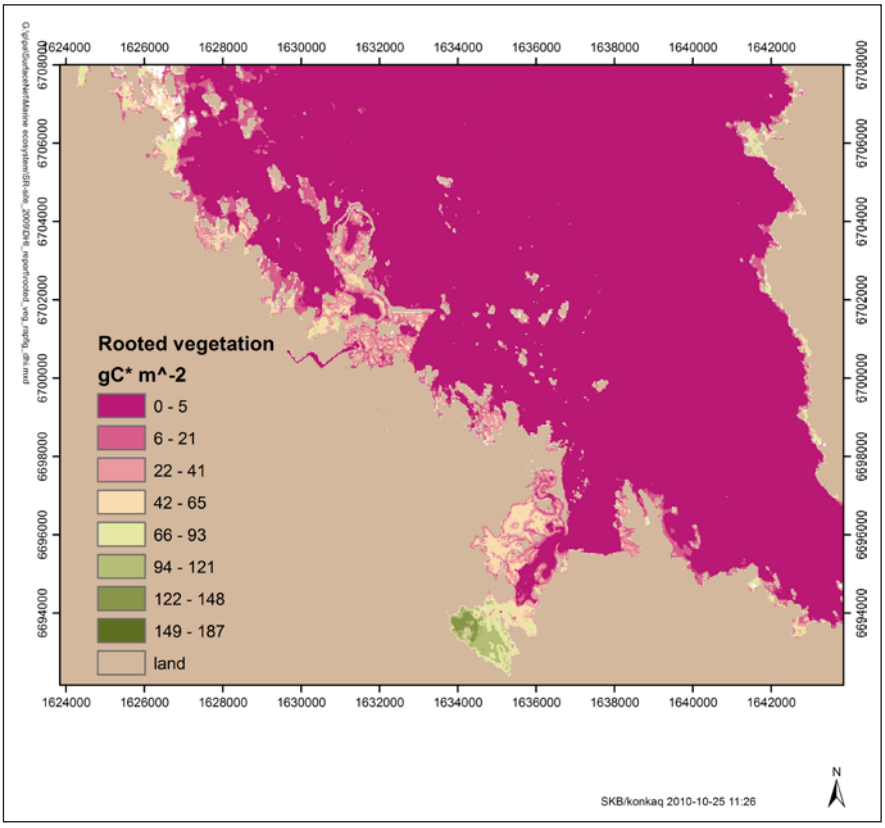


***Figure 4-7.*** *GIS-model result for biomass of rooted vegetation. From /Wijnbladh et al. 2008/.*

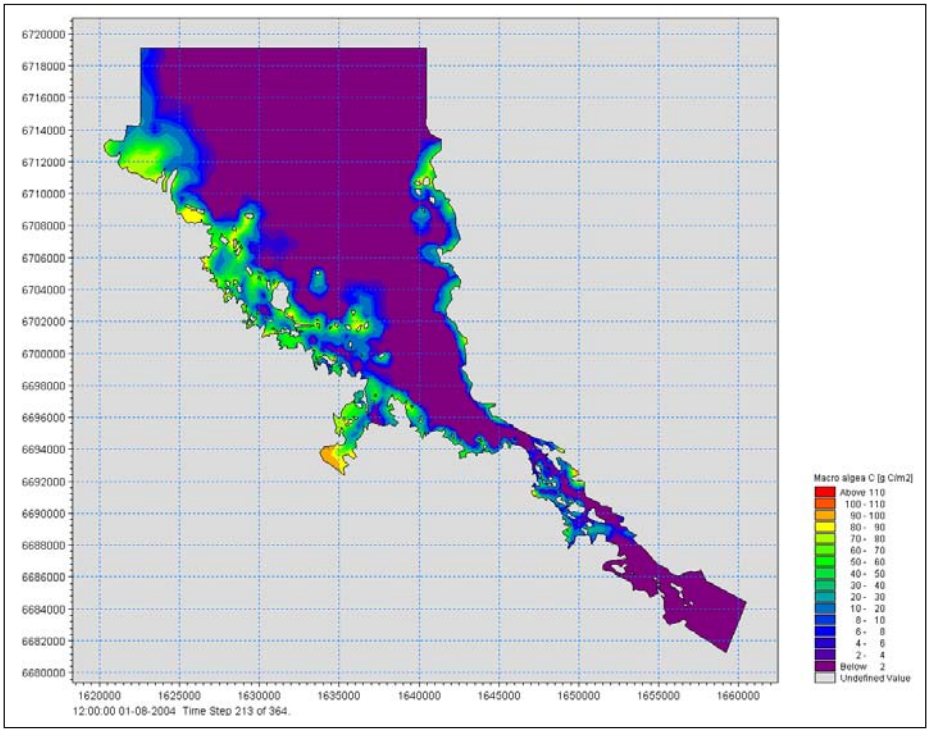


***Figure 4-8.*** *Modelled distributions of perennial macroalgae (g C/m²) on 1 August 2004.*

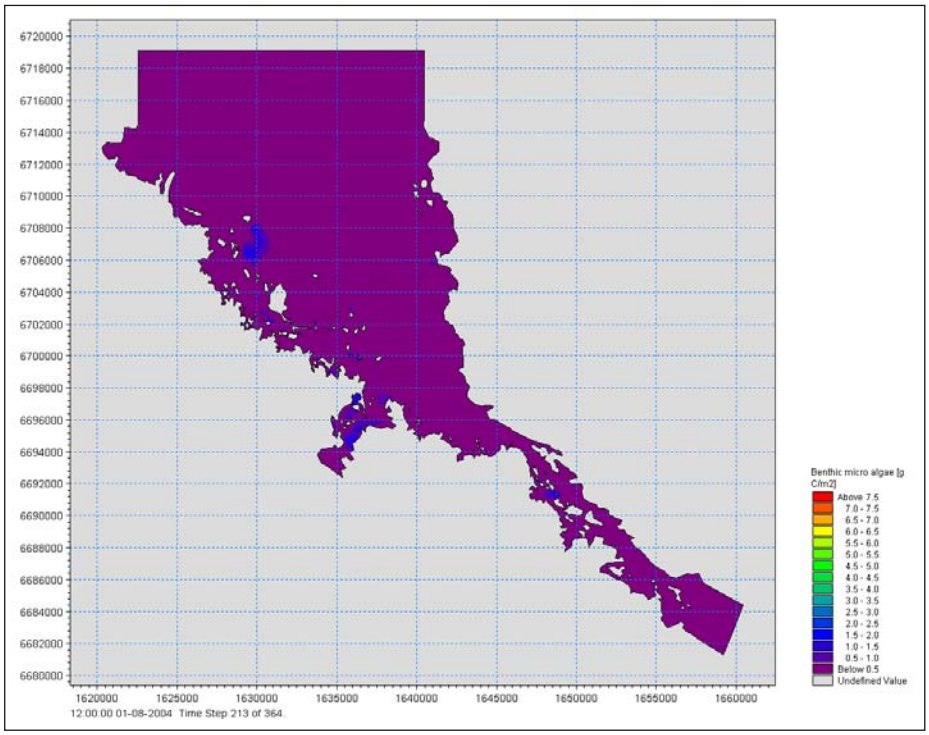


***Figure 4-9.*** *Modelled distributions of microalgae (sum of benthic microalgae, annual macroalgae) (g C/m²) on 1 August 2004.*

## 4.5 Deposit-feeders and benthic feeding fish

Modelled distribution of deposit-feeders and benthic feeding fish/predatory invertebrates is shown in Figure 4-10 and 4-11. Benthic deposit-feeders show the highest biomass (ca 10 gC $m^{-2}$) in the deepest parts of Öregrundsgrepen and where sedimentation rate is highest. The level is comparable to the data from the site investigation (average over entire area 4 gC $m^{-2}$) /Wijnbladh et al. 2008/. Biomass of bentivorus fish range between 0.05 and 0.5 gC $m^{-3}$ and levels are comparable with data from the site investigation (average 0.1 gC $m^{-2}$ over entire Öregrundsgrepen), see /Wijnbladh et al. 2008/.

## 4.6 Planktivorous fish

Modelled distribution of planktivorus fish is shown in Figure 4-12. Their main distribution and highest biomass (0.3–0.4 gC $m^{-3}$) is confined to the narrow strait where currents and thus flux of food is highest. Averaged over the entire Öregrundsgrepen modelled biomass is higher compared to values from site investigation, ca 0.1 gC $m^{-2}$ /Wijnbladh et al. 2008/.

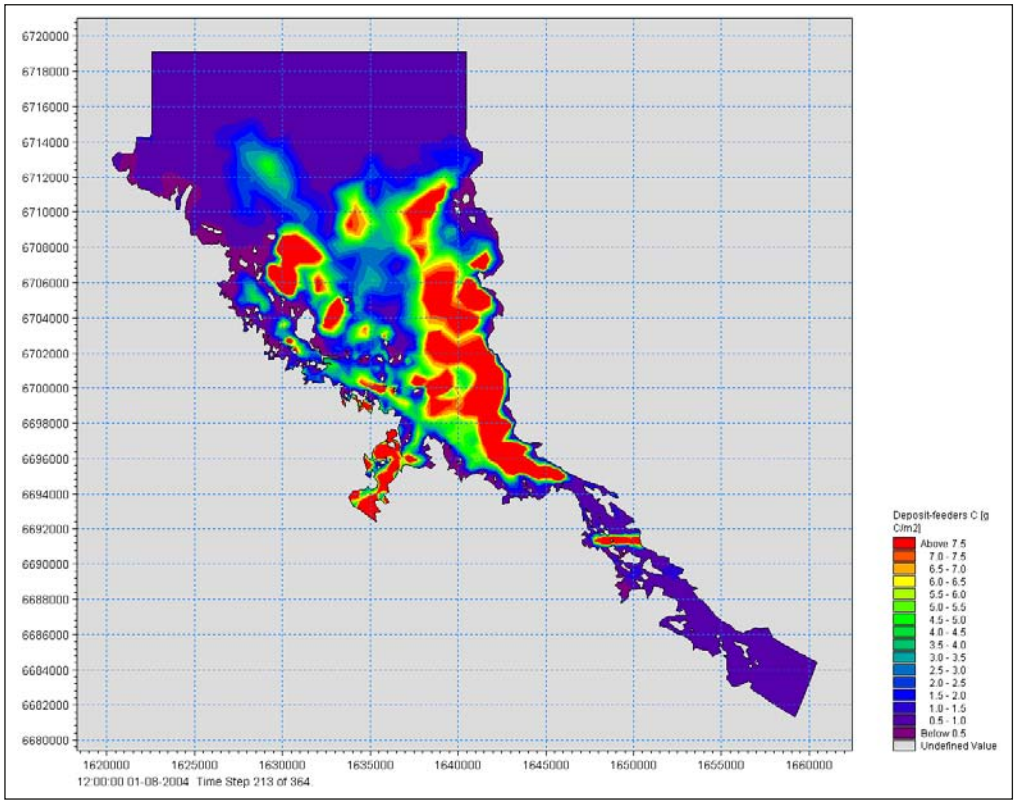


***Figure 4-10.*** *Modelled distributions of deposit feeders (g C/m²) on 1 August 2004.*

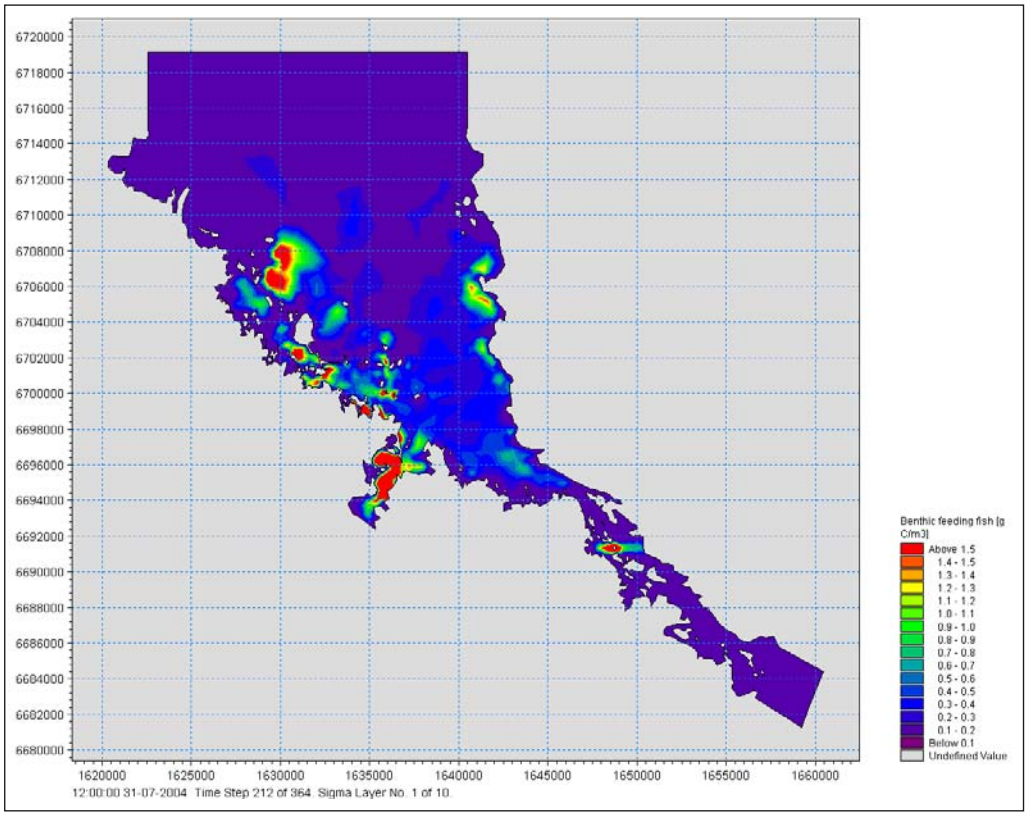


***Figure 4-11.*** *Modelled distributions of benthic feeding fish (g C/m³) on 1 August 2004.*

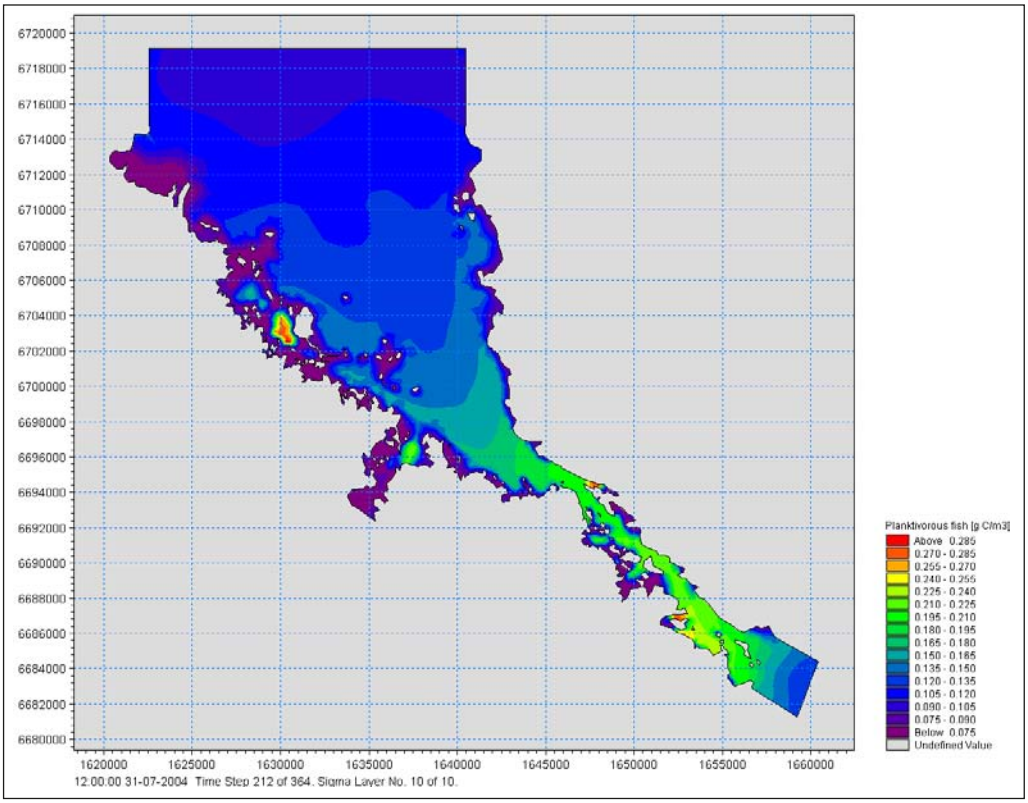


***Figure 4-12.*** *Modelled distribution in the surface waters of planktivorus fish (g C/m³) on 1 August 2004.*

# 5 Description of radionuclide model

## 5.1 Methodology

The radionuclide model builds on the ecosystem model developed for the Öregrundsgrepen that in turn builds on the hydrodynamic model for the same area (see Section 2.4 for an extended presentation on how models are interlinked).

## 5.2 Model overview

Radionuclides are found in the environment as either dissolved in the water and sediment pore-water, adsorbed to surfaces (inorganic and organic), within organisms or precipitated in the sediment. The distribution between these states is dependent on the nature of the radionuclide and the composition of inorganic and organic matter and organisms in the ecosystem. In the radionuclide model the flow of radionuclides is assumed to be proportional to the flow of carbon in the ecosystem model, for the following processes:

- Diffusion
- Sedimentation and resuspension
- Consolidation of the sediment (transport from surface sediment to deeper layers)
- Mixing due to deposit feeder burrowing and feeding activity
- Uptake by plants
- Assimilation and excretion by animals
- Respiration by plants and animals
- Death of plants and animals
- Mineralisation

Furthermore, processes specific for radionuclides were included in the model:

- Decay
- Adsorption and desorption
- Precipitation and dissolution in the sediment

The ECO Lab template for the radionuclide processes in the Forsmark area was developed to encompass the following phases:

1. An inorganic ECOLab template describing radionuclides (RN) as (Figure 5-1):
   a. RN dissolved in water and sediment pore water layer 1 and 2.
   b. RN adsorbed to inorganic suspended solids and inorganic sediment layer 1 and 2.
   c. RN precipitated in sediment layer 1 and 2.
2. An inorganic/organic ECOLab template including radionuclides related to phytoplankton, zooplankton, detritus and organic sediment compartments as (Figure 5-2):
   a. RN adsorbed to detritus, phytoplankton, zooplankton and organic sediment layer 1 and 2.
   b. RN accumulated internally in detritus, phytoplankton, zooplankton and organic sediment layer 1 and 2.
3. An inorganic/organic ECO Lab template further including radionuclides related to all biotic compartments described in the ecological model (Figure 5-3 and Figure 5-4):
   a. RN adsorbed to microalgae and epiphytes, macroalgae, macrophytes, herbivorous invertebrates, deposit feeders, planktivorous fish, benthic feeding fish/benthic predatory invertebrates and dead fish.
   b. RN accumulated internally in microalgae and epiphytes, macroalgae, macrophytes, herbivorous invertebrates, deposit feeders, planktivorous fish, benthic feeding fish/benthic predatory invertebrates and dead fish.

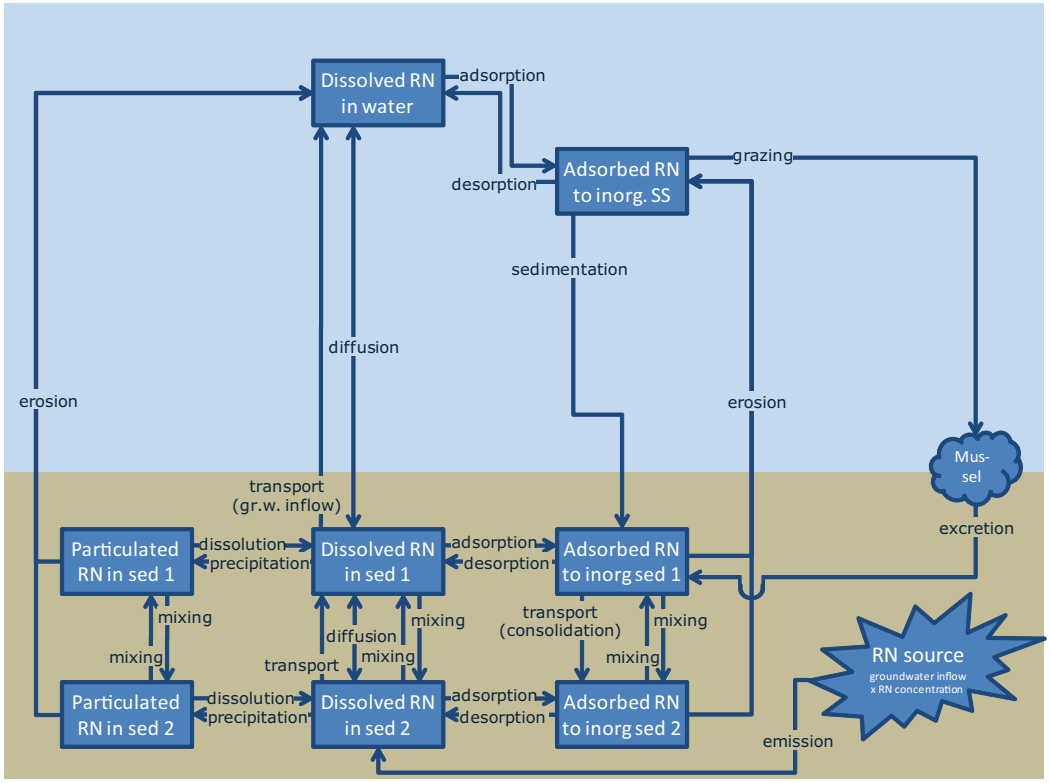


***Figure 5-1.*** *Flow of radionuclides between inorganic compartments.*

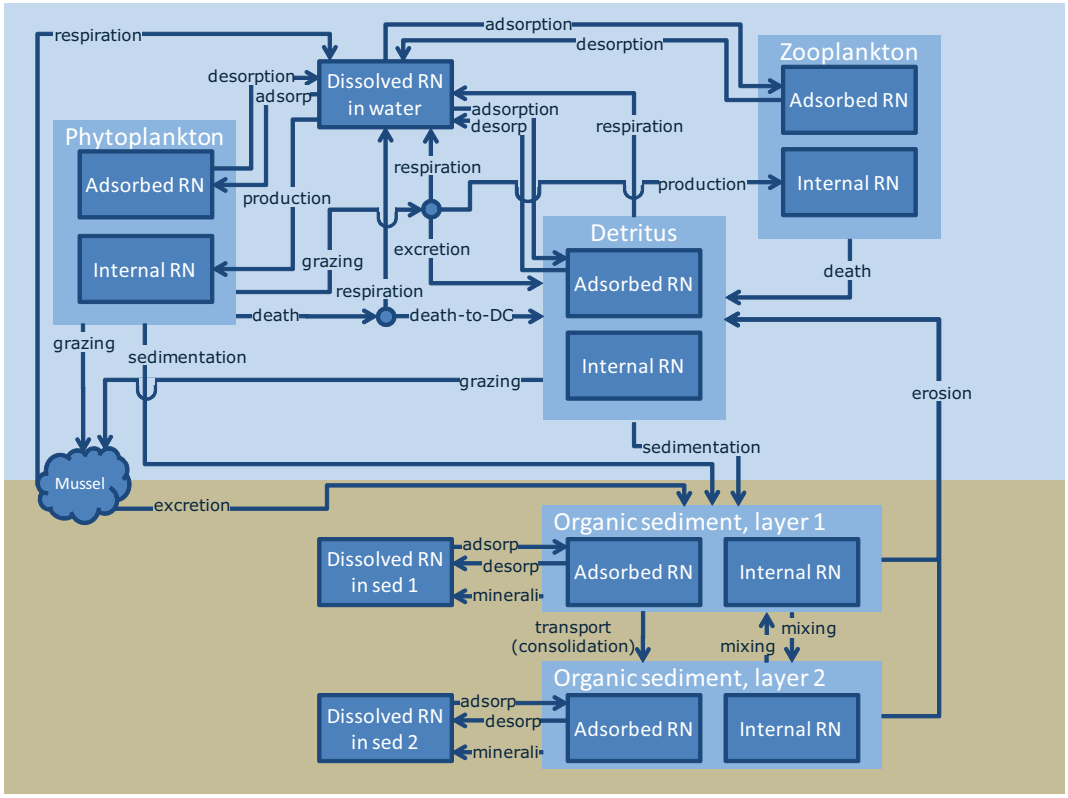


***Figure 5-2.*** *Flow of radionuclides between compartments of plankton, detritus and organic sediment.*

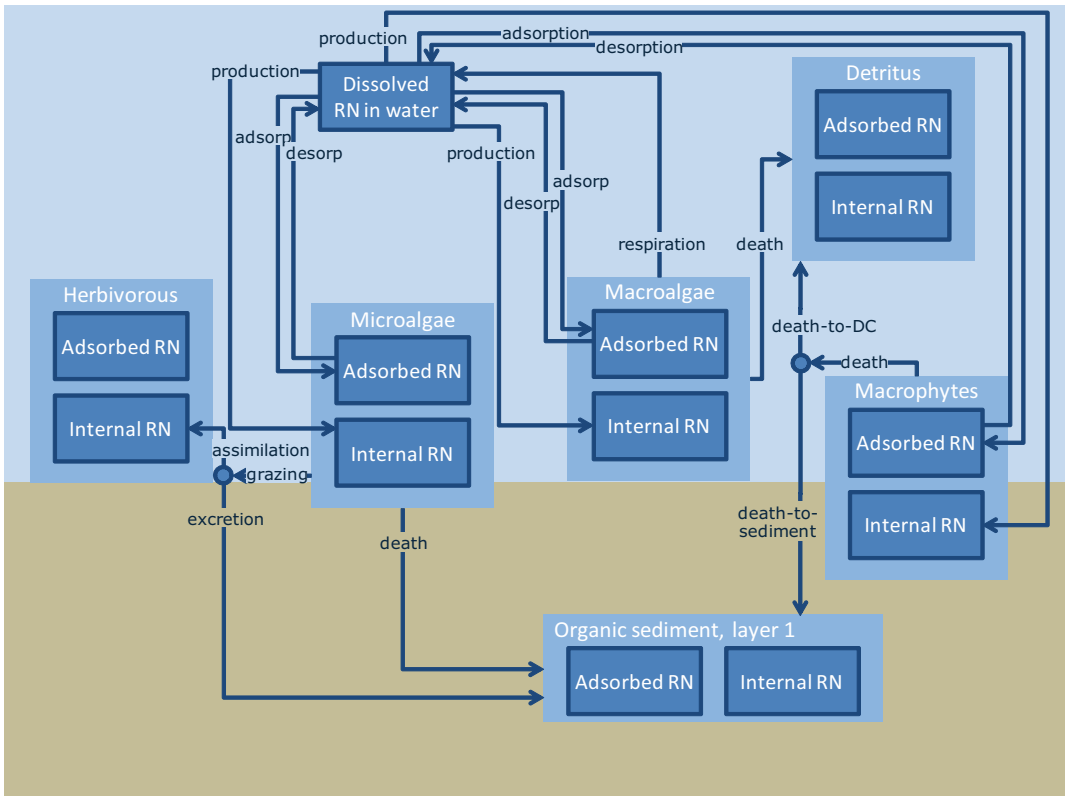


***Figure 5-3.*** *Flow of radionuclides between autotrophic compartments.*

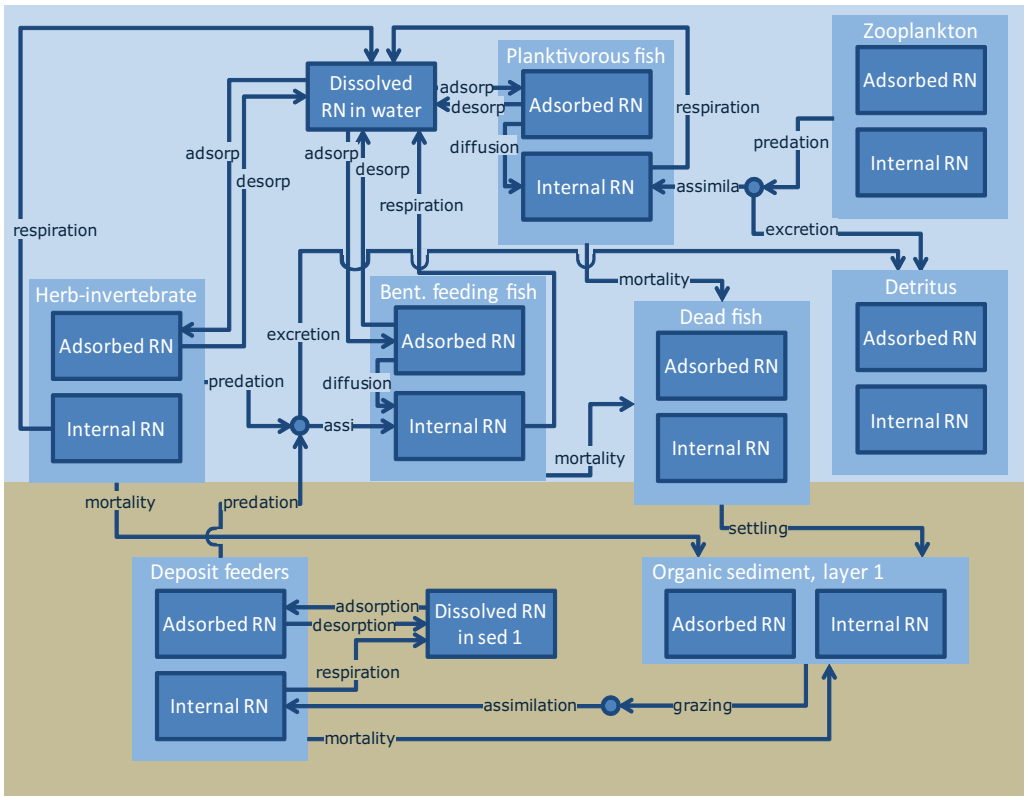


***Figure 5-4.*** *Flow of radionuclides between heterotrophic compartments.*

## 5.3 Structure of the radionuclide model

Radionuclides are introduced to the pore water of the lower sediment layer (layer 2) via groundwater inflow (Figure 5-1). From the pore-water in sediment layer 2 the dissolved radionuclide is either adsorbed to inorganic sediment (particles) or organic sediment, precipitates or is transported to the pore-water in the upper sediment layer (layer 1) driven by the groundwater inflow or due to diffusion. Analogous to processes in layer 2 sorption, precipitation and transport to the near-bed water due to diffusion or groundwater inflow takes place in sediment layer 1. Besides the transport of dissolved radionuclides from sediment layer 1 to the near-bed water radionuclides are introduced to the near-bed water via erosion of sediments and hence as dissolved (from pore water), adsorbed to inorganic or organic suspended sediments.

In the biotic components radionuclides are either adsorbed to surfaces or accumulated internally in the organisms. In the autotrophic organisms radionuclide uptake and accumulation are driven by and scaled to their photosynthetic activity. In heterotrophic organisms radionuclides are taken up through food chain by grazing or predation.

### 5.3.1 Assumptions

Processes related to diffusion, sedimentation and resuspension, mineralization, consolidation, mixing due to deposit feeder activity, uptake by plants, assimilation and excretion by animals, respiration and death follows the flow of carbon described in the ecosystem model, as shown with the example of zooplankton grazing of phytoplankton:

$$\frac{Phyt_{RNin} \cdot grazing}{PhytConc}$$

where $Phyt_{RNin}$ is the concentration of radionuclides internally in phytoplankton (g $m^{-3}$), grazing is the zooplankton grazing on phytoplankton (g $m^{-3}$ $d^{-1}$) and PhytConc is the concentration of phytoplankton (g C $m^{-3}$). The process rates and variation in state variables were not modelled explicitly in the RN model. Instead, relevant outputs from the ecosystem model were used as forcing values to drive processes and state variables in the RN model.

Some types of radionuclides are respired and excreted at a slower rate than carbon due to storage in the organism. Therefore, an option was built into the RN template to vary the rate of respiration of radionuclides by macroalgae and animals and the excretion of radionuclides by animals by a factor (between 0 and 1).

The biomass of organisms is estimated as a concentration per volume (g $m^{-3}$), but adsorption is related to the surface of an organism. Adsorption to organisms larger than phytoplankton was therefore multiplied with a volume-to-area factor, which is specific for each organismic state variable and related to the typical organisms present in the ecosystem. The biomass of organisms is estimated as a concentration per volume (g $m^{-3}$), but adsorption is related to the surface of an organism. Adsorption to organisms larger than phytoplankton was therefore multiplied with a volume-to-area factor, which is specific for each organismic state variable and related to the typical organisms present in the ecosystem (Table 5-1 to Table 5-3).

**Table 5-1. Area, volume and weight of zooplankton (Copepods), herbivorous invertebrates (Idotea and Hydrobia) and deposit feeders (divided into polychaetes and the bivalve Macoma balthica). All animals including the gills and siphons of the bivalve is assumed to have a cylindrical form. For the bivalve siphons absorption inside and outside is considered, which doubles the surface.**

| | Amount (no per animal) | Length (mm) | Diameter (mm) | Area ($mm^2$) | Volume ($mm^3$) | Weight (mg C/ $mm^3$) | Weight (mg C/ animal) | Reference |
|---|---|---|---|---|---|---|---|---|
| Zooplankton | – | 0.25 | 0.05 | 0.043 | 0.00049 | 0.07 | – | (a) |
| Herbivorous invertebrates | – | 10 | 2 | 69 | 31 | 0.07 | – | t.s. |
| Deposit feeders | – | 30 | 4 | 402 | 377 | 0.07 | – | t.s. |
| Polychaetes | | | | | | | | |
| Bivalve gills | 250 | 12 | 0.02 | 189 | – | – | 5 | t.s. |
| Bivalve siphons | 4 | 50 | 1.5 | 943 | – | – | 5 | t.s. |

References: (a) /Hernroth 1985/; t.s. calculated in this study.

**Table 5-2. Area per volume and weight of phytoplankton (Skeletonema costatum), microalgae (benthic microalgae, annual algae), perennial macroalgae (Fucus), rooted macrophytes (Potamogeton pectinatus) and fish gills (Common mackerel).**

| | Area per volume<br>Primary producers: 1/mm<br>Fish gills: $mm^2$/mg WW) | Weight<br>Primary producers: mg C/$mm^3$<br>Fish gills: mg C/mg WW | Reference |
|---|---|---|---|
| Phytoplankton | 900 | 0.07 | (b) |
| Microalgae/annual algae | 300 | 0.07 | (c), (d) |
| Perennial macroalgae | 35.0 | 0.07 | (e) |
| Rooted macrophytes | 13.4 | 0.07 | (f) |
| Fish gills | 1.16 | 0.105 | (g), (h) |

References: (b) /Hernroth 1985/; (c) /Smayda and Boleyn 1966a, b/; (d) /Smayda and Boleyn 1965/; (e) /Hernández et al. 1999/; (f) /Sand-Jensen and Borum 1991/; (g) /Wijnbladh et al. 2008/; (h) /Gray 1954/.

**Table 5-3. Area per mg carbon estimated from Table 5-1 and Table 5-2 and relative area to volume ratio, with phytoplankton as basis. For the deposit feeders the relative area to volume ratio was scaled to the biomass of (88% bivalve and 12% polychaete), from /Borgiel 2005/.**

| | Area per weight ($mm^2$/mg C) | Relative area to volume ratio |
|---|---|---|
| Phytoplankton | 12,857 | 1.0 |
| Microalgae/annual algae | 4,286 | 0.33 |
| Perennial macroalgae | 500 | 0.039 |
| Rooted macrophytes | 191 | 0.015 |
| Zooplankton | 1,257 | 0.098 |
| Herbivorous invertebrates | 31 | 0.0024 |
| Deposit feeders | (226) | (0.018) |
| Polychaetes | | |
| Bivalves | (15) | (0.0012) |
| Total | – | 0.016 |
| Fish gills | 11 | 0.00086 |

## 5.4 Detailed description of radionuclide model

### 5.4.1 General processes

Radioactive decay is considered for all compartments of radionuclides and described by a first-order process:

$$\lambda \cdot RN \qquad 5\text{-}1$$

where $\lambda$ is the decay rate ($d^{-1}$), and RN is the concentration of radionuclides (g $m^{-3}$). The decay rate is estimated from the half life of radionuclides ($T_{0.5}$, d):

$$\frac{\ln 2}{T_{0.5}} \qquad 5\text{-}2$$

#### *Sorption of radionuclides*

The degree by which radionuclides adsorb to surfaces is described by the distribution coefficient ($k_d$, l/kg). The distribution coefficient is defined as the relation between the amount of sorbed radionuclides to dissolved radionuclides i.e. the quantity of sorbed radionuclides per unit weight of solids (mg RN/kg solid) divided by the quantity of dissolved radionuclides (mg RN/l). The affinity of radionuclides to surfaces differs according to the nature of radionuclide and the surface property of solids.

We have taken a pragmatic approach and calculated partition coefficients for the organic part of marine sediments and the inorganic part, knowing that particle sizes and nature of particles such as their surface charge will differ among sediments. Briefly, using in situ data from comparable environments linear relations between organic carbon concentration in sediment (gC/kg DW) and concentration of radionuclide (or corresponding stable element) (per sediment DW) was developed and, the slope·1,000/y-intercept then represents the ratio in element affinity between organic C and inorganic sediment (see Figure 5-5).

Using such information the adsorption of radionuclides to surfaces was differentiated between inorganic and organic compartments by two different distribution coefficients, one relating to inorganic surfaces and the other relating to organic surfaces. Furthermore, a relative area to volume ratio is considered and related to the size of phytoplankton (Table 5-3).

The surfaces of detritus and inorganic suspended solids are assumed to have approximately the same size as phytoplankton. Thus, all other compartments than phytoplankton, detritus, inorganic suspended solids and organic and inorganic sediment are multiplied with a volume to area factor. This is summarized with adsorption to inorganic suspended solids and to zooplankton:

$$k_w \cdot kd_{in} \cdot 10^{-6} \cdot RN_{dis} \cdot SS_{in} \qquad 5\text{-}3$$

$$k_w \cdot kd_{oc} \cdot 10^{-6} \cdot RN_{dis} \cdot ZC \cdot area_{zc} \qquad 5\text{-}4$$

where $k_w$ is the sorption rate in water ($d^{-1}$), $kd_{in}$ the partitioning coefficient for inorganic matter ($l\ kg^{-1}$), $kd_{oc}$ the partitioning coefficient for organic carbon ($l\ kg\ C^{-1}$), $RN_{dis}$ the concentration of dissolved radionuclides in water ($g\ RN\ m^{-3}$), $SS_{in}$ the concentration of inorganic suspended solids ($g\ m^{-3}$), ZC the concentration of zooplankton ($g\ m^{-3}$), and $area_{zc}$ the zooplankton specific volume-to-area-factor (lenght).

Sorption rates are slower in the sediment compared to sorption processes in water. Therefore, sorption processes were differentiated between processes taking place in the sediment and water as shown with the two examples of desorption of radionuclides from surfaces of zooplankton and inorganic sediment:

$$k_w \cdot ZC_{XRN} \cdot areazc \qquad 5\text{-}5$$

$$k_s \cdot Sin1_{XRN} \qquad 5\text{-}6$$

where $k_w$ and $k_s$ is the sorption rate in water and sediment, respectively ($d^{-1}$), $ZC_{XRN}$ the concentration of radionuclides adsorbed to zooplankton ($g\ m^{-3}$), $Sin_{XRN}$ the concentration of radionuclides adsorbed to inorganic sediment layer 1 ($g\ m^{-2}$), and areazc the zooplankton specific volume-to-area-factor (dimensionless).

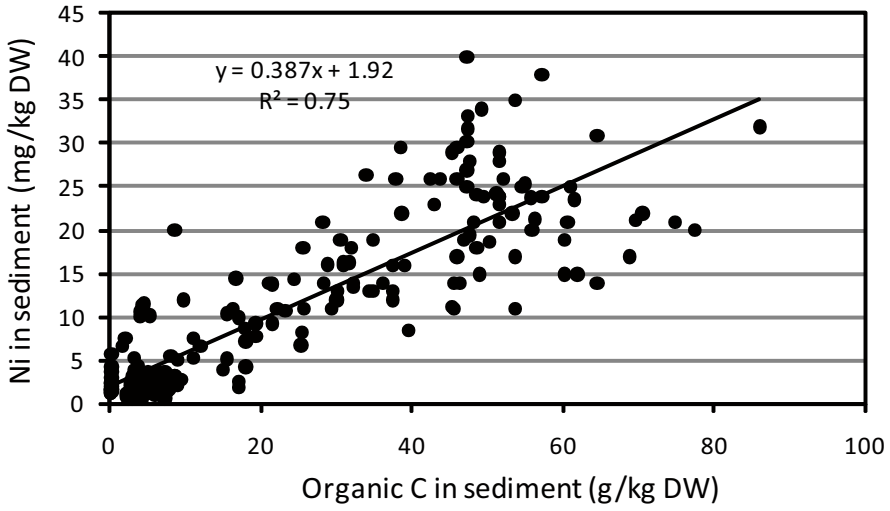


***Figure 5-5.*** *Linear regression between sediment organic carbon concentration and Ni concentration in surface sediment from Danish estuaries and coastal waters. Relative affinity of Ni to organic C in sediment is expressed by the slope, while the intercept 1.92 represents the relative affinity to the inorganic sediment fraction.*

**Table 5-4. Values used in the model scenarios of radionuclide half-life, organic carbon partitioning coefficient ($Kd_c$) and inorganic partitioning coefficient ($Kd_{in}$). For comparison, Kd values recommended by the International Atomic Energy Agency /IAEA 2004/, Kd values used in an earlier study (a) /Kumblad and Kautsky 2004/ and Kd values for particulate matter (b) and for sediment layer 1 (c) in the landscape dose model /Nordén et al. 2010/ are also shown.**

| RN | Half-life (y) | $Kd_{oc}$ ($m^3$/kg C) | $Kd_{in}$ ($m^3$/kg DW) | $K_d$-IAEA ---- ($m^3$/kg DW) ---- | $K_d$ a) | $K_d$ b) ---- ($m^3$/kg DW) ---- | $K_d$ c) |
|---|---|---|---|---|---|---|---|
| C-14 | 5.73E+03 | 0 | 0 | 1 | 0 | 0 | 0 |
| Cl-36 | 3.01E+05 | 6.0E-05 | 2.0E-05 | 3.0E-05 | 0.03 | 0.001 | 0.01 |
| Cs-135 | 2.30E+06 | 20 | 0.13 | 4.00 | 1.00 | 11 | 22 |
| Nb-94 | 2.03E+04 | 4 | 0.50 | 800 | 500 | 196 | 85 |
| Ni-59 | 7.60E+04 | 2.13 | 0.015 | 20 | 100 | 14 | 8.2 |
| Ra-226 | 1.60E+03 | 10 | 0.050 | 2.00 | 5.00 | 4 | 2.5 |
| Th-230 | 7.54E+04 | 417 | 1.67 | 3.0E+03 | 2.0E+03 | 995 | 97 |

### 5.4.2 Uptake of radionuclides in primary producers

Besides adsorption and desorption the flow of radionuclides related to primary producers is controlled by primary production, respiration and death. The uptake of radionuclides due to primary production incorporates the radionuclides internally in the primary producer as shown below for macroalgae:

$$\frac{RN_{dis} \cdot prbc}{BC} \qquad 5\text{-}7$$

where $RN_{dis}$ is dissolved radionuclides in the water (g $m^{-3}$), prbc is the macroalgae primary production (g C $m^{-2}$ $d^{-1}$) and BC the biomass of macroalgae (g C $m^{-2}$).

Many macroalgae such as fucoids can accumulate radionuclides in to high concentrations and in contrast to the other primary producers modelled in the ecosystem model the respiration of radionuclides for macroalgae are scaled with a factor:

$$\frac{BC_{INRN} \cdot rebc \cdot frep}{BC} \qquad 5\text{-}8$$

where $BC_{INRN}$ is the concentration of radionuclides internally in macroalgae (g $m^{-3}$), rebc the macroalgae respiration of carbon (g C $m^{-2}$ $d^{-1}$), BC the biomass of macroalgae (g C $m^{-2}$), and frep the fraction of radionuclides "respired" by macroalgae (dimensionless). The factor for regulation is allowed to vary between 0 and 1. In the model execution only accumulation is considered, i.e. frep is fixed at zero.

### 5.4.3 Uptake of radionuclides in herbivores and predators

Radionuclides related to herbivores and predators via adsorption and desorption are incorporated in the organisms by grazing or predation. The assimilation of radionuclides is a function of the amount consumed minus the amount respired and excreted. For herbivores and predators storage of radionuclides decreases the amount of radionuclide respired and excreted. Therefore, a factor for regulation of respiration and excretion is included in the processes, and is similar to the procedure described for the macroalgae above.

### 5.4.4 Temporal and spatial variation in BCF

The bioconcentration factor (BCF, L $(kg\ C)^{-1}$) of radionuclides is defined as the concentration of radionuclides associated to a biotic component in relation to the concentration of radionuclides in water as illustrated with the zooplankton bioconcentration factor:

$$\frac{ZC_{RN}}{ZC}\frac{1}{RN_{dis}}10^6 \qquad 5\text{-}9$$

where, $RN_{dis}$ is dissolved radionuclides (mg RN $l^{-1}$), $ZC_{RN}$ the radionuclides related to zooplankton (mg RN $l^{-1}$) and ZC the concentration of zooplankton (mg C $l^{-1}$). Thus BCF characterizes the accumulation of radionuclides in the biotic components.

## 5.5 Detailed flow of radionuclides

The RN model is dependent on process rates and concentration of state variables described in the ecosystem model. These parameters are used as forcings in the RN model and symbolised with a "F_".

### 5.5.1 Dissolved radionuclides in sediment pore water

***Dissolved radionuclides in pore water in "lower sediment layer"***

An accidental release of radionuclides from the final geological repository of spent nuclear fuel is introduced to the marine environment through groundwater inflow in the sediment. The concentration of dissolved radionuclides in the sediment pore water of model layer 2 (lowest layer) is described by (Figure 5-1 to Figure 5-4):

*+emission –transport –decay –adsorption +desorption +mineralisation –diffusion +dissolution –precipitation +mixing1 –mixing2*

Groundwater inflow through the sediment causes an emission of dissolved radionuclides from the source to sediment pore water in model layer 2 and a further transport of dissolved radionuclides from model layer 2 to surface sediment, i.e. model layer 1 (emisou and tragw2, g RN m–2 d–1), described by:

$$\text{emisou} = \text{RN}_{\text{source}} \cdot \text{GW} \qquad 5\text{-}10$$

$$\text{tragw2} = \frac{\text{RN}_{\text{dis2}} \cdot \text{GW}}{\text{dzs2}} \qquad 5\text{-}11$$

where $RN_{source}$ is the source of radionuclides in sediment pore water layer 2 (g RN $m^{-3}$), $RN_{dis2}$ the concentration of radionuclides in pore water sediment layer 2 (g RN $m^{-2}$), GW the inflow of groundwater (m $d^{-1}$) and dzs2 the thickness of sediment layer 2 (m).

Decay of dissolved radionuclides in sediment pore water layer 2 (dksed2, g RN $m^{-2}$ $d^{-1}$) is described according to Equation 5-1. Adsorption and desorption of radionuclides related to the surfaces of inorganic and organic sediment layer 2 is described by (adssrn2 and dessrn2, g RN $m^{-2}$ $d^{-1}$):

$$\text{adssrn2} = \text{adsin2} + \text{adssoc2} \qquad 5\text{-}12$$

$$\text{dessrn2} = \text{desin2} + \text{dessoc2} \qquad 5\text{-}13$$

where the processes of adsorption and desorption is described under the relevant sections (Sections 5.5.15 and 5.5.16).

Mineralisation of organic sediment layer 2 (minsoca2, g RN $m^{-2}$ $d^{-1}$) increases the concentration of dissolved radionuclides in the sediment pore water. The process of mineralisation is described under the sections of adsorbed and internal radionuclides in organic sediment layer 2 (Section 5.5.16). Diffusion of dissolved radionuclides between sediment pore water layer 2 and 1 (difa2, g RN $m^{-2}$ $d^{-1}$) is described by:

$$\text{difa2} = \text{difw} \cdot \text{fbiot} \cdot \left( \frac{\frac{\text{RN}_{\text{dis2}}}{\text{dzs2} \cdot \text{pors2}} - \frac{\text{RN}_{\text{dis1}}}{\text{dzs1} \cdot \text{pors1}}}{\text{dzs2}} \right) \qquad 5\text{-}14$$

where $RN_{dis1}$ and $RN_{dis2}$ is the concentration of dissolved radionuclides in sediment pore water layer 1 and 2 (g RN $m^{-2}$), dzs1 and dzs2 the thickness of sediment layer 1 and 2 (m), pors1 and pors2 the

porosity of sediment layer 1 and 2 ($m^3_{H2O}$ $m^{-3}_{bulk}$), difw the diffusion coefficient of radionuclides ($m^2$ $d^{-1}$) and fbiot is a factor for diffusion due to bioturbation (m $d^{-1}$), described by:

$$fbiot = kf_{biot} \cdot \frac{F\_DO_{WB}}{F\_DO_{WB} + kh_{DOwb}} \cdot \frac{F\_DFC}{F\_DFC + kh_{DFC}} \quad 5\text{-}15$$

where $kf_{biot}$ is the diffusion rate due to bioturbation (dimensionless), $kh_{DOwb}$ the half saturation concentration for processes related to dissolved oxygen in the water bed (g $O_2$ $m^{-3}$), $kh_{DFC}$ the half saturation constant for processes related to sediment deposit feeder carbon (g C $m^{-2}$) and the ecosystem model outputs of $F\_DO_{WB}$ is the concentration of dissolved oxygen in the water bed (g $O_2$ $m^{-3}$) and F_DFC the mass of deposit feeder carbon (g C $m^{-2}$).

Precipitation and dissolution of radionuclides in sediment pore water layer 2 (prec2 and diss2, g RN $m^{-2}$ $d^{-1}$) is described under the section of precipitated radionuclides in layer 2 (Section 5.5.17). Mixing of the sediment due to invertebrate consumption leads to a downward and an upward mixing of dissolved radionuclides between sediment pore water layer 1 and 2 (mixs1 and mixs2, g RN $m^{-2}$ $d^{-1}$), described by:

$$mixs1 = k_{mixdown} \cdot RN_{Sed1} \frac{F\_DO_{WB}}{F\_DO_{WB} + kh_{DOwb}} \cdot \frac{F\_DFC}{F\_DFC + kh_{DFC}} \quad 5\text{-}16$$

$$mixs2 = k_{mixup} \cdot RN_{Sed2} \frac{F\_DO_{WB}}{F\_DO_{WB} + kh_{DOwb}} \cdot \frac{F\_DFC}{F\_DFC + kh_{DFC}} \quad 5\text{-}17$$

where $RN_{Sed1}$ and $RN_{Sed2}$ are the concentration of radionuclides in sediment pore water layer 1 and 2 (g RN $m^{-2}$), $k_{mixdown}$ and $k_{mixup}$ are the downward and upward mixing rates due to invertebrate consumption ($d^{-1}$), $kh_{DOwb}$ the half saturation concentration for processes related to dissolved oxygen in the water bed (g $O_2$ $m^{-3}$), $kh_{DFC}$ the half saturation constant for processes related to sediment deposit feeder carbon (g C $m^{-2}$) and the ecosystem model outputs of $F\_DO_{WB}$ is the concentration of dissolved oxygen in the water bed (g $O_2$ $m^{-3}$) and F_DFC the mass of deposit feeder carbon (g C $m^{-2}$).

#### *Dissolved radionuclides in sediment pore water of surface sediment layer*

The concentration of dissolved radionuclides in the sediment pore water layer 1 is described by (Figure 5-1 to Figure 5-4):

*–decay ±transport –adsorption +desorption + mineralisation ±diffusion +dissolution –precipitation +respiration –mixing1 +mixing2*

Decay of dissolved radionuclides in sediment pore water layer 1 (dksed1, g RN $m^{-2}$ $d^{-1}$) is described according to Equation 5-1. Groundwater inflow through the sediment causes a transport of dissolved radionuclides from sediment pore water layer 2 to layer 1 and an outflow from layer 1 to the water bed (tragw2 and tragw1, g RN $m^{-2}$ $d^{-1}$). The transport from layer 2 to layer 1 is earlier described in this section (Equation 5-11). The outflow from layer 1 to the water bed is described by:

$$tragw1 = \frac{RN_{dis1} \cdot GW}{dzs1} \quad 5\text{-}18$$

where dzs1 is the thickness of sediment layer 1 (m), $RN_{dis1}$ the concentration of radionuclides in pore water sediment layer 1 (g RN $m^{-2}$) and GW the inflow of groundwater (m $d^{-1}$).

Adsorption and desorption of radionuclides related to the surfaces of inorganic sediment layer 1, organic sediment layer 1 and deposit feeders are described by (adssrn1 and dessrn1, g RN $m^{-2}$ $d^{-1}$):

$$adssrn1 = adsin1 + adssoc1 + adsdfc \quad 5\text{-}19$$

$$dessrn1 = desin1 + dessoc1 + desdfc \quad 5\text{-}20$$

where the processes of adsorption and desorption is described under the relevant sections (Sections 5.5.11, 5.5.15 and 5.5.16).

Mineralisation of organic sediment layer 1 (minsoca1, g RN $m^{-2}$ $d^{-1}$) increases the concentration of dissolved radionuclides in the sediment pore water. The process of mineralisation is described under the sections of adsorbed and internal radionuclides in organic sediment layer 1 (Section 5.5.16).

Diffusion of dissolved radionuclides between sediment pore water layer 2 and 1 (difa2, g RN $m^{-2}$ $d^{-1}$) is earlier described in this section (Equation 5-14). Diffusion of dissolved radionuclides from sediment pore water layer 1 to the bottom water (difa1, g RN $m^{-2}$ $d^{-1}$) is described by:

$$\text{difa1} = \text{difw} \cdot \text{fbiot} \cdot \text{F\_fdbl1} \cdot \left( \frac{\frac{\text{RN}_{\text{dis1}}}{\text{dzs1} \cdot \text{pors1}} - \text{RN}_{\text{dis}}}{\text{dzs1}} \right) \qquad 5\text{-}21$$

where $RN_{dis}$ and $RN_{dis1}$ are the concentrations of dissolved radionuclides in water and sediment pore water layer 1 (g RN $m^{-3}$ and g RN $m^{-2}$), dzs1 the thickness of sediment layer 1 (m), pors1 the porosity of sediment layer 1 ($m^3_{H2O}$ $m^{-3}_{bulk}$), difw the diffusion coefficient of radionuclides ($m^2$ $d^{-1}$), F_fdbl1 the change in diffusion between water and sediment due to current and waves (dimensionless) and fbiot a factor for diffusion due to bioturbation (Equation 5-15, m $d^{-1}$).

Precipitation and dissolution of radionuclides in sediment pore water layer 1 (prec1 and diss1, g RN $m^{-2}$ $d^{-1}$) is described under the section of precipitated radionuclides in layer 1 (Section 5.5.17). Radionuclides are released to sediment pore water layer 1 due to respiration by deposit feeders (redfci, g RN $m^{-2}$ $d^{-1}$), described under the section for internal radionuclides in deposit feeders (Section 5.5.11). Mixing of the sediment due to invertebrate consumption leads to a downward and an upward mixing of dissolved radionuclides between sediment pore water layer 1 and 2 (mixs1 and mixs2, g RN $m^{-2}$ $d^{-1}$), earlier described in this section (Equation 5-16 and 5-17).

### 5.5.2 Dissolved radionuclides in water column

The concentration of dissolved radionuclides in the water column is described by (Figure 5-1 to Figure 5-4):

*–decay +transport –adsorption +desorption +diffusion +erosion –production +respiration*

Decay of dissolved radionuclides in the water column (dksrn, g RN $m^{-3}$ $d^{-1}$) is described according to Equation 5-1. Groundwater inflow through the sediment causes a transport of dissolved radionuclides from sediment pore water in layer 1 to the water (tragw, g RN $m^{-3}$ $d^{-1}$):

$$\text{tragw} = \frac{\text{tragw1}}{\text{dz}} \qquad 5\text{-}22$$

where tragw1 is inflow of dissolved radionuclides per area (Equation 5-8, g RN $m^{-2}$ $d^{-1}$) and dz the water layer height (m).

Adsorption and desorption of radionuclides related to the surfaces of inorganic suspended solids, phytoplankton, detritus, zooplankton, planktivorous fish, benthic feeding fish, microalgae, macroalgae, macrophytes and herbivorous invertebrates (adssrn and dessrn, g RN $m^{-3}$ $d^{-1}$) is described by:

$$\text{adssrn} = \text{adsin} + \text{adspc} + \text{adsdc} + \text{adszc} + \text{adsfcp} + \text{adsfcb} + \left( \frac{\text{adsbdc} + \text{adsbc} + \text{adsec} + \text{adshc}}{\text{dz}} \right) \qquad 5\text{-}23$$

$$\text{dessrn} = \text{desin} + \text{despc} + \text{desdc} + \text{deszc} + \text{desfcp} + \text{desfcb} + \left( \frac{\text{desbdc} + \text{desbc} + \text{desec} + \text{deshc}}{\text{dz}} \right) \qquad 5\text{-}24$$

where dz is the water layer height (m) and the processes of adsorption and desorption is described under the relevant sections (Sections 5.5.3 to 5.5.10 and 5.5.12 to 5.5.13).

Diffusion of dissolved radionuclides from sediment pore water layer 1 to the bottom water (difv, g RN $m^{-3}$ $d^{-1}$) is described by:

$$difv = \frac{difa1}{dz} \qquad 5\text{-}25$$

where difa1 is diffusion of radionuclides per area (Equation 5-21, g RN $m^{-2}$ $d^{-1}$) and dz the water layer height (m).

Erosion of precipitated radionuclides adds to the pool of dissolved radionuclides in water due to dissolution (eroprn, g RN $m^{-3}$ $d^{-1}$) which is the sum of erosion of precipitated radionuclides from sediment layer 1 and 2 divided by the water layer height (dz, m). The erosion of precipitated radionuclides is described under sections for precipitated radionuclides in sediment layer 1 and 2 (Section 5.5.17).

Radionuclides are incorporated internally in the autotrophic organisms due to primary production of phytoplankton, microalgae, macroalgae and macrophytes (prpci, prbdcim3, prbcim3 and precim3, g RN $m^{-3}$ $d^{-1}$), which is described under the relevant sections (Sections 5.5.4 and 5.5.6 to 5.5.8). However, the primary production of microalgae, macroalgae and macrophytes are converted to "per volume" by dividing the processes with the water layer height (dz, m).

Radionuclides are released to the water due to respiration of detritus, zooplankton, mussels, planktivorous fish, benthic feeding fish, herbivorous invertebrates and macroalgae. The respiration of detritus (redca and redci, g RN $m^{-3}$ $d^{-1}$), zooplankton (rezca and rezci, g RN $m^{-3}$ $d^{-1}$), planktivorous and benthic feeding fish (refcpi and refcbi, g RN $m^{-3}$ $d^{-1}$) are described under the associated sections (Sections 5.5.5, 5.5.9, 5.5.12 and 5.5.13). Also the respiration of macroalgae (rebca and rebci, g RN $m^{-2}$ $d^{-1}$) and herbivorous invertebrates (rehci, g RN $m^{-2}$ $d^{-1}$) are described in the associated sections (Section 5.5.7 and 5.5.10), but with the respiration converted to "per volume" by dividing with the water layer height (dz, m). The respiration by mussels (remca and remci, g RN $m^{-3}$ $d^{-1}$) is described under the sections for adsorbed and internal radionuclides related to organic sediment layer 1 (Section 5.5.16).

Death of phytoplankton causes transfer of adsorbed and internal radionuclides to detritus. However, at phytoplankton death a part is leaked (respirated) immediately as dissolved substances, and thus phytoplankton death also adds to the pool of dissolved radionuclides. The respiration due to phytoplankton death (repca and repci, g RN $m^{-3}$ $d^{-1}$) is described as the difference between the death of phytoplankton and the part that is transferred to detritus (repca = depca-depc2dca and repci = depci-depc2dci, g RN $m^{-3}$ $d^{-1}$). The death of phytoplankton (depca and depci, g RN $m^{-3}$ $d^{-1}$) and the transfer of dead phytoplankton to detritus (depc2dca and depc2dci, g RN $m^{-3}$ $d^{-1}$) is described under the section of phytoplankton and detritus (Sections 5.5.4 and 5.5.5).

### 5.5.3 Inorganic suspended solid adsorbed radionuclides

The amount of radionuclides adsorbed to inorganic suspended solids is described by (Figure 5-1):

*–decay +adsorption –desorption –sedimentation +erosion –filtration*

Decay of radionuclides adsorbed to inorganic suspended solids (dkssin, g RN $m^{-3}$ $d^{-1}$) is described according to Equation 5-1. Adsorption of radionuclides to inorganic suspended solids (adsin, g RN $m^{-3}$ $d^{-1}$) is described by:

$$adsin = k_w \cdot kd_{in} \cdot 10^{-6} \cdot RN_{dis} \cdot F\_SSin \qquad 5\text{-}26$$

where $k_w$ is the sorption rate in water ($d^{-1}$), $kd_{in}$ the partitioning coefficient for inorganic matter (l $kg^{-1}$), $RN_{dis}$ the concentration of dissolved radionuclides in water (g RN $m^{-3}$) and F_SSin the ecosystem model output of the concentration of inorganic suspended solids (g $m^{-3}$). Desorption of radionuclides from inorganic suspended solids (desin, g RN $m^{-3}$ $d^{-1}$) follows:

$$desin = k_w \cdot SSin_{XRN} \qquad 5\text{-}27$$

where $k_w$ is the sorption rate in water ($d^{-1}$) and $SSin_{XRN}$ the concentration of radionuclides adsorbed to inorganic suspended solids (g RN $m^{-3}$).

Sedimentation of radionuclides adsorbed to inorganic suspended solids is described by a general sedimentation in the water column (sedin, g RN $m^{-3}$ $d^{-1}$). However, at the water bed (WB, the bottom layer in connection with the sediment) a different sedimentation is considered, therefore the general sedimentation in the water column is subtracted from this layer (sedincomp, g RN $m^{-3}$ $d^{-1}$) and a deposition from the layer to the sediment is considered instead (sedinWB, g RN $m^{-3}$ $d^{-1}$):

$$\text{sedin} = \frac{\text{SSin}_{\text{XRN}} \cdot \text{F\_sed}_{\text{SSin-WC}}}{\text{F\_SSin}} \qquad 5\text{-}28$$

$$\text{sedincomp} = \frac{\text{SSin}_{\text{XRN}} \cdot \text{F\_compsed}_{\text{SSin-WB}}}{\text{F\_SSin}} \qquad 5\text{-}29$$

$$\text{sedinWB} = \frac{\text{SSin}_{\text{XRN}} \cdot \text{F\_sed}_{\text{SSin-WB}}}{\text{F\_SSin}} \qquad 5\text{-}30$$

where $SSin_{XRN}$ is the concentration of radionuclides adsorbed to inorganic suspended solids (g RN $m^{-3}$), and the ecosystem model outputs of F_SSin is the concentration of inorganic suspended solids (g $m^{-3}$), $F\_sed_{SSin-WC}$, $F\_compsed_{SSin-WB}$ and $F\_sed_{SSin-WB}$ the sedimentation of inorganic suspended solids in the water column, compensation in the water bed and deposition on the sediment from the water bed, respectively (g $m^{-3}$ $d^{-1}$).

Erosion of radionuclides adsorbed to inorganic sediment layer 1 and 2 adds to the concentration of radionuclides adsorbed to inorganic suspended solids (eroin, g RN $m^{-3}$ $d^{-1}$) and is described as the sum of erosion from sediment layer 1 and 2 (eroin1+eroin2, g RN $m^{-2}$ $d^{-1}$):

$$\text{eroin} = \frac{(\text{eroin1} + \text{eroin2})}{\text{dz}} \qquad 5\text{-}31$$

where dz is the thickness of the water layer (m), and eroin1 and eroin2 is described under the sections for radionuclides adsorbed to inorganic sediment layer 1 and 2, respectively (Section 5.5.15).

Mussel filtration and excretion activities causes a transport of radionuclides adsorbed to inorganic suspended solids (grmin, g RN $m^{-3}$ $d^{-1}$) to the sediment inorganic layer 1:

$$\text{grmin} = \frac{\text{SSin}_{\text{XRN}} \cdot \text{F\_grm}_{\text{SSin}}}{\text{F\_SSin}} \qquad 5\text{-}32$$

where $SSin_{XRN}$ is the concentration of radionuclides adsorbed to inorganic suspended solids (g RN $m^{-3}$), and the ecosystem model outputs of F_SSin is the concentration of inorganic suspended solids (g $m^{-3}$) and $Fgrm_{SSin}$ the mussel filtration of inorganic suspended solids (g $m^{-3}$ $d^{-1}$).

### 5.5.4 Phytoplankton

#### *Adsorbed radionuclides*

The amount of radionuclides adsorbed to phytoplankton is described by (Figure 5-2):

*–decay +adsorption –desorption –sedimentation –death –grazing –filtration*

Decay of radionuclides adsorbed to phytoplankton (dkpca, g RN $m^{-3}$ $d^{-1}$) is described according to Equation 5-1. Adsorption of radionuclides to phytoplankton (adspc, g RN $m^{-3}$ $d^{-1}$) is described by:

$$\text{adspc} = k_w \cdot kd_{oc} \cdot 10^{-6} \cdot RN_{dis} \cdot \text{F\_PC} \qquad 5\text{-}33$$

where $k_w$ is the sorption rate in water ($d^{-1}$), $kd_{oc}$ the partitioning coefficient for organic carbon (l $kgC^{-1}$), $RN_{dis}$ the concentration of dissolved radionuclides in water (g RN $m^{-3}$) and F_PC the ecosystem model output of the concentration of phytoplankton carbon (g C $m^{-3}$). Desorption of radionuclides from phytoplankton (despc, g RN $m^{-3}$ $d^{-1}$) follows:

$$\text{despc} = k_w \cdot PC_{XRN} \qquad 5\text{-}34$$

where $k_w$ is the sorption rate in water ($d^{-1}$) and $PC_{XRN}$ the concentration of radionuclides adsorbed to phytoplankton (g RN $m^{-3}$).

Sedimentation of radionuclides adsorbed to phytoplankton is described by a general sedimentation in the water column (sedpca, g RN $m^{-3}$ $d^{-1}$). However, at the water bed a different sedimentation is considered, therefore the general sedimentation in the water column is subtracted from this layer (sedpcacomp, g RN $m^{-3}$ $d^{-1}$) and deposition from the bottom water to the sediment is considered instead (sedpcaWB, g RN $m^{-3}$ $d^{-1}$):

$$\text{sedpca} = \frac{PC_{XRN} \cdot F\_sed_{PC\text{-}WC}}{F\_PC} \quad 5\text{-}35$$

$$\text{sedpcacomp} = \frac{PC_{XRN} \cdot F\_compsed_{PC\text{-}WB}}{F\_PC} \quad 5\text{-}36$$

$$\text{sedpcaWB} = \frac{PC_{XRN} \cdot F\_sed_{PC\text{-}WB}}{F\_PC} \quad 5\text{-}37$$

where $PC_{XRN}$ is the concentration of radionuclides adsorbed to phytoplankton (g RN $m^{-3}$) and the ecosystem model output of F_PC is the concentration of phytoplankton carbon (g C $m^{-3}$), $F\_sed_{PC\text{-}WC}$, $F\_compsed_{PC\text{-}WB}$ and $F\_sed_{PC\text{-}WB}$ the sedimentation of phytoplankton carbon in the water column, compensation in the water bed and deposition on the sediment from the water bed, respectively (g C $m^{-3}$ $d^{-1}$).

Loss of radionuclides adsorbed to phytoplankton due to death of phytoplankton, zooplankton grazing and mussel filtration (depca, grpca and grmpca, g RN $m^{-3}$ $d^{-1}$) is described by:

$$\text{depca} = \frac{PC_{XRN} \cdot F\_depc}{F\_PC} \quad 5\text{-}38$$

$$\text{grpca} = \frac{PC_{XRN} \cdot F\_grpc}{F\_PC} \quad 5\text{-}39$$

$$\text{grmpca} = \frac{PC_{XRN} \cdot F\_grmpc}{F\_PC} \quad 5\text{-}40$$

where $PC_{XRN}$ is the concentration of radionuclides adsorbed to phytoplankton (g RN $m^{-3}$), and the ecosystem model outputs of F_PC is the concentration of phytoplankton carbon (g C $m^{-3}$) and F_depc, F_grpc and F_grmpc the phytoplankton death, zooplankton grazing and mussel filtration, respectively (g C $m^{-3}$ $d^{-1}$).

### *Internal radionuclides*

The amount of radionuclides internal in phytoplankton is described by (Figure 5-2):

*–decay +production –sedimentation –death –grazing –filtration*

Decay of radionuclides internal in phytoplankton (dkpci, g RN $m^{-3}$ $d^{-1}$) is described according to Equation 5-1. Radionuclides are incorporated internally in phytoplankton due to primary production (prpci, g RN $m^{-3}$ $d^{-1}$) following:

$$\text{prpci} = \frac{RN_{dis} \cdot F\_prpc}{F\_PC} \quad 5\text{-}41$$

where $RN_{dis}$ is the concentration of dissolved radionuclides (g RN $m^{-3}$) and the ecosystem model outputs of F_PC is the concentration of phytoplankton carbon (g C $m^{-3}$) and F_prpc, the phytoplankton primary production (g C $m^{-3}$ $d^{-1}$).

Sedimentation of radionuclides internal in phytoplankton is similar to the sedimentation of radionuclides adsorbed to phytoplankton (Equation 5-35 to 5-37), only the concentration of radionuclides is exchanged with the internal concentration of radionuclides ($PC_{INRN}$, g RN $m^{-3}$). Also loss of radionuclides internal in phytoplankton due to death of phytoplankton, zooplankton grazing and mussel filtration (depci, grpci and grmpci, g RN $m^{-3}$ $d^{-1}$) are similar to the equations for radionuclides adsorbed to phytoplankton (Equation 5-38 to 5-40), again with the adsorbed radionuclides replaced with internal concentration of radionuclides ($PC_{INRN}$, g RN $m^{-3}$).

### 5.5.5 Detritus

#### *Adsorbed radionuclides*

The amount of radionuclides adsorbed to detritus is described by (Figure 5-2):

*–decay +adsorption –desorption –sedimentation +erosion –respiration + death –filtration +excretion*

Decay of radionuclides adsorbed to detritus (dkdca, g RN $m^{-3}$ $d^{-1}$) is described according to Equation 5-1. Adsorption of radionuclides to detritus (adsdc, g RN $m^{-3}$ $d^{-1}$) is described by:

$$\text{adsdc} = k_w \cdot kd_{oc} \cdot 10^{-6} \cdot RN_{dis} \cdot F\_DC \qquad 5\text{-}42$$

where $k_w$ is the sorption rate in water ($d^{-1}$), $kd_{oc}$ the partitioning coefficient for organic carbon (l $kgC^{-1}$), $RN_{dis}$ the concentration of dissolved radionuclides in water (g RN $m^{-3}$) and F_DC the ecosystem model output of the concentration of detritus carbon (g C $m^{-3}$). Desorption of radionuclides from the surface of detritus (desdc, g RN $m^{-3}$ $d^{-1}$) follows:

$$\text{desdc} = k_w \cdot DC_{XRN} \qquad 5\text{-}43$$

where $k_w$ is the sorption rate in water ($d^{-1}$) and $DC_{XRN}$ the concentration of radionuclides adsorbed to detritus (g RN $m^{-3}$).

Sedimentation of radionuclides adsorbed to detritus is described by a general sedimentation in the water column (seddca, g RN $m^{-3}$ $d^{-1}$). However, at the water bed a different sedimentation is considered, therefore the general sedimentation in the water column is subtracted from this layer (seddcacomp, g RN $m^{-3}$ $d^{-1}$) and deposition from the bottom water to the sediment is considered instead (seddcaWB, g RN $m^{-3}$ $d^{-1}$):

$$\text{seddca} = \frac{DC_{XRN} \cdot F\_sed_{DC\text{-}WC}}{F\_DC} \qquad 5\text{-}44$$

$$\text{seddcacomp} = \frac{DC_{XRN} \cdot F\_compsed_{DC\text{-}WB}}{F\_DC} \qquad 5\text{-}45$$

$$\text{seddcaWB} = \frac{DC_{XRN} \cdot F\_sed_{DC\text{-}WB}}{F\_DC} \qquad 5\text{-}46$$

where $DC_{XRN}$ is the concentration of radionuclides adsorbed to detritus (g RN $m^{-3}$), and the ecosystem model outputs of F_DC is the concentration of detritus carbon (g C $m^{-3}$), $F\_sed_{DC\text{-}WC}$, $F\_compsed_{DC\text{-}WB}$ and $F\_sed_{DC\text{-}WB}$ the sedimentation of detritus carbon in the water column, compensation in the water bed and deposition on the sediment from the water bed, respectively (g C $m^{-3}$ $d^{-1}$).

Erosion of radionuclides adsorbed to organic sediment layer 1 and 2 adds to the concentration of radionuclides adsorbed to detritus (erosoca, g RN $m^{-3}$ $d^{-1}$) and is described as the sum of erosion from sediment layer 1 and 2 (erosoca1+erosoca2, g RN $m^{-2}$ $d^{-1}$):

$$\text{erosoca} = \frac{(\text{erosoca1} + \text{erosoca2})}{dz} \qquad 5\text{-}47$$

where dz is the thickness of the water layer (m), and erosoca1 and erosoca2 is described under the sections for radionuclides adsorbed to organic sediment layer 1 and 2, respectively (Section 5.5.16).

Bacterial respiration of detritus carbon and nitrate leads to a release of radionuclides adsorbed to detritus to the pool of dissolved radionuclides (redca, RN $m^{-3}$ $d^{-1}$), following:

$$\text{redca} = \frac{DC_{XRN} \cdot (F\_redc + F\_denwc)}{F\_DC} \qquad 5\text{-}48$$

where $DC_{XRN}$ is the concentration of radionuclides adsorbed to detritus (g RN $m^{-3}$), and the ecosystem model outputs of F_DC is the concentration of detritus carbon (g C $m^{-3}$), F_redc and F_denwc the respiration of detritus carbon and nitrate related to carbon, respectively (g C $m^{-3}$ $d^{-1}$).

Death of phytoplankton, zooplankton, macrophytes and macroalgae leads to an addition of adsorbed radionuclides to detritus (depc2dca, dezca, debcam3 and deeca2dc, RN $m^{-3}$ $d^{-1}$) described by:

$$\text{depc2dca} = \frac{PC_{XRN} \cdot F\_depc2dc}{F\_PC} \quad 5\text{-}49$$

$$\text{dezca} = \frac{ZC_{XRN} \cdot F\_dezc}{F\_ZC} \quad 5\text{-}50$$

$$\text{debcam3} = \frac{BC_{XRN} \cdot F\_debc}{F\_BC \cdot dz} \quad 5\text{-}51$$

$$\text{deeca2dc} = \frac{\text{deeca} - \text{deeca2soc1}}{dz} \quad 5\text{-}52$$

where dz is the layer height (m), $PC_{XRN}$ and $ZC_{XRN}$ are the concentrations of radionuclides adsorbed to phytoplankton and zooplankton, respectively (g RN $m^{-3}$), $BC_{XRN}$ the concentration of radionuclides adsorbed to macroalgae (g RN $m^{-2}$) and the ecosystem model outputs of F_PC and F_ZC are the concentrations of phytoplankton and zooplankton carbon, respectively (g C $m^{-3}$), F_BC the mass of macroalgae (g C $m^{-2}$), F_depc2dc and F_dezc the part of dead phytoplankton and zooplankton which are transferred to detritus, respectively (g C $m^{-3}$ $d^{-1}$) and F_debc the death of macroalgae (g C $m^{-2}$ $d^{-1}$). By macrophytes death (deeca, g C $m^{-2}$ $d^{-1}$, Section 5.5.6) the adsorbed radionuclides is partly transferred to organic sediment layer 1 (deeca2soc1, g C $m^{-2}$ $d^{-1}$, Section 5.5.16) and the rest is transferred to detritus.

Loss of radionuclides adsorbed to detritus due to mussel filtration (grmdca, g RN $m^{-3}$ $d^{-1}$) is described by:

$$\text{grmdca} = \frac{DC_{XRN} \cdot F\_grmdc}{F\_DC} \quad 5\text{-}53$$

where $DC_{XRN}$ is the concentration of radionuclides adsorbed to detritus (g RN $m^{-3}$), and the ecosystem model outputs of F_DC is the concentration of detritus carbon (g C $m^{-3}$) and F_grmdc the mussel filtration of detritus (g C $m^{-3}$ $d^{-1}$).

Excretion by zooplankton, planktivorous fish and benthic feeding fish adds to the pool of detritus and thus to the pool of radionuclides adsorbed to detritus (exzca, exfcpa and exfcba, g RN $m^{-3}$ $d^{-1}$):

$$\text{exzca} = \frac{\text{fek} \cdot PC_{XRN} \cdot F\_ekzc}{F\_PC} \quad 5\text{-}54$$

$$\text{exfcpa} = \frac{\text{fek} \cdot ZC_{XRN} \cdot F\_ExcFCpla}{F\_ZC} \quad 5\text{-}55$$

$$\text{exfcba} = \frac{\text{fek} \cdot \left(HC_{XRN} + DFC_{XRN}\right) \cdot F\_ExcFCben}{F\_HerbC + F\_DFC} \quad 5\text{-}56$$

where fek is the fraction of radionuclides excreted (dimensionless, Section 5.3.1), $PC_{XRN}$ and $ZC_{XRN}$ the concentration of radionuclides adsorbed to phytoplankton and zooplankton (g RN $m^{-3}$), $HC_{XRN}$ and $DFC_{XRN}$ the concentration of radionuclides adsorbed to herbivorous invertebrates and detritus feeders (g RN $m^{-2}$), the ecosystem model outputs of F_PC and F_ZC is the concentration of phytoplankton and zooplankton carbon (g C $m^{-3}$), F_HerbC and F_DFC the biomass of herbivorous invertebrates and detritus feeders (g C $m^{-2}$) and F_ekzc, F_excFCpla and F_ExcFCben the excretion by zooplankton, planktivorous fish and benthic feeding fish (g C $m^{-3}$ $d^{-1}$).

### *Internal radionuclides*

The amount of radionuclides internal in detritus is described by (Figure 5-2):

*–decay –sedimentation +erosion –respiration + death –filtration +excretion*

Decay of radionuclides internal in detritus (dkdci, g RN $m^{-3}$ $d^{-1}$) is described according to Equation 5-1. The processes of sedimentation, erosion, respiration, death, filtration and excretion are similar to the processes described for the radionuclides adsorbed to detritus; only the concentration of adsorbed radionuclides is exchanged with the internal concentration in the equations (Equation 5-44 to 5-56).

### 5.5.6 Rooted macrophytes

#### *Adsorbed radionuclides*

The amount of radionuclides adsorbed to rooted macrophytes is described by (Figure 5-3):

*–decay +adsorption –desorption – death*

Decay of radionuclides adsorbed to macrophytes (dkeca, g RN $m^{-2}$ $d^{-1}$) is described according to Equation 5-1. Adsorption of radionuclides to macrophytes (adsec, g RN $m^{-2}$ $d^{-1}$) is described by:

$$\text{adsec} = \text{areaec} \cdot k_w \cdot kd_{oc} \cdot 10^{-6} \cdot RN_{dis} \cdot F\_EC \qquad 5\text{-}57$$

where areaec is the volume to area factor for macrophytes (Table 5-3), $k_w$ is the sorption rate in water ($d^{-1}$), $kd_{oc}$ the partitioning coefficient for organic carbon (l $kgC^{-1}$), $RN_{dis}$ the concentration of dissolved radionuclides in water (g RN $m^{-3}$) and F_EC the ecosystem model output of the biomass of macrophytes (g C $m^{-2}$). Desorption of radionuclides from the surface of rooted macrophytes (desec, g RN $m^{-2}$ $d^{-1}$) follows:

$$\text{desec} = \text{areaec} \cdot k_w \cdot EC_{XRN} \qquad 5\text{-}58$$

where areaec is the volume to area factor for rooted macrophytes (Table 5-3), $k_w$ is the sorption rate in water ($d^{-1}$) and $EC_{XRN}$ the amount of radionuclides adsorbed to rooted macrophytes (g RN $m^{-2}$).

Loss of radionuclides adsorbed to rooted macrophytes due to death of macrophytes (deeca, g RN $m^{-2}$ $d^{-1}$) is described by:

$$\text{deeca} = \frac{EC_{XRN} \cdot F\_deec}{F\_EC} \qquad 5\text{-}59$$

where $EC_{XRN}$ is the concentration of radionuclides adsorbed to rooted macrophytes (g RN $m^{-2}$), and the ecosystem model outputs of F_EC is the concentration of macrophyte carbon (g C $m^{-2}$) and F_deec death of macrophytes (g C $m^{-2}$ $d^{-1}$).

#### *Internal radionuclides*

The amount of radionuclides internal in rooted macrophytes is described by (Figure 5-3):

*–decay +production –death*

Decay of radionuclides internal in macrophytes (dkeci, g RN $m^{-2}$ $d^{-1}$) is described according to Equation 5-1. Radionuclides are incorporated internally in rooted macrophytes due to primary production (preci, g RN $m^{-2}$ $d^{-1}$) following:

$$\text{preci} = \frac{RN_{dis} \cdot F\_prec}{F\_EC} \qquad 5\text{-}60$$

where $RN_{dis}$ is the concentration of dissolved radionuclides (g RN $m^{-3}$) and the ecosystem model outputs of F_EC is the biomass of macrophyte carbon (g C $m^{-2}$) and F_prec the macrophyte primary production (g C $m^{-2}$ $d^{-1}$).

Loss of radionuclides internal in macrophytes due to death of macrophytes (deeci, g RN $m^{-2}$ $d^{-1}$) is similar to the loss described for radionuclides adsorbed to macrophytes (Equation 5-59), only with the adsorbed radionuclides replaced with internal concentration of radionuclides ($EC_{INRN}$, g RN $m^{-2}$).

### 5.5.7 Perennial macroalgae

#### *Adsorbed radionuclides*

The amount of radionuclides adsorbed to perennial macroalgae is described by (Figure 5-3):

*–decay +adsorption –desorption –respiration –death –grazing*

Decay of radionuclides adsorbed to macroalgae (dkbca, g RN $m^{-2}$ $d^{-1}$) is described according to Equation 5-1. Adsorption of radionuclides to macroalgae (adsbc, g RN $m^{-2}$ $d^{-1}$) is described by:

$$\text{adsbc} = \text{areabc} \cdot k_w \cdot kd_{oc} \cdot 10^{-6} \cdot RN_{dis} \cdot \text{F\_BC} \qquad 5\text{-}61$$

where areabc is the volume to area factor for macroalgae (Table 5-3), $k_w$ is the sorption rate in water ($d^{-1}$), $kd_{oc}$ the partitioning coefficient for organic carbon (l $kgC^{-1}$), $RN_{dis}$ the concentration of dissolved radionuclides in water (g RN $m^{-3}$) and F_BC the ecosystem model output of the biomass of macroalgae (g C $m^{-2}$). Desorption of radionuclides from the surface of macroalgae (desbc, g RN $m^{-2}$ $d^{-1}$) follows:

$$\text{desbc} = \text{areabc} \cdot k_w \cdot BC_{XRN} \qquad 5\text{-}62$$

where areabc is the volume to area factor for macroalgae (Table 5-3), $k_w$ the sorption rate in water ($d^{-1}$) and $BC_{XRN}$ the amount of radionuclides adsorbed to macroalgae (g RN $m^{-2}$).

Loss of radionuclides adsorbed to macroalgae due to respiration and death of macroalgae and grazing by herbivorous invertebrate (rebca, debca and grbca, g RN $m^{-2}$ $d^{-1}$) is described by:

$$\text{rebca} = \frac{\text{frep} \cdot BC_{XRN} \cdot \text{F\_rebc}}{\text{F\_BC}} \qquad 5\text{-}63$$

$$\text{debca} = \frac{BC_{XRN} \cdot \text{F\_debc}}{\text{F\_BC}} \qquad 5\text{-}64$$

$$\text{grbca} = \frac{BC_{XRN} \cdot \text{F\_grhcbc}}{\text{F\_BC}} \qquad 5\text{-}65$$

where frep is the fraction of radionuclides respired by macroalgae (dimensionless) $BC_{XRN}$ is the concentration of radionuclides adsorbed to macroalgae (g RN $m^{-2}$), and the ecosystem model outputs of F_BC is the concentration of macroalgae carbon (g C $m^{-2}$), F_rebc and F_debc the death of macroalgae (g C $m^{-2}$ $d^{-1}$) and F_grhcbc the grazing by herbivorous invertebrates on macroalgae (g C $m^{-2}$ $d^{-1}$).

#### *Internal radionuclides*

The amount of radionuclides internal in perennial macroalgae is described by (Figure 5-3):

*–decay +production –respiration –death –grazing*

Decay of radionuclides internal in macroalgae (dkbci, g RN $m^{-2}$ $d^{-1}$) is described according to Equation 5-1. Radionuclides are incorporated internally in macroalgae due to primary production (prbci, g RN $m^{-2}$ $d^{-1}$) following:

$$\text{prbci} = \frac{RN_{dis} \cdot \text{F\_prbc}}{\text{F\_BC}} \qquad 5\text{-}66$$

where $RN_{dis}$ is the concentration of dissolved radionuclides (g RN $m^{-3}$) and the ecosystem model outputs of F_BC is the biomass of macroalgae carbon (g C $m^{-2}$) and F_prbc the macroalgae primary production (g C $m^{-2}$ $d^{-1}$).

Loss of radionuclides internal in macroalgae due to respiration and death of macroalgae (rebci and debci, g RN $m^{-2}$ $d^{-1}$) and herbivorous invertebrate grazing (grbci, g RN $m^{-2}$ $d^{-1}$) are similar to the loss described for radionuclides adsorbed to macroalgae (Equation 5-63 to 5-65), only with the adsorbed radionuclides replaced with internal concentration of radionuclides ($BC_{INRN}$, g RN $m^{-2}$).

### 5.5.8 Microalgae and annual macroalgae

#### *Adsorbed radionuclides*

The amount of radionuclides adsorbed to benthic microalgae and annual macroalgae (abbr. microalgae) is described by (Figure 5-3):

*–decay +adsorption –desorption –death –grazing*

Decay of radionuclides adsorbed to microalgae (dkbdca, g RN $m^{-2}$ $d^{-1}$) is described according to Equation 5-1.

Adsorption of radionuclides to microalgae (adsbdc, g RN $m^{-2}$ $d^{-1}$) is described by:

$$\text{adsbdc} = \text{areabdc} \cdot k_w \cdot kd_{oc} \cdot 10^{-6} \cdot RN_{dis} \cdot \text{F\_BDC} \qquad 5\text{-}67$$

where areabdc is the volume to area factor for microalgae (Table 5-3), $k_w$ the sorption rate in water ($d^{-1}$), $kd_{oc}$ the partitioning coefficient for organic carbon (l $kgC^{-1}$), $RN_{dis}$ the concentration of dissolved radionuclides in water (g RN $m^{-3}$) and F_BDC the ecosystem model output of the biomass of microalgae (g C $m^{-2}$). Desorption of radionuclides from the surface of microalgae (desbdc, g RN $m^{-2}$ $d^{-1}$) follows:

$$\text{desbdc} = \text{areabdc} \cdot k_w \cdot BDC_{XRN} \qquad 5\text{-}68$$

where areabdc is the volume to area factor for microalgae (Table 5-3), $k_w$ the sorption rate in water ($d^{-1}$) and $BDC_{XRN}$ the amount of radionuclides adsorbed to microalgae (g RN $m^{-2}$).

Loss of radionuclides adsorbed to microalgae due to death of microalgae and grazing by herbivorous invertebrates (debdca and grbdca, g RN $m^{-2}$ $d^{-1}$) is described by:

$$\text{debdca} = \frac{BDC_{XRN} \cdot \text{F\_debdc}}{\text{F\_BDC}} \qquad 5\text{-}69$$

$$\text{grbdca} = \frac{BDC_{XRN} \cdot \text{F\_grhcbdc}}{\text{F\_BDC}} \qquad 5\text{-}70$$

where $BDC_{XRN}$ is the concentration of radionuclides adsorbed to microalgae (g RN $m^{-2}$), and the ecosystem model outputs of F_BDC is the concentration of microalgae carbon (g C $m^{-2}$), F_debdc the death of microalgae (g C $m^{-2}$ $d^{-1}$) and F_grhcbdc the grazing by herbivorous invertebrates on microalgae (g C $m^{-2}$ $d^{-1}$).

#### *Internal radionuclides*

The amount of radionuclides internal in benthic microalgae and annual macroalgae (abbr. microalgae) is described by (Figure 5-3):

*–decay +production –death –grazing*

Decay of radionuclides internal in microalgae (dkbdci, g RN $m^{-2}$ $d^{-1}$) is described according to Equation 5-1.

Radionuclides are incorporated internally in microalgae due to primary production (prbdci, g RN $m^{-2}$ $d^{-1}$) following:

$$\text{prbdci} = \frac{RN_{dis} \cdot \text{F\_prbdc}}{\text{F\_BDC}} \qquad 5\text{-}71$$

where $RN_{dis}$ is the concentration of dissolved radionuclides (g RN $m^{-3}$) and the ecosystem model outputs of F_BDC is the biomass of microalgae carbon (g C $m^{-2}$) and F_prbdc the microalgae primary production (g C $m^{-2}$ $d^{-1}$).

Loss of radionuclides internal in microalgae due to death of microalgae and grazing by herbivorous invertebrates (debdci and grbdci, g RN $m^{-2}$ $d^{-1}$) are similar to the loss described for radionuclides adsorbed to microalgae (Equation 5-69 and 5-70), only with the adsorbed radionuclides replaced with internal concentration of radionuclides ($BDC_{INRN}$, g RN $m^{-2}$).

### 5.5.9 Zooplankton

#### *Adsorbed radionuclides*

The amount of radionuclides adsorbed to zooplankton is described by (Figure 5-2 and Figure 5-4):

*–decay +adsorption –desorption –death –predation*

Decay of radionuclides adsorbed to zooplankton (dkzca, g RN $m^{-3}$ $d^{-1}$) is described according to Equation 5-1.

Adsorption of radionuclides to zooplankton (adszc, g RN $m^{-3}$ $d^{-1}$) is described by:

$$\text{adszc} = \text{areazc} \cdot k_w \cdot kd_{oc} \cdot 10^{-6} \cdot RN_{dis} \cdot F\_ZC \qquad 5\text{-}72$$

where areazc is the volume to area factor for zooplankton (Table 5-3), $k_w$ the sorption rate in water ($d^{-1}$), $kd_{oc}$ the partitioning coefficient for organic carbon (l $kgC^{-1}$), $RN_{dis}$ the concentration of dissolved radionuclides in water (g RN $m^{-3}$) and F_ZC the ecosystem model output of the concentration of zooplankton (g C $m^{-3}$). Desorption of radionuclides from the surface of zooplankton (deszc, g RN $m^{-3}$ $d^{-1}$) follows:

$$\text{deszc} = \text{areazc} \cdot k_w \cdot ZC_{XRN} \qquad 5\text{-}73$$

where areazc is the volume to area factor for zooplankton (Table 5-3), $k_w$ is the sorption rate in water ($d^{-1}$) and $ZC_{XRN}$ the amount of radionuclides adsorbed to zooplankton (g RN $m^{-3}$).

Loss of radionuclides adsorbed to zooplankton due to death of zooplankton and predation by planktivorous fish (dezca and predzca, g RN $m^{-3}$ $d^{-1}$) is described by:

$$\text{dezca} = \frac{ZC_{XRN} \cdot F\_dezc}{F\_ZC} \qquad 5\text{-}74$$

$$\text{predzca} = \frac{ZC_{XRN} \cdot F\_predzc}{F\_ZC} \qquad 5\text{-}75$$

where $ZC_{XRN}$ is the concentration of radionuclides adsorbed to zooplankton (g RN $m^{-3}$), and the ecosystem model outputs of F_ZC is the concentration of zooplankton carbon (g C $m^{-3}$), F_dezc the death of zooplankton (g C $m^{-3}$ $d^{-1}$) and F_predzc the predation of zooplankton by planktivorous fish (g C $m^{-3}$ $d^{-1}$).

#### *Internal radionuclides*

The amount of radionuclides internal in zooplankton is described by (Figure 5-2 and Figure 5-4):

*–decay +production –death –predation*

Decay of radionuclides internal in zooplankton (dkzci, g RN $m^{-3}$ $d^{-1}$) is described according to Equation 5-1.

The production of zooplankton leads to an assimilation of radionuclides internally in zooplankton (przci, g RN $m^{-3}$ $d^{-1}$). The production is described as the net-production, hence excretion and respiration is subtracted from the amount grazed:

$$\text{przci} = \text{grpca} + \text{grpci} - \text{exzca} - \text{exzci} - \text{rezca} - \text{rezci} \qquad 5\text{-}76$$

where grpca and grpci are the grazing of phytoplankton adsorbed and internal radionuclides by zooplankton (g RN $m^{-3}$ $d^{-1}$, Section 5.5.4), exzca and exzci are the excretion of phytoplankton adsorbed and internal radionuclides by zooplankton (g RN $m^{-3}$ $d^{-1}$, Section 5.5.5) and rezca is the zooplankton respiration of phytoplankton adsorbed radionuclides (g RN $m^{-3}$ $d^{-1}$), described by:

$$\text{rezca} = \frac{\text{fre} \cdot PC_{XRN} \cdot F\_rezc}{F\_PC} \qquad 5\text{-}77$$

where fre is the fraction of radionuclides respirated by animals (dimensionless), $PC_{XRN}$ is the concentration of radionuclides adsorbed to phytoplankton (g RN $m^{-3}$), and the ecosystem model outputs

of F_PC is the concentration of phytoplankton carbon (g C $m^{-3}$) and F_rezc the zooplankton respiration (g C $m^{-3}$ $d^{-1}$). The respiration of radionuclides internal in phytoplankton (rezci, g RN $m^{-3}$ $d^{-1}$) is described likewise, only with the adsorbed radionuclides replaced with internal concentration of radionuclides ($PC_{INRN}$, g RN $m^{-3}$).

Loss of radionuclides internal in zooplankton due to death of zooplankton and predation by planktivorous fish (dezci and predzci, g RN $m^{-3}$ $d^{-1}$) are similar to the loss described for radionuclides adsorbed to zooplankton (Equation 5-74 and 5-75), only with the adsorbed radionuclides replaced with internal concentration of radionuclides ($ZC_{INRN}$, g RN $m^{-3}$).

### 5.5.10 Herbivorous invertebrates

#### *Adsorbed radionuclides*

The amount of radionuclides adsorbed to herbivorous invertebrates is described by (Figure 5-3 and Figure 5-4):

*–decay +adsorption –desorption –death –predation*

Decay of radionuclides adsorbed to herbivorous invertebrates (dkhca, g RN $m^{-2}$ $d^{-1}$) is described according to Equation 5-1.

Adsorption of radionuclides to herbivorous invertebrates (adshc, g RN $m^{-2}$ $d^{-1}$) is described by:

$$\text{adshc} = \text{areahc} \cdot k_w \cdot kd_{oc} \cdot 10^{-6} \cdot RN_{dis} \cdot F\_HC \cdot dz \qquad 5\text{-}78$$

where dz is the water layer height (m), areahc the volume to area factor for herbivorous invertebrates (Table 5-3), $k_w$ the sorption rate in water ($d^{-1}$), $kd_{oc}$ the partitioning coefficient for organic carbon (l $kgC^{-1}$), $RN_{dis}$ the concentration of dissolved radionuclides in water (g RN $m^{-3}$) and F_HC the ecosystem model output of the concentration of herbivorous invertebrates (g C $m^{-2}$). Desorption of radionuclides from the surface of herbivorous invertebrates (deshc, g RN $m^{-2}$ $d^{-1}$) follows:

$$\text{deshc} = \text{areahc} \cdot k_w \cdot HC_{XRN} \qquad 5\text{-}79$$

where areahc is the volume to area factor for herbivorous invertebrates (Table 5-3), $k_w$ the sorption rate in water ($d^{-1}$) and $HC_{XRN}$ the amount of radionuclides adsorbed to herbivorous invertebrates (g RN $m^{-2}$).

Loss of radionuclides adsorbed to herbivorous invertebrates due to death of herbivorous invertebrates and predation by benthic feeding fish (dehca and predhca, g RN $m^{-2}$ $d^{-1}$) is described by:

$$\text{dehca} = \frac{HC_{XRN} \cdot F\_dehc}{F\_HC} \qquad 5\text{-}80$$

$$\text{predhca} = \frac{HC_{XRN} \cdot F\_predhc}{F\_HC} \qquad 5\text{-}81$$

where $HC_{XRN}$ is the concentration of radionuclides adsorbed to herbivorous invertebrates (g RN $m^{-2}$), and the ecosystem model outputs of F_HC is the concentration of herbivorous invertebrates carbon (g C $m^{-2}$), F_dehc the death of herbivorous invertebrates (g C $m^{-2}$ $d^{-1}$) and F_predhc the predation of herbivorous invertebrates by benthic feeding fish (g C $m^{-2}$ $d^{-1}$).

#### *Internal radionuclides*

The amount of radionuclides internal in herbivorous invertebrates is described by (Figure 5-3 and Figure 5-4):

*–decay +production –respiration –death –predation*

Decay of radionuclides internal in herbivorous invertebrates (dkhci, g RN $m^{-2}$ $d^{-1}$) is described according to Equation 5-1.

The production of herbivorous invertebrates leads to an assimilation of radionuclides internally in herbivorous invertebrates (prhci, g RN $m^{-2}$ $d^{-1}$). The production is described as the grazing subtracted excretion:

$$\begin{aligned} prhci = {} & grbdca + grbdci + grbca + grbci \\ & - exbdchca - exbdchci - exbchca - exbchci \end{aligned} \quad 5\text{-}82$$

where grbdca, grbdci, grbca and grbci is the grazing of microalgae and macroalgae adsorbed and internal radionuclides by herbivorous invertebrates (g RN $m^{-2}$ $d^{-1}$, Sections 5.5.7 and 5.5.8) and exbdchca and exbchca is the excretion of microalgae and macroalgae adsorbed radionuclides by herbivorous invertebrates (g RN $m^{-2}$ $d^{-1}$), described by:

$$exbdchca = \frac{fek \cdot BDC_{XRN} \cdot F\_exhcbdc}{F\_BDC} \quad 5\text{-}83$$

$$exbchca = \frac{fek \cdot BC_{XRN} \cdot F\_exhcbc}{F\_BC} \quad 5\text{-}84$$

where fek is the fraction of radionuclides excreted by animals (dimensionless), $BDC_{XRN}$ and $BC_{XRN}$ are the concentration of radionuclides adsorbed to microalgae and macroalgae (g RN $m^{-2}$), and the ecosystem model outputs of F_BDC and F_BC are the biomass of microalgae and macroalgae carbon (g C $m^{-2}$) and F_exhcbdca and F_exhcbca the herbivorous invertebrates excretion of microalgae and macroalgae, respectively (g C $m^{-2}$ $d^{-1}$). The excretion of radionuclides internal in microalgae and macroalgae (exbdchci and exbchci, g RN $m^{-2}$ $d^{-1}$) are described likewise, only with the adsorbed radionuclides replaced with internal concentration of radionuclides ($BDC_{INRN}$ and $BC_{INRN}$ g RN $m^{-2}$).

Loss of herbivorous invertebrate internal radionuclides due to respiration (rehci, g RN $m^{-2}$ $d^{-1}$) is described by:

$$rehci = \frac{fre \cdot HC_{INRN} \cdot F\_rehc}{F\_HC} \quad 5\text{-}85$$

where fre is the fraction of radionuclides respirated by animals (dimensionless), $HC_{INRN}$ the concentration of radionuclides internal in herbivorous invertebrates (g RN $m^{-2}$), and the ecosystem model outputs of F_HC is the biomass of herbivorous invertebrates carbon (g C $m^{-2}$) and F_rehc the respiration by herbivorous invertebrates (g C $m^{-2}$ $d^{-1}$).

Loss of radionuclides internal in herbivorous invertebrates due to death of herbivorous invertebrates and predation by benthic feeding fish (dehci and predhci, g RN $m^{-2}$ $d^{-1}$) are similar to the loss described for radionuclides adsorbed to herbivorous invertebrates (Equation 5-80 and 5-81), only with the adsorbed radionuclides replaced with internal concentration of radionuclides ($HC_{INRN}$, g RN $m^{-2}$).

### 5.5.11 Deposit-feeders

#### *Adsorbed radionuclides*

The amount of radionuclides adsorbed to deposit feeders is described by (Figure 5-4):

*–decay +adsorption –desorption –death –predation*

Decay of radionuclides adsorbed to deposit feeders (dkdfca, g RN $m^{-2}$ $d^{-1}$) is described according to Equation 5-1.

Adsorption of radionuclides to deposit feeders (adsdfc, g RN $m^{-2}$ $d^{-1}$) is described by:

$$adsdfc = \frac{areadfc \cdot k_s \cdot kd_{oc} \cdot 10^{-6} \cdot RN_{dis1} \cdot F\_DFC}{dzs1 \cdot pors1} \quad 5\text{-}86$$

where dzs1 is the thickness of sediment layer 1 (m), pors1 the porosity of sediment layer 1 ($m^3_{H2O}$ $m^{-3}_{bulk}$), areadfc the volume to area factor for deposit feeders (Table 5-3), $k_s$ the sorption rate in sediment ($d^{-1}$), $kd_{oc}$ the partitioning coefficient for organic carbon (l $kgC^{-1}$), $RN_{dis1}$ the concentration of dissolved radionuclides in sediment layer 1 (g RN $m^{-2}$) and F_DFC the ecosystem model output of the concentration of deposit feeders (g C $m^{-2}$).

Desorption of radionuclides from the surface of deposit feeders (desdfc, g RN $m^{-2}$ $d^{-1}$) follows:

$$\text{desdfc} = \text{areadfc} \cdot k_s \cdot \text{DFC}_{\text{XRN}} \qquad 5\text{-}87$$

where areadfc is the volume to area factor for deposit feeders (Table 5-3), $k_s$ the sorption rate in sediment ($d^{-1}$) and $\text{DFC}_{\text{XRN}}$ the amount of radionuclides adsorbed to deposit feeders (g RN $m^{-2}$).

Loss of radionuclides adsorbed to deposit feeders due to death of deposit feeders and predation by benthic feeding fish (dedfca and preddfca, g RN $m^{-2}$ $d^{-1}$) is described by:

$$\text{dedfca} = \frac{\text{DFC}_{\text{XRN}} \cdot \text{F\_dedfc}}{\text{F\_DFC}} \qquad 5\text{-}88$$

$$\text{preddfca} = \frac{\text{DFC}_{\text{XRN}} \cdot \text{F\_preddfc}}{\text{F\_DFC}} \qquad 5\text{-}89$$

where $\text{DFC}_{\text{XRN}}$ is the concentration of radionuclides adsorbed to deposit feeders (g RN $m^{-2}$), and the ecosystem model outputs of F_DFC is the biomass of deposit feeders carbon (g C $m^{-2}$), F_dedfc the death of deposit feeders (g C $m^{-2}$ $d^{-1}$) and F_preddfc the predation of deposit feeders by benthic feeding fish (g C $m^{-2}$ $d^{-1}$).

### *Internal radionuclides*

The amount of radionuclides internal in deposit feeders is described by (Figure 5-4):

*–decay +production –respiration –death –predation*

Decay of radionuclides internal in deposit feeders (dkdfci, g RN $m^{-2}$ $d^{-1}$) is described according to Equation 5-1.

Deposit feeders feed on organic sediment layer 1 and the assimilation of radionuclides internally in deposit feeders (prdfci, g RN $m^{-2}$ $d^{-1}$) is described by:

$$\text{prdfci} = \text{grsoc1a} + \text{grsoc1i} \qquad 5\text{-}90$$

where grsoc1a is the grazing of radionuclides adsorbed to organic sediment layer 1 by deposit feeders (g RN $m^{-2}$ $d^{-1}$), described by:

$$\text{grsoc1a} = \frac{\text{SOC1}_{\text{XRN}} \cdot \text{F\_grdfc}}{\text{F\_SOC1}} \qquad 5\text{-}91$$

where $\text{SOC1}_{\text{XRN}}$ is the amount of radionuclides adsorbed to organic sediment layer 1 (g RN $m^{-2}$), and the ecosystem model outputs of F_SOC1 is the mass of organic sediment layer 1 (g C $m^{-2}$) and F_grdfc the deposit feeders grazing on organic sediment layer 1 (g C $m^{-2}$ $d^{-1}$). The grazing of radionuclides internal in organic sediment layer 1 (grsoc1i, g RN $m^{-2}$ $d^{-1}$) is described likewise, only with the adsorbed radionuclides replaced with internal concentration of radionuclides ($\text{SOC1}_{\text{INRN}}$, g RN $m^{-2}$).

Loss of deposit feeder internal radionuclides due to respiration (redfci, g RN $m^{-2}$ $d^{-1}$) is described by:

$$\text{redfci} = \frac{\text{fre} \cdot \text{DFC}_{\text{INRN}} \cdot \text{F\_redfc}}{\text{F\_DFC}} \qquad 5\text{-}92$$

where fre is the fraction of radionuclides respirated by animals (dimensionless), $\text{DFC}_{\text{INRN}}$ the concentration of radionuclides internal in deposit feeders (g RN $m^{-2}$), and the ecosystem model outputs of F_DFC is the biomass of deposit feeders carbon (g C $m^{-2}$) and F_redfc the respiration by deposit feeders (g C $m^{-2}$ $d^{-1}$).

Loss of radionuclides internal in deposit feeders due to death of deposit feeders and predation by benthic feeding fish (dedfci and preddfci, g RN $m^{-2}$ $d^{-1}$) are similar to the loss described for radionuclides adsorbed to deposit feeders (Equation 5-88 and 5-89), only with the adsorbed radionuclides replaced with internal concentration of radionuclides ($\text{DFC}_{\text{INRN}}$, g RN $m^{-2}$).

### 5.5.12 Planktivorous fish

#### *Adsorbed radionuclides*

The amount of radionuclides adsorbed to planktivorous fish gills is described by (Figure 5-4):

*–decay +adsorption –desorption –death –diffusion*

Decay of radionuclides adsorbed to planktivorous fish gills (dkfcpa, g RN $m^{-3}$ $d^{-1}$) is described according to Equation 5-1.

The area of fish gills are considerable larger than the surface area of the fish, and therefore the adsorption of radionuclides is related to the area of fish gills. Adsorption of radionuclides to planktivorous fish gills (adsfcp, g RN $m^{-3}$ $d^{-1}$) is described by:

$$\text{adsdfcp} = \text{areagill} \cdot k_w \cdot kd_{oc} \cdot 10^{-6} \cdot RN_{dis} \cdot \text{F\_FCP} \qquad 5\text{-}93$$

where areagill is the volume to area factor for fish gills (Table 5-3), $k_w$ the sorption rate in water ($d^{-1}$), $kd_{oc}$ the partitioning coefficient for organic carbon (l $kgC^{-1}$), $RN_{dis}$ the concentration of dissolved radionuclides in water (g RN $m^{-3}$) and F_FCP the ecosystem model output of the biomass of planktivorous fish (g C $m^{-3}$).

Desorption of radionuclides from the surface of planktivorous fish gills (desfcp, g RN $m^{-3}$ $d^{-1}$) follows:

$$\text{desfcp} = \text{areagill} \cdot k_w \cdot FCP_{XRN} \qquad 5\text{-}94$$

where areagill is the volume to area factor for planktivorous fish gills (Table 5-3), $k_w$ the sorption rate in water ($d^{-1}$) and $FCP_{XRN}$ the amount of radionuclides adsorbed to planktivorous fish gills (g RN $m^{-3}$).

Loss of radionuclides adsorbed to planktivorous fish gills due to death of planktivorous fish (defcpa, g RN $m^{-3}$ $d^{-1}$) is described by:

$$\text{defcpa} = \frac{FCP_{XRN} \cdot \text{F\_defcp}}{\text{F\_FCP}} \qquad 5\text{-}95$$

where $FCP_{XRN}$ is the amount of radionuclides adsorbed to planktivorous fish gills (g RN $m^{-3}$), and the ecosystem model outputs of F_FCP is the biomass of planktivorous fish carbon (g C $m^{-3}$) and F_defcp the death of planktivorous fish (g C $m^{-3}$ $d^{-1}$).

Diffusion of radionuclides from planktivorous fish gills into the fish (diffcp, g C $m^{-3}$ $d^{-1}$) is considered if the concentration of adsorbed radionuclides on the gills is larger than the internal concentration ($FCP_{XRN} > FCP_{INRN}$). The diffusion is described by:

$$\text{diffcp} = \text{kdiffc} \cdot FCP_{XRN} - FCP_{INRN} \qquad 5\text{-}96$$

where kdiffc is the diffusion coefficient of radionuclides over fish gills ($d^{-1}$) and $FCP_{XRN}$ and $FCP_{INRN}$ the concentration of adsorbed and internal radionuclides related to planktivorous fish (g RN $m^{-3}$).

#### *Internal radionuclides*

The amount of radionuclides internal in planktivorous fish is described by (Figure 5-4):

*–decay +production –respiration –death +diffusion*

Decay of radionuclides internal in planktivorous fish (dkfcpi, g RN $m^{-3}$ $d^{-1}$) is described according to Equation 5-1.

Planktivorous fishs' predation on zooplankton leads to an assimilation of radionuclides internally in the fish (prfcpi, g RN $m^{-3}$ $d^{-1}$). The assimilation is described as the production subtracted excretion:

$$\text{prfcpi} = \text{predzca} + \text{predzci} - \text{exfcpa} - \text{exfcpi} \qquad 5\text{-}97$$

where predzca and predzci are the predation of planktivorous fish on zooplankton adsorbed and internal radionuclides (g RN $m^{-3}$ $d^{-1}$, Section 5.5.9) and exfcpa and exfcpi is the excretion by planktivorous fish of zooplankton adsorbed and internal radionuclides (g RN $m^{-3}$ $d^{-1}$, Section 5.5.5).

Loss of planktivorous fish internal radionuclides due to respiration (refcpi, g RN $m^{-3}$ $d^{-1}$) is described by:

$$\text{refcpi} = \frac{\text{fre} \cdot \text{FCP}_{\text{INRN}} \cdot \text{F\_refcp}}{\text{F\_FCP}} \qquad 5\text{-}98$$

where fre is the fraction of radionuclides respirated by animals (dimensionless), $FCP_{INRN}$ is the concentration of radionuclides internal in planktivorous fish (g RN $m^{-3}$), and the ecosystem model outputs of F_FCP is the biomass of planktivorous fish carbon (g C $m^{-3}$) and F_refcp the respiration by planktivorous fish (g C $m^{-3}$ $d^{-1}$).

Loss of radionuclides internal in planktivorous fish due to death of planktivorous fish (defcpi, g RN $m^{-3}$ $d^{-1}$) are similar to the loss described for radionuclides adsorbed to planktivorous fish gills (Equation 5-95), only with the adsorbed radionuclides replaced with internal concentration of radionuclides ($FCP_{INRN}$, g RN $m^{-2}$). Diffusion (diffcp, g RN $m^{-3}$ $d^{-1}$) takes place when the concentration of fish gill adsorbed radionuclides is larger than the internal concentration ($FCP_{XRN} > FCP_{INRN}$). This leads to an increase of concentration of internal radionuclides in planktivorous fish (Equation 5-96).

### 5.5.13 Benthic feeding fish and predatory invertebrates

#### *Adsorbed radionuclides*

The amount of radionuclides adsorbed to benthic feeding fish gills (and predatory invertebrates, i.e. *Saduria*) is described by (Figure 5-4):

*–decay +adsorption –desorption –death –diffusion*

Decay of radionuclides adsorbed to benthic feeding fish gills (dkfcba, g RN $m^{-3}$ $d^{-1}$) is described according to Equation 5-1.

The area of fish gills are considerable larger than the surface area of the fish, and therefore the adsorption of radionuclides are related to the fish gills. Adsorption of radionuclides to benthic feeding fish gills (adsfcb, g RN $m^{-3}$ $d^{-1}$) is described by:

$$\text{adsfcb} = \text{areagill} \cdot k_w \cdot kd_{oc} \cdot 10^{-6} \cdot RN_{dis} \cdot \text{F\_FCB} \qquad 5\text{-}99$$

where areagill is the volume to area factor for fish gills (Table 5-3), $k_w$ the sorption rate in water ($d^{-1}$), $kd_{oc}$ the partitioning coefficient for organic carbon (l $kgC^{-1}$), $RN_{dis}$ the concentration of dissolved radionuclides in water (g RN $m^{-3}$) and F_FCB the ecosystem model output of the biomass of benthic feeding fish (g C $m^{-3}$). Desorption of radionuclides from the surface of benthic feeding fish gills (desfcb, g RN $m^{-3}$ $d^{-1}$) follows:

$$\text{desfcb} = \text{areagill} \cdot k_w \cdot FCB_{XRN} \qquad 5\text{-}100$$

where areagill is the volume to area factor for benthic feeding fish gills (Table 5-3), $k_w$ the sorption rate in water ($d^{-1}$) and $FCB_{XRN}$ the amount of radionuclides adsorbed to benthic feeding fish gills (g RN $m^{-3}$).

Loss of radionuclides adsorbed to benthic feeding fish gills due to death of benthic feeding fish (defcba, g RN $m^{-3}$ $d^{-1}$) is described by:

$$\text{defcba} = \frac{FCB_{XRN} \cdot \text{F\_defcb}}{\text{F\_FCB}} \qquad 5\text{-}101$$

where $FCB_{XRN}$ is the amount of radionuclides adsorbed to benthic feeding fish gills (g RN $m^{-3}$), and the ecosystem model outputs of F_FCB is the biomass of benthic feeding fish carbon (g C $m^{-3}$) and F_defcb the death of benthic feeding fish (g C $m^{-3}$ $d^{-1}$).

Diffusion of radionuclides from benthic feeding fish gills into the fish (diffcb, g C $m^{-3}$ $d^{-1}$) is considered if the concentration of adsorbed radionuclides on the gills is larger than the internal concentration ($FCB_{XRN} > FCB_{INRN}$). The diffusion is described by:

$$diffcb = kdiffc \cdot FCB_{XRN} - FCB_{INRN} \quad 5\text{-}102$$

where kdiffc is the diffusion coefficient of radionuclides over fish gills ($d^{-1}$) and $FCB_{XRN}$ and $FCB_{INRN}$ is the concentration of adsorbed and internal radionuclides related to benthic feeding fish (g RN $m^{-3}$).

#### *Internal radionuclides*

The amount of radionuclides internal in benthic feeding fish (and predatory invertebrates) is described by (Figure 5-4):

*–decay +production –respiration –death +diffusion*

Decay of radionuclides internal in benthic feeding fish (dkfcbi, g RN $m^{-3}$ $d^{-1}$) is described according to Equation 5-1.

Benthic feeding fish predation on herbivorous invertebrates and deposit-feeders leads to an assimilation of radionuclides internally in the fish (prfcbi, g RN $m^{-3}$ $d^{-1}$). The assimilation is described as the production subtracted excretion:

$$prfcbi = \frac{predhca + predhci + preddfca + preddfci}{dz} - exfcba - exfcbi \quad 5\text{-}103$$

where predhca, predhci, preddfca and preddfci are the predation by benthic feeding fish on herbivorous invertebrates and deposit-feeders adsorbed and internal (g RN $m^{-3}$ $d^{-1}$, Sections 5.5.10 and 5.5.11) and exfcba and exfcbi are the excretion by benthic feeding fish (g RN $m^{-3}$ $d^{-1}$, Section 5.5.5).

Loss of benthic feeding fishs' internal radionuclides due to respiration (refcbi, g RN $m^{-3}$ $d^{-1}$) is described by:

$$refcbi = \frac{fre \cdot FCB_{INRN} \cdot F\_refcb}{F\_FCB} \quad 5\text{-}104$$

where fre is the fraction of radionuclides respirated by animals (dimensionless), $FCB_{INRN}$ is the concentration of radionuclides internal in benthic feeding fish (g RN $m^{-3}$), and the ecosystem model outputs of F_FCB is the biomass of benthic feeding fish carbon (g C $m^{-3}$) and F_refcb the respiration by benthic feeding fish (g C $m^{-3}$ $d^{-1}$).

Loss of radionuclides internal in benthic feeding fish due to death of benthic feeding fish (defcbi, g RN $m^{-3}$ $d^{-1}$) are similar to the loss described for radionuclides adsorbed to benthic feeding fish gills (Equation 5-101), only with the adsorbed radionuclides replaced with internal concentration of radionuclides ($FCB_{INRN}$, g RN $m^{-2}$). Diffusion (diffcb, g RN $m^{-3}$ $d^{-1}$) takes place when the concentration of fish gill adsorbed radionuclides is larger than the internal concentration ($FCB_{XRN} > FCB_{INRN}$). This leads to an increase of concentration of internal radionuclides in benthic feeding fish (Equation 5-102).

### 5.5.14 Dead fish

#### *Adsorbed radionuclides to dead fish gills*

The amount of radionuclides adsorbed to dead fish gills is described by (Figure 5-4):

*–decay +death –sedimentation*

Decay of radionuclides adsorbed to dead fish gills (dkfcda, g RN $m^{-3}$ $d^{-1}$) is described according to Equation 5-1.

Death of planktivorous and benthic feeding fish are transferred to a pool of dead fish leading to an increase of the concentration of radionuclides adsorbed to dead fish gills (defcpa +defcba, g RN $m^{-3}$ $d^{-1}$, Sections 5.5.12 and 5.5.13). The pool of dead fish is necessary in the ecosystem

model, because the fish are described as a fixed process type, which cannot settle out to the sediment. Dead fish is described as a transformation process type, and the settling is described as:

$$\text{sedfcda} = \frac{\text{FCD}_{\text{XRN}} \cdot \text{F\_sedfcd}}{\text{F\_FCD}} \qquad 5\text{-}105$$

where $FCD_{XRN}$ is the concentration of radionuclides adsorbed to dead fish (g RN $m^{-3}$), and the ecosystem model outputs of F_FCD is the biomass of dead fish carbon (g C $m^{-3}$) and F_sedfcd the settling of dead fish (g C $m^{-3}$ $d^{-1}$).

#### *Internal radionuclides*

The amount of radionuclides internal in dead fish is described by (Figure 5-4):

*–decay +death –sedimentation*

Decay of radionuclides internal in dead fish (dkfcdi, g RN $m^{-3}$ $d^{-1}$) is described according to Equation 5-1. Death of planktivorous and benthic feeding fish are transferred to a pool of dead fish leading to an increase of the concentration of radionuclides internal in dead fish (defcpi +defcbi, g RN $m^{-3}$ $d^{-1}$, Sections 5.5.12 and 5.5.13).

Loss of radionuclides internal in dead fish due to settling of dead fish (sedfcdi, g RN $m^{-3}$ $d^{-1}$) is similar to the loss described for radionuclides adsorbed to dead fish gills (Equation 5-105), only with the adsorbed radionuclides replaced with internal concentration of radionuclides ($FCD_{INRN}$, g RN $m^{-2}$).

### 5.5.15 Inorganic sediment

#### *Adsorbed radionuclides to inorganic sediment layer 1*

The amount of radionuclides adsorbed to inorganic sediment in surface layer (i.e. model layer 1) is described by (Figure 5-1):

*–decay +adsorption –desorption +sedimentation –erosion +excretion –transport –mixing1 +mixing2*

Decay of radionuclides adsorbed to inorganic sediment layer 1 (dkssin1, g RN $m^{-2}$ $d^{-1}$) is described according to Equation 5-1.

Adsorption of radionuclides to inorganic sediment layer 1 (adsin1, g RN $m^{-2}$ $d^{-1}$) is described by:

$$\text{adsin1} = \frac{k_s \cdot kd_{in} \cdot 10^{-6} \cdot RN_{dis1} \cdot \text{F\_Sin1}}{dzs1 \cdot pors1} \qquad 5\text{-}106$$

where dzs1 is the thickness of sediment layer 1 (m), pors1 the porosity of sediment layer 1 ($m^3_{H2O}$ $m^{-3}_{bulk}$), $k_s$ the sorption rate in sediment ($d^{-1}$), $kd_{in}$ the partitioning coefficient for inorganic matter (l $kg^{-1}$), $RN_{dis1}$ the concentration of dissolved radionuclides in sediment layer 1 (g RN $m^{-2}$) and F_Sin1 the ecosystem model output of the mass of inorganic sediment layer 1 (g $m^{-2}$). Desorption of radionuclides from inorganic sediment layer 1 (desin1, g RN $m^{-2}$ $d^{-1}$) follows:

$$\text{desin1} = k_s \cdot \text{Sin1}_{\text{XRN}} \qquad 5\text{-}107$$

where $k_s$ is the sorption rate in sediment ($d^{-1}$) and $Sin1_{XRN}$ the amount of radionuclides adsorbed to inorganic sediment layer 1 (g RN $m^{-2}$).

Deposition (sedimentation from the water bed) of radionuclides adsorbed to inorganic suspended solids to sediment layer 1 (sedin1, g RN $m^{-2}$ $d^{-1}$) is described by:

$$\text{sedin1} = \frac{\text{SSin}_{\text{XRN}} \cdot \text{F\_dep}_{\text{SSin}}}{\text{F\_SSin}} \qquad 5\text{-}108$$

where $SSin_{XRN}$ is the concentration of radionuclides adsorbed to inorganic suspended solids (g RN $m^{-3}$), and the ecosystem model outputs of F_SSin is the concentration of inorganic suspended solids (g $m^{-3}$) and $F\_dep_{SSin}$ the deposition of inorganic suspended solids from the water bed to the sediment layer 1 (g $m^{-2}$ $d^{-1}$).

Erosion of radionuclides adsorbed to inorganic sediment layer 1 (eroin1, g RN $m^{-2}$ $d^{-1}$) add to the concentration of radionuclides adsorbed to inorganic suspended solids and is described by:

$$\text{eroin1} = \frac{\text{Sin1}_{\text{XRN}} \cdot \text{F\_ero}_{\text{Sin1}}}{\text{F\_Sin1}} \qquad 5\text{-}109$$

where $\text{Sin1}_{\text{XRN}}$ is the concentration of radionuclides adsorbed to inorganic sediment layer 1 (g RN $m^{-2}$) and the ecosystem model outputs of F_Sin1 is the mass of inorganic sediment layer 1 (g $m^{-2}$) and $\text{F\_ero}_{\text{Sin1}}$ the erosion of inorganic sediment layer 1 (g $m^{-2}$ $d^{-1}$).

Mussel filtration and excretion activities cause a transport of radionuclides adsorbed to inorganic suspended solids to inorganic sediment layer 1 (grmin1, g RN $m^{-2}$ $d^{-1}$):

$$\text{grmin1} = \frac{\text{SSin}_{\text{XRN}} \cdot \text{F\_grm}_{\text{SSin-m2}}}{\text{F\_SSin}} \qquad 5\text{-}110$$

where $\text{SSin}_{\text{XRN}}$ is the concentration of radionuclides adsorbed to inorganic suspended solids (g RN $m^{-3}$), and the ecosystem model outputs of F_SSin is the concentration of inorganic suspended solids (g $m^{-3}$) and $\text{Fgrm}_{\text{SSin-m2}}$ the mussel filtration of inorganic suspended solids per area (g $m^{-2}$ $d^{-1}$).

Consolidation of the sediment cause a transport of radionuclides adsorbed to inorganic sediment from layer 1 to layer 2 (train, g RN $m^{-2}$ $d^{-1}$), described by:

$$\text{train1} = \frac{\text{Sin1}_{\text{XRN}} \cdot \text{F\_tran}_{\text{Sin1}}}{\text{F\_Sin1}} \qquad 5\text{-}111$$

where $\text{Sin1}_{\text{XRN}}$ is the concentration of radionuclides adsorbed to inorganic sediment layer 1 (g RN $m^{-2}$) and the ecosystem model outputs of F_Sin1 is the mass of inorganic sediment layer 1 (g $m^{-2}$) and $\text{F\_tran}_{\text{Sin1}}$ the transport of inorganic sediment (g $m^{-2}$ $d^{-1}$).

Mixing of the sediment due to invertebrate consumption leads to a downward and an upward mixing of radionuclides adsorbed to inorganic sediment between layer 1 and 2 (mixx1 and mixx2, g RN $m^{-2}$ $d^{-1}$), described by:

$$\text{mixx1} = \text{k}_{\text{mixdown}} \cdot \text{SIN1}_{\text{XRN}} \frac{\text{F\_DO}_{\text{WB}}}{\text{F\_DO}_{\text{WB}} + \text{kh}_{\text{DOwb}}} \cdot \frac{\text{F\_DFC}}{\text{F\_DFC} + \text{kh}_{\text{DFC}}} \qquad 5\text{-}112$$

$$\text{mixx2} = \text{k}_{\text{mixup}} \cdot \text{SIN2}_{\text{XRN}} \frac{\text{F\_DO}_{\text{WB}}}{\text{F\_DO}_{\text{WB}} + \text{kh}_{\text{DOwb}}} \cdot \frac{\text{F\_DFC}}{\text{F\_DFC} + \text{kh}_{\text{DFC}}} \qquad 5\text{-}113$$

where $\text{SIN1}_{\text{XRN}}$ and $\text{SIN2}_{\text{XRN}}$ are the concentration of radionuclides adsorbed to inorganic sediment layer 1 and 2 (g RN $m^{-2}$), $k_{mixdown}$ and $k_{mixup}$ are the downward and upward mixing rates due to invertebrate consumption ($d^{-1}$), $kh_{DOwb}$ the half saturation concentration for processes related to dissolved oxygen in the water bed (g $O_2$ $m^{-3}$), $kh_{DFC}$ the half saturation constant for processes related to sediment deposit feeder carbon (g C $m^{-2}$) and the ecosystem model outputs of $\text{F\_DO}_{\text{WB}}$ is the concentration of dissolved oxygen in the water bed (g $O_2$ $m^{-3}$) and F_DFC the mass of deposit feeder carbon (g C $m^{-2}$).

### *Adsorbed radionuclides to inorganic sediment layer 2*

The amount of radionuclides adsorbed to inorganic sediment in subsurface sediment (i.e. model layer 2) is described by (Figure 5-1):

*–decay +adsorption –desorption –erosion +transport +mixing1 –mixing2*

Decay of radionuclides adsorbed to inorganic sediment layer 2 (dkssin2, g RN $m^{-2}$ $d^{-1}$) is described according to Equation 5-1.

Adsorption and desorption of radionuclides to inorganic sediment layer 2 (adsin2 and desin2, g RN $m^{-2}$ $d^{-1}$) are similar to the sorption processes described for radionuclides related to inorganic sediment layer 1 (Equation 5-106 and 5-107), but with parameters related to layer 2 instead of layer 1 ($RN_{dis2}$, $\text{Sin2}_{\text{XRN}}$, F_Sin2, dzs2, pors2).

Erosion of radionuclides adsorbed to inorganic sediment layer 2 (eroin2, g RN $m^{-2}$ $d^{-1}$) is similar to the erosion described for layer 1 (Equation 5-109), but with the parameters related to layer 2 instead of layer 1 ($Sin2_{XRN}$, F_Sin2, $F\_ero_{Sin2}$). The processes of transport due to consolidation and mixing due to invertebrate consumption are described under the section of radionuclides adsorbed to inorganic sediment layer 1 (Equation 5-111 to 5-113).

### 5.5.16 Organic sediment

#### *Adsorbed radionuclides to organic sediment layer 1*

The amount of radionuclides adsorbed to organic sediment in surface layer (i.e. model layer 1) is described by (Figure 5-2 to Figure 5-4):

*–decay +adsorption –desorption +sedimentation –erosion –mineralisation –grazing +excretion +death –transport –mixing1 +mixing2*

Decay of radionuclides adsorbed to organic sediment layer 1 (dksoca1, g RN $m^{-2}$ $d^{-1}$) is described according to Equation 5-1.

Adsorption of radionuclides to organic sediment layer 1 (adssoc1, g RN $m^{-2}$ $d^{-1}$) is described by:

$$\text{adssoc1} = \frac{k_s \cdot kd_{oc} \cdot 10^{-6} \cdot RN_{dis1} \cdot F\_Soc1}{dzs1 \cdot pors1} \qquad 5\text{-}114$$

where dzs1 is the thickness of sediment layer 1 (m), pors1 the porosity of sediment layer 1 ($m^3_{H2O}$ $m^{-3}_{bulk}$), $k_s$ the sorption rate in sediment ($d^{-1}$), $kd_{oc}$ the partitioning coefficient for organic carbon (l $kgC^{-1}$), $RN_{dis1}$ the concentration of dissolved radionuclides in sediment layer 1 (g RN $m^{-2}$) and F_SOC1 the ecosystem model output of the mass of organic sediment layer 1 (g C $m^{-2}$). Desorption of radionuclides from organic sediment layer 1 (desoc1, g RN $m^{-2}$ $d^{-1}$) follows:

$$\text{desoc1} = k_s \cdot SOC1_{XRN} \qquad 5\text{-}115$$

where $k_s$ is the sorption rate in sediment ($d^{-1}$) and $SOC1_{XRN}$ the amount of radionuclides adsorbed to organic sediment layer 1 (g RN $m^{-2}$).

Deposition (sedimentation from the water bed) of radionuclides adsorbed to phytoplankton and detritus onto sediment layer 1 (sedpca1 and seddca1, g RN m–2 d–1) is described by:

$$\text{sedpca1} = \frac{PC_{XRN} \cdot F\_dep_{PC}}{F\_PC} \qquad 5\text{-}116$$

$$\text{seddca1} = \frac{DC_{XRN} \cdot F\_dep_{DC}}{F\_DC} \qquad 5\text{-}117$$

where $PC_{XRN}$ and $DC_{XRN}$ are the concentration of radionuclides adsorbed to phytoplankton and detritus (g RN $m^{-3}$), and the ecosystem model outputs of F_PC and F_DC are the concentration of phytoplankton and detritus (g C $m^{-3}$) and $F\_dep_{PC}$ and $F\_dep_{DC}$ the deposition of phytoplankton and detritus from the water bed to sediment layer 1 (g C $m^{-2}$ $d^{-1}$).

Erosion of radionuclides adsorbed to organic sediment layer 1 (erosoca1, g RN $m^{-2}$ $d^{-1}$) add to the concentration of radionuclides adsorbed detritus and is described by:

$$\text{erosoca1} = \frac{SOC1_{XRN} \cdot F\_ero_{SOC1}}{F\_SOC1} \qquad 5\text{-}118$$

where $SOC1_{XRN}$ is the concentration of radionuclides adsorbed to organic sediment layer 1 (g RN $m^{-2}$) and the ecosystem model outputs of F_SOC1 is the mass of organic sediment layer 1 (g C $m^{-2}$) and $F\_ero_{SOC1}$ the erosion of organic sediment layer 1 (g C $m^{-2}$ $d^{-1}$).

Mineralisation of organic sediment causes a release of radionuclides adsorbed to organic sediment layer 1 (minsoca1, g RN $m^{-2}$ $d^{-1}$) to the pool of dissolved radionuclides in the pore water of sediment layer 1 and is described by:

$$\text{minsoca1} = \frac{SOC1_{XRN} \cdot F\_min_{SOC1}}{F\_SOC1} \qquad 5\text{-}119$$

where $SOC1_{XRN}$ is the concentration of radionuclides adsorbed to organic sediment layer 1 (g RN $m^{-2}$) and the ecosystem model outputs of F_SOC1 is the mass of organic sediment layer 1 (g C $m^{-2}$) and $F\_min_{SOC1}$ the erosion of organic sediment layer 1 (g C $m^{-2}$ $d^{-1}$). Organic sediment layer 1 is grazed by deposit feeders causing a reduction of the amount of radionuclides adsorbed to organic sediment layer 1 (grsoca1, g RN $m^{-2}$ $d^{-1}$), earlier described under the section of deposit feeders (Section 5.5.11).

Mussels are not described by a state variable, why the amount of grazed phytoplankton and detritus are not used for production but entirely to mussel respiration and excretion. The excretion cause a transport of radionuclides adsorbed to phytoplankton and detritus to organic sediment layer 1 (exmca1, g RN $m^{-2}$ $d^{-1}$):

$$exmca1 = (grmpca + grmdca - remca) \cdot dz \qquad 5\text{-}120$$

where dz is the water layer height (m), grmpca and grmdca the mussel grazing on radionuclides adsorbed to phytoplankton and detritus (g RN $m^{-2}$ $d^{-1}$, Sections 5.5.4 and 5.5.5) and remca the mussel respiration of adsorbed radionuclides (g RN $m^{-3}$ $d^{-1}$) described by:

$$remca = F\_remc \cdot \left( \frac{grmpca}{(F\_grmpc + F\_grmdc)} + \frac{grmdca}{(F\_grmpc + F\_grmdc)} \right) \qquad 5\text{-}121$$

where the ecosystem model outputs of F_remc is the mussel respiration of organic particles (g C $m^{-3}$ $d^{-1}$) and F_grmcp and F_grmdc the mussel filtration of phytoplankton and detritus (g C $m^{-3}$ $d^{-1}$).

Excretion by herbivorous invertebrates increases the amount of radionuclides adsorbed to organic sediment layer 1 (exbdchca and exbchca, g RN $m^{-2}$ $d^{-1}$), earlier described under the section for herbivorous invertebrates adsorbed radionuclides (Section 5.5.10). Death of macrophytes is divided into a part in water which adds to the pool of detritus and a part in sediment which adds to the pool of organic sediment layer 1 and thus to the amount of adsorbed radionuclides (deeca2soc1, g RN $m^{-2}$ $d^{-1}$), described by:

$$deeca2soc1 = \frac{EC_{XRN} \cdot F\_deec2SOC}{F\_EC} \qquad 5\text{-}122$$

where $EC_{XRN}$ is the amount of radionuclides adsorbed to macrophytes (g RN $m^{-2}$) and the ecosystem model outputs of F_EC the biomass of macrophytes (g C $m^{-2}$) and F_deec2SOC the part of dead macrophytes which is transferred to organic sediment layer 1 (g C $m^{-2}$ $d^{-1}$).

Death of macroalgae is transferred entirely to the organic sediment layer 1 (debdca, g C $m^{-2}$ $d^{-1}$) and is described under the section of macroalgae adsorbed radionuclides (Section 5.5.7). Also death of herbivorous invertebrates and deposit feeders (dehca and dedfca, g C $m^{-2}$ $d^{-1}$) adds to the pool of adsorbed radionuclides to organic sediment layer 1 earlier described under the respective sections (Sections 5.5.10 and 5.5.11). Settling of dead fish to the sediment causes a transfer of radionuclides adsorbed to dead fish gills to the organic sediment layer 1 (sedfcdam2, g C $m^{-2}$ $d^{-1}$), earlier described under the section of radionuclides adsorbed to dead fish (Section 5.5.14) multiplied with the water layer height (dz, m).

Consolidation of the sediment cause a transport of radionuclides adsorbed to organic sediment from layer 1 to 2 (trasoca, g RN $m^{-2}$ $d^{-1}$), described by:

$$trasoca = \frac{SOC1_{XRN} \cdot F\_tran_{SOC1}}{F\_SOC1} \qquad 5\text{-}123$$

where $SOC1_{XRN}$ is the concentration of radionuclides adsorbed to organic sediment layer 1 (g RN $m^{-2}$) and the ecosystem model outputs of F_SOC1 is the mass of organic sediment layer 1 (g C $m^{-2}$) and $F\_tran_{SOC1}$ the transport of organic sediment (g C $m^{-2}$ $d^{-1}$).

Mixing of the sediment due to invertebrate consumption leads to a downward and an upward mixing of radionuclides adsorbed to organic sediment between layer 1 and 2 (mixsoca1 and mixsoca2, g RN $m^{-2}$ $d^{-1}$), described by:

$$mixsoca1 = k_{mixdown} \cdot SOC1_{XRN} \frac{F\_DO_{WB}}{F\_DO_{WB} + kh_{DOwb}} \cdot \frac{F\_DFC}{F\_DFC + kh_{DFC}} \qquad 5\text{-}124$$

$$\text{mixsoca2} = k_{\text{mixup}} \cdot SOC2_{XRN} \frac{F\_DO_{WB}}{F\_DO_{WB} + kh_{DOwb}} \cdot \frac{F\_DFC}{F\_DFC + kh_{DFC}} \qquad 5\text{-}125$$

where $SOC1_{XRN}$ and $SOC2_{XRN}$ are the concentration of radionuclides adsorbed to organic sediment layer 1 and 2 (g RN $m^{-2}$), $k_{mixdown}$ and $k_{mixup}$ are the downward and upward mixing rates due to invertebrate consumption ($d^{-1}$), $kh_{DOwb}$ the half saturation concentration for processes related to dissolved oxygen in the water bed (g $O_2$ $m^{-3}$), $kh_{DFC}$ the half saturation constant for processes related to sediment deposit feeder carbon (g C $m^{-2}$) and the ecosystem model outputs of $F\_DO_{WB}$ is the concentration of dissolved oxygen in the water bed (g $O_2$ $m^{-3}$) and F_DFC the mass of deposit feeder carbon (g C $m^{-2}$).

### *Adsorbed radionuclides to organic sediment layer 2*

The amount of radionuclides adsorbed to organic sediment in subsurface layer (i.e. model layer 2) is described by (Figure 5-2 to Figure 5-4):

*–decay +adsorption –desorption –erosion –mineralisation +transport +mixing1 –mixing2*

Decay of radionuclides adsorbed to organic sediment layer 2 (dksoca2, g RN $m^{-2}$ $d^{-1}$) is described according to Equation 5-1. Adsorption and desorption of radionuclides to organic sediment layer 2 (adssoc2 and dessoc2, g RN $m^{-2}$ $d^{-1}$) are similar to the sorption processes described for radionuclides related to organic sediment layer 1 (Equation 5-114 and 5-115), but with parameters related to layer 2 instead of layer 1 ($RN_{dis2}$, $SOC2_{XRN}$, F_SOC2, dzs2, pors2).

Erosion and mineralisation of radionuclides adsorbed to organic sediment layer 2 (erosoca2 and minsoca2, g RN $m^{-2}$ $d^{-1}$) are similar to the erosion and mineralisation described for layer 1 (Equation 5-118 and 5-119), but with the parameters related to layer 2 instead of layer 1 ($SOC2_{XRN}$, F_SOC2, $F\_ero_{SOC2}$ and $F\_min_{SOC2}$). Transport due to consolidation and mixing due to invertebrate consumption (trasoci, mixsoca1 and mixsoca2, g RN $m^{-2}$ $d^{-1}$) is described under the section for radionuclides adsorbed to organic sediment layer 1 (Equation 5-123 to 5-125).

### *Internal radionuclides in organic sediment layer 1*

The amount of radionuclides internal in organic sediment in surface layer (model layer 1) is described by (Figure 5-2 to Figure 5-4):

*–decay +sedimentation –erosion –mineralisation –grazing +excretion +death –transport –mixing1 +mixing2*

Decay of radionuclides internal in organic sediment layer 1 (dksoci1, g RN $m^{-2}$ $d^{-1}$) is described according to Equation 5-1. The processes describing the flow of radionuclides internal in organic sediment layer 1 are similar to the processes for radionuclides adsorbed to organic sediment layer 1, only with the adsorbed radionuclides replaced with internal concentration of radionuclides:

Deposition of radionuclides internal in phytoplankton and detritus onto sediment layer 1 (sedpci1 and seddci1, g RN $m^{-2}$ $d^{-1}$) are similar to Equation 5-116 and 5-117, with adsorbed radionuclides replaced with internal ($PC_{INRN}$ and $DC_{INRN,}$ g RN $m^{-3}$). Erosion of radionuclides internal in organic sediment layer 1 (erosoci1, g RN $m^{-2}$ $d^{-1}$) is similar to Equation 5-118, with adsorbed radionuclides replaced with internal ($SOC1_{INRN}$, g RN $m^{-2}$).

Mineralisation of radionuclides internal in organic sediment layer 1 (minsoci1, g RN $m^{-2}$ $d^{-1}$) is similar to Equation 5-119, with adsorbed radionuclides replaced with internal ($SOC1_{INRN}$, g RN $m^{-2}$). Grazing by deposit feeders on radionuclides internal in organic sediment layer 1 (grsoci1, g RN $m^{-2}$ $d^{-1}$), is earlier described under the section for deposit feeders (Section 5.5.11).

Excretion by mussels (exmci1, g RN $m^{-2}$ $d^{-1}$) are similar to Equation 5-120 and 5-121, with processes related to adsorption replaced with internal (grmpci, grmdci and remci, g RN $m^{-2}$ $d^{-1}$). Excretion by herbivorous invertebrates (exbdchci and exbchci, g RN $m^{-2}$ $d^{-1}$), is earlier described under the section for herbivorous invertebrates (Section 5.5.10).

Death of macrophytes adding to the pool of radionuclides internal in organic sediment layer 1 (deeci2soc1, g RN $m^{-2}$ $d^{-1}$), is similar to Equation 5-122, with adsorbed radionuclides replaced with internal for $EC_{INRN}$ (g RN $m^{-2}$). Death of macroalgae (debdci, g C $m^{-2}$ $d^{-1}$) is earlier described under the sections of macroalgae (Section 5.5.7). Death of herbivorous invertebrates (dehci, g C $m^{-2}$ $d^{-1}$) and deposit feeders dedfci, g C $m^{-2}$ $d^{-1}$) are earlier described under their respective sections (Sections 5.5.10 and 5.5.11). Settling of radionuclides internal in dead fish (sedfcdim2, g C $m^{-2}$ $d^{-1}$), is earlier described under the sections of dead fish (Section 5.5.14) multiplied with the water layer height (dz, m).

Transport of radionuclides internal in organic sediment layer 1 due to consolidation (trasoci, g RN $m^{-2}$ $d^{-1}$) is similar to Equation 5-123, with adsorbed radionuclides replaced with internal ($SOC1_{INRN}$, g RN $m^{-2}$). Mixing of the sediment due to invertebrate consumption leads to a downward and an upward mixing of radionuclides internal in organic sediment between layer 1 and 2 (mixsoci1 and mixsoci2, g RN $m^{-2}$ $d^{-1}$) similar to Equation 5-124 and 5-125, with adsorbed radionuclides replaced with internal ($SOC1_{INRN}$ and $SOC2_{INRN}$, g RN $m^{-2}$).

#### *Internal radionuclides in organic sediment layer 2*

The amount of radionuclides internal in organic sediment subsurface layer (model layer 2) is described by (Figure 5-2 to Figure 5-4):

*–decay –erosion –mineralisation +transport +mixing1 –mixing2*

Decay of radionuclides internal in sediment layer 2 (dksoci2, g RN $m^{-2}$ $d^{-1}$) is described according to Equation 5-1. Erosion and mineralisation of radionuclides internal in organic sediment layer 2 (erosoci2 and minsoci2, g RN $m^{-2}$ $d^{-1}$) are similar to the erosion and mineralisation described for radionuclides adsorbed to organic sediment layer 1 (Equation 5-118 and 5-119), but with the parameters related to internal concentrations and to layer 2 instead of layer 1 ($SOC2_{INRN}$, F_SOC2, $F\_ero_{SOC2}$ and $F\_min_{SOC2}$).

Transport due to consolidation and mixing due to invertebrate consumption (trasoci, mixsoci1 and mixsoci2, g RN $m^{-2}$ $d^{-1}$) similar to the transport and mixing described for radionuclides adsorbed to organic sediment layer 1 (Equation 5-123 to 5-125), but with adsorbed radionuclides replaced with internal ($SOC1_{INRN}$ and $SOC2_{INRN}$, g RN $m^{-2}$).

### 5.5.17 Precipitated radionuclides

#### *Precipitated radionuclides in sediment layer 1*

The amount of radionuclides precipitated in sediment surface layer (model layer 1) is described by (Figure 5-1):

*–decay +precipitation –dissolution –erosion –transport –mixing1 +mixing2*

Decay of radionuclides precipitated in sediment layer 1 (dkprn1, g RN $m^{-2}$ $d^{-1}$) is described according to Equation 5-1.

Precipitation of radionuclides takes place in anoxic sediment and dissolution of precipitated radionuclides takes place when oxygen is present (prec1 and diss1, g RN $m^{-2}$ $d^{-1}$):

$$prec1 = k_{prec} \cdot RN_{dis1} \cdot \frac{dzs1 - \min(F\_KDOX, dzs1)}{dzs1} \qquad 5\text{-}126$$

$$diss1 = k_{diss} \cdot Sed1_{PRN} \cdot \left(1 - \frac{dzs1 - \min(F\_KDOX, dzs1)}{dzs1}\right) \qquad 5\text{-}127$$

where $k_{prec}$ and $k_{diss}$ are the precipitation and dissolution rates ($d^{-1}$), $RN_{dis1}$ the concentration of dissolved radionuclides in sediment pore water layer 1 (g RN $m^{-2}$), $Sed1_{PRN}$ the amount of precipitated radionuclides in sediment pore water. The fraction describes the depth of oxygen penetration, i.e. the percentage of sediment without and with oxygen in layer 1, where dzs1 is the thickness of sediment layer 1 (m), F_KDOX the depth of nitrate penetration in the sediment (m) and min(a,b) returns the minimum value.

Erosion of precipitated radionuclides from the sediment to the water causes dissolution of the radionuclides and thus the erosion add to the pool dissolved radionuclides. The erosion of precipitated radionuclides in sediment layer 1 (eroprn1, g RN $m^{-2}$ $d^{-1}$) is described by:

$$eroprn1 = \frac{Sed1_{PRN} \cdot F\_ero_{Sin1}}{F\_Sin1} \qquad 5\text{-}128$$

where $Sed1_{PRN}$ is the concentration of precipitated radionuclides in sediment layer 1 (g RN $m^{-2}$) and the ecosystem model outputs of F_Sin1 is the mass of inorganic sediment layer 1 (g $m^{-2}$) and $F\_ero_{Sin1}$ the erosion of inorganic sediment layer 1 (g $m^{-2}$ $d^{-1}$).

Consolidation of the sediment cause a transport of precipitated radionuclides from sediment layer 1 to 2 (traprn, g RN $m^{-2}$ $d^{-1}$), described by:

$$traprn1 = \frac{Sed1_{PRN} \cdot F\_tran_{Sin1}}{F\_Sin1} \qquad 5\text{-}129$$

where $Sed1_{PRN}$ is the concentration of precipitated radionuclides in sediment layer 1 (g RN $m^{-2}$) and the ecosystem model outputs of F_Sin1 is the mass of inorganic sediment layer 1 (g $m^{-2}$) and $F\_tran_{Sin1}$ the transport of inorganic sediment (g $m^{-2}$ $d^{-1}$).

Mixing of the sediment due to invertebrate consumption leads to a downward and an upward mixing of precipitated radionuclides between sediment layer 1 and 2 (mixp1 and mixp2, g RN $m^{-2}$ $d^{-1}$), described by:

$$mixp1 = k_{mixdown} \cdot Sed1_{PRN} \frac{F\_DO_{WB}}{F\_DO_{WB} + kh_{DOwb}} \cdot \frac{F\_DFC}{F\_DFC + kh_{DFC}} \qquad 5\text{-}130$$

$$mixp2 = k_{mixup} \cdot Sed2_{PRN} \frac{F\_DO_{WB}}{F\_DO_{WB} + kh_{DOwb}} \cdot \frac{F\_DFC}{F\_DFC + kh_{DFC}} \qquad 5\text{-}131$$

where $Sed1_{PRN}$ and $Sed2_{PRN}$ are the amount of precipitated radionuclides in sediment layer 1 and 2 (g RN $m^{-2}$), $k_{mixdown}$ and $k_{mixup}$ are the downward and upward mixing rates due to invertebrate consumption ($d^{-1}$), $kh_{DOwb}$ the half saturation concentration for processes related to dissolved oxygen in the water bed (g $O_2$ $m^{-3}$), $kh_{DFC}$ the half saturation constant for processes related to sediment deposit feeder carbon (g C $m^{-2}$) and the ecosystem model outputs of $F\_DO_{WB}$ is the concentration of dissolved oxygen in the water bed (g $O_2$ $m^{-3}$) and F_DFC the mass of deposit feeder carbon (g C $m^{-2}$).

### *Precipitated radionuclides in sediment layer 2*

The amount of radionuclides precipitated in subsurface sediment (model layer 2) is described by (Figure 5-1):

*–decay +precipitation –dissolution –erosion +transport +mixing1 –mixing2*

Decay of radionuclides precipitated in sediment layer 2 (dkprn2, g RN $m^{-2}$ $d^{-1}$) is described according to Equation 5-1.

Precipitation in sediment layer 2 ( prec2, g RN $m^{-2}$ $d^{-1}$) is described by:

$$prec2 = k_{prec} \cdot RN_{dis2} \qquad 5\text{-}132$$

if F_KDOX < dzs1, and by

$$prec2 = k_{prec} \cdot RN_{dis2} \cdot \frac{dzs2 - MIN(F\_KDOX - dzs1, dzs2)}{dzs2} \qquad 5\text{-}133$$

if F_KDOX ≥ dzs1

Dissolution of radionuclides in sediment layer 2 (diss2, g RN $m^{-2}$ $d^{-1}$) is described by:

$$diss2 = 0 \qquad 5\text{-}134$$

if F_KDOX < dzs1, and by

$$diss2 = k_{diss} \cdot Sed2_{PRN} \cdot \left(1 - \frac{dzs2 - MIN(F\_KDOX - dzs1, dzs2)}{dzs2}\right) \quad 5\text{-}135$$

if F_KDOX ≥ dzs1

where $k_{prec}$ and $k_{diss}$ are the precipitation and dissolution rates ($d^{-1}$), $RN_{dis2}$ the concentration of dissolved radionuclides in sediment pore water layer 2 (g RN $m^{-2}$), $Sed2_{PRN}$ the amount of precipitated radionuclides in pore water of sediment layer 2. The status of F_KDOX < dzs1 describes whether oxygen is already depleted in layer 1. In numerical terms the fraction describes the depth of oxygen penetration, i.e. the percentage of sediment without and with oxygen in layer 2, where dzs1 and dzs2 is the thickness of sediment layer 1 and 2 (m), F_KDOX the depth of nitrate penetration in the sediment (m) and *MIN*(a,b) returns the minimum value.

Erosion of precipitated radionuclides in sediment layer 2 (eroprn2, g RN $m^{-2}\,d^{-1}$) are similar to the erosion described for precipitated radionuclides in sediment layer 1 (Equation 5-128), but with the parameters related to layer 2 instead of layer 1 ($Sed2_{PRN}$, F_SIN2 and $F\_ero_{Sin2}$). Transport due to consolidation and mixing due to invertebrate consumption (traprn, mixp1 and mixp2, g RN $m^{-2}\,d^{-1}$) are described under the section of precipitated radionuclides in sediment layer 1 (Equation 5-129 to 5-131).

# 6 Application of the radionuclide model to the Forsmark area

## 6.1 Release scenario and radionuclides selected for modelling

Various radionuclides may potentially be released to the aquatic environment from a deep repository of spent nuclear fuel. Six radionuclides were chosen to be included in the radionuclide model. In addition, C-14 was included for comparison, as this element can be regarded as a tracer for organic carbon (C-12), being subject to accumulation, metabolism to $^{14}CO_2$ and excretion. The radionuclides were chosen because in earlier studies they appeared to be of interest in the safety assessment and because they represent a wide range of partitioning coefficients ($K_d$). Table 5-4 shows the radionuclides selected and the values of partition coefficients chosen for modelling in comparison with $K_d$ values recommended by the IAEA, $K_d$ values from a previous study and site specific $K_d$ values used by SKB in the safety assessment (SR-Site) /IAEA 2004, Kumblad and Kautsky 2004, Nordén et al. 2010/.

The radionuclides were introduced to the model by groundwater inflow at a rate of 1 Bq/year, total for all basins. Individual radionuclides were introduced to the groundwater at a flow-proportional rate, and groundwater was then introduced to sediment Layer 2. The location of release areas is depicted in Figure 6-1.

Annual groundwater flow, $A_{gwf}$ ($m^3\ year^{-1}$ *or* $L\ year^{-1}$), was calculated from daily groundwater flow, $D_{gwf}$ ($m^3\ day^{-1}$ *or* $L\ Day^{-1}$), based on data from the discharge areas ($mm\ d^{-1}$) in the model area assuming mm $d^{-1}$ is equal to L $m^{-2}$. The daily groundwater flow was calculated based on MIKE SHE modelling /Bosson et al. 2008/.

$$\sum_{t365}^{t0} Dgwf1 + Dgwf2 \ldots$$

The total annual groundwater flow in the Forsmark area was calculated to be 92.3 $m^3$, resulting in an average daily groundwater flow of 0.253 $m^3$, and an average radionuclide concentration in groundwater of 0.0108 Bq $m^{-3}$. The distribution of total groundwater flow and radionuclide release between basins is shown in Table 6-1.

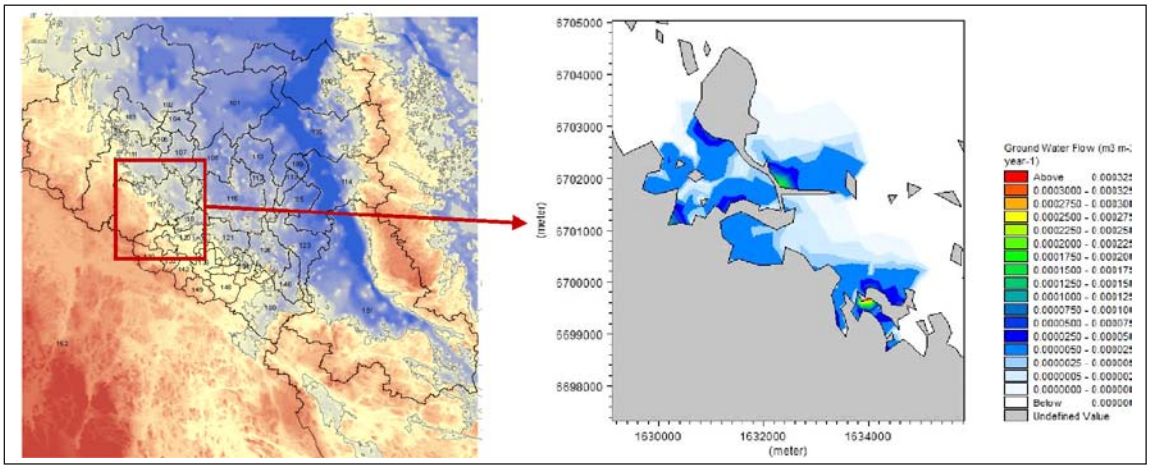


***Figure 6-1.*** *Locations of groundwater inflow and input of radionuclides into the model area.*

**Table 6-1. Groundwater flow into and radionuclide input to 6 model basins, from /Bosson et al. 2008/.**

| Basin | Groundwater flow ($m^3$ $year^{-1}$) | RN release Bq $year^{-1}$ |
|---|---|---|
| 116 | 22.5 | 0.24 |
| 117 | 14.4 | 0.16 |
| 118 | 16.0 | 0.17 |
| 120 | 5.2 | 0.06 |
| 121 | 23.5 | 0.25 |
| 134 | 10.7 | 0.12 |
| Total | 92.3 | 1.00 |

## 6.2 Results

The fate of the modelled radionuclides in water and in organisms invariable will be a result of the assumptions and definitions made as well as how the hydrodynamic, ecosystem and radionuclide models have been linked. In the following we focus on presenting the results from the following perspectives:

- Relative distribution of radionuclides in abiotic fractions (sediment and water column).
- Spatial variation of radionuclides in water, sediment and biota.
- Temporal and spatial variation of bioconcentration factors (BCFs), using Ra-226 as an example.
- BCF per functional group and radionuclide.
- BCF per functional group and basin.
- Comparative analysis for basin 116.

It should be pointed out that uneven distribution of radionuclides in water and matter, especially occurrences of very low concentrations, can bias comparisons between basins if based on average values. Accordingly, in the following presentation of results, median values of radionuclide distribution and concentration have been used in all cases except the temporal analysis of BCF (see below).

### 6.2.1 Radionuclide concentrations in abiotic compartments of sediment and water

Modelled concentrations of radionuclides in water and sediment (Bq $m^{-3}$) are shown in Table 6-2 for Basin 116. Basically, the resulting concentrations are a result of the amount of radionuclide released, the characteristics of the receiving water and sediment, and the model assumptions concerning partition coefficients between sediments and water.

**Table 6-2. Modelled concentration (Bq $m^{-3}$) of 6 radionuclides in abiotic fractions in Basin 116 following release of 0.24 Bq $y^{-1}$ of each radionuclide. Data after 8 years of simulation. Values represent median values of all grid cells in the basin.**

| Compartment | Cl-36 | Cs-135 | Nb-94 | Ni-59 | Ra-226 | Th-230 |
|---|---|---|---|---|---|---|
| Water: dissolved | 1.92E-08 | 1.31E-08 | 1.76E-08 | 1.87E-08 | 1.72E-08 | 6.01E-9 |
| Water: particle bound | 6.10E-11 | 2.98E-10 | 1.94E-09 | 7.38E-10 | 5.86E-10 | 1.28E-09 |
| Sed layer 1: pore water | 7.32E-11 | 8.78E-11 | 2.08E-10 | 1.98E-10 | 2.20E-10 | 2.06E-11 |
| Sed layer 1: adsorb to inorganic | 2.84E-09 | 2.23E-08 | 1.76E-07 | 5.25E-08 | 4.61E-08 | 3.90E-08 |
| Sed layer 1: adsorb to organic | 1.71E-11 | 1.75E-08 | 1.80E-08 | 4.37E-08 | 7.43E-08 | 1.02E-07 |
| Sed layer 1: absorb into organic | - | 7.50E-09 | 5.06E-09 | 1.43E-08 | 2.23E-08 | 2.78E-08 |
| Sed layer 2: pore water | 4.39E-10 | 5.15E-09 | 2.12E-08 | 1.46E-08 | 1.98E-08 | 2.01E-08 |
| Sed layer 2: adsorb to inorganic | 2.50E-09 | 2.13E-08 | 1.70E-07 | 4.99E-08 | 4.39E-08 | 3.73E-08 |
| Sed layer 2: adsorb to organic | 1.46E-11 | 1.65E-08 | 1.70E-08 | 4.22E-08 | 7.36E-08 | 9.69E-08 |
| Sed layer 2: absorb into organic | 3.66E-12 | 7.16E-09 | 4.85E-09 | 1.36E-08 | 2.12E-08 | 2.62E-08 |

By applying a dimensionless approach, the inherent physico-chemical properties of the different radionuclides can be illustrated (Figure 6-2). Cl-36, which is characterized by a very low affinity to inorganic and organic surfaces and low partition coefficients (0.06 and 0.02, see Table 6-2), primarily occurs in the water column (76%), while the sediment-associated fractions add up to 12% in Layers 1 and 2. At the other end of the spectrum, only 2% of Th-230, with the highest partition coefficients among the selected radionuclides, occurs in the water column, while sediment fractions account for 51% and 47% of the "abiotic activity" in Layer 2 and Layer 1. The low mobility of radionuclides with high partition coefficients is illustrated by the difference in concentrations in Layer 2 and Layer 1, i.e. a higher enrichment in Layer 2 – where the radionuclide is released – compared with Layer 1. In contrast, the concentration of Cl-36 was similar in the two sediment layers due to the high mobility of chloride.

The analysis was repeated for several basins in the Forsmark area, and except for absolute concentrations, the distribution between the inorganic compartments was comparable to the results for basin 116. This leads to the conclusion that the main driver that affects the relative distribution of radionuclides between abiotic components such as water and sediment is the partition coefficients, rather than differences in the characteristics of the different basins.

### 6.2.2 Spatial variations of radionuclides in water, sediment and biota – comparisons of Cs-135 and Ra-226

Due to high partition coefficients, $K_d$s, most radionuclides are associated with sediments. Their spread from release areas primarily occurs through resuspension events and subsequent sedimentation, especially for those radionuclides with high $K_d$s such as Cs-135. Figure 6-3 shows the spatial distribution of Cs-135 and Ra-226 in the upper sediment layer in terms of activity (Bq/m$^2$) after 8 years of modelling in the whole model area.

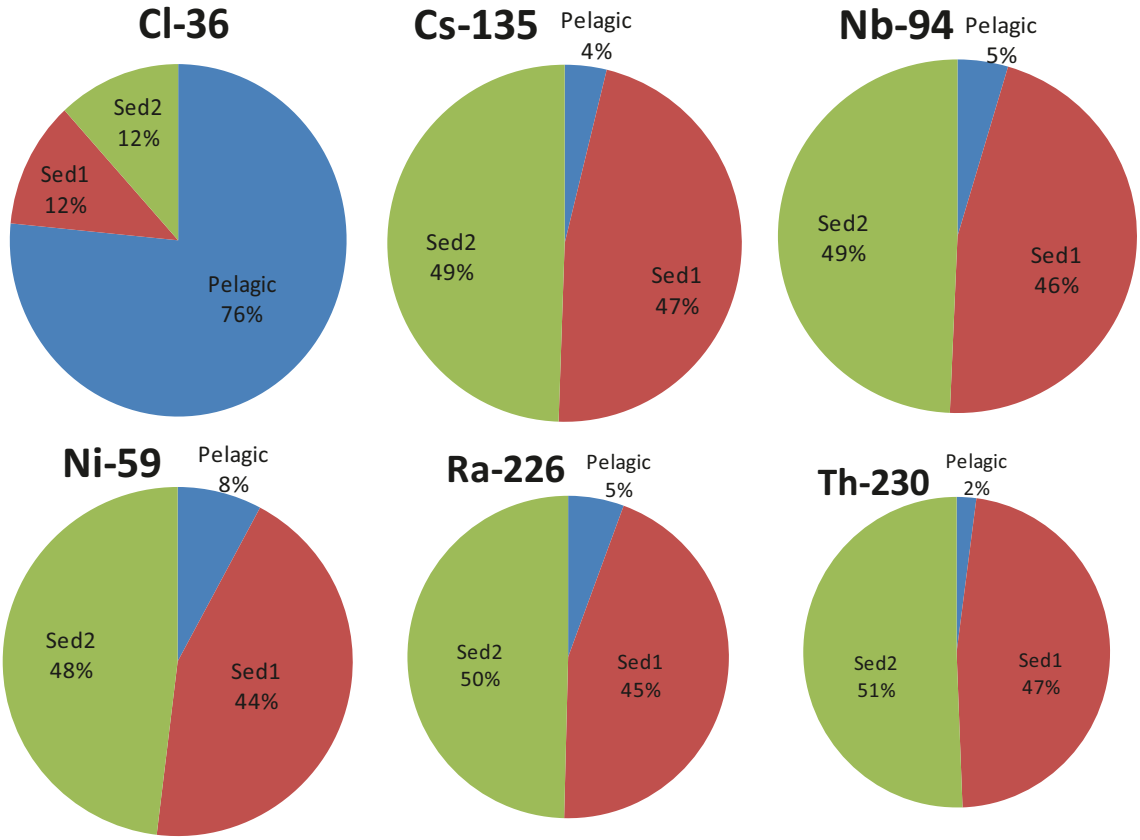


***Figure 6-2.*** *Relative distribution of 6 radionuclides, in basin 116, between non-biotic components in the ecosystem model. Sediment compartments include radionuclides adsorbed to inorganic and organic surfaces, absorbed into organic matter and dissolved in pore water. Radionuclides in the pelagic compartment include radionuclides in solution and radionuclides adsorbed to non-living particles.*

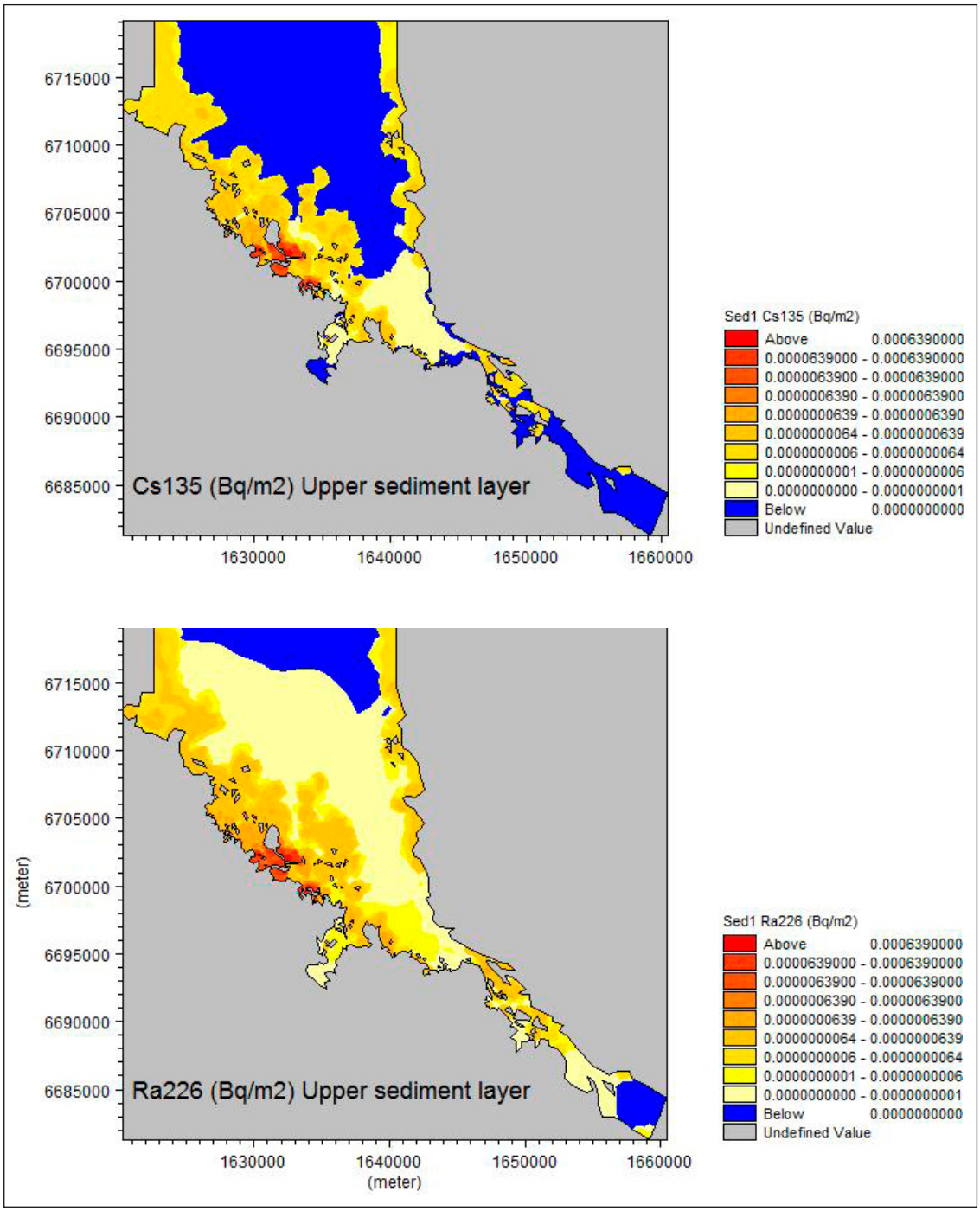


***Figure 6-3.*** *Modelled concentration of Cs-135 and Ra-226 in upper sediment layer; concentrations given in activity (Bq/m²). The source strength was identical for both radionuclides at 1 Bq/y for the whole model area. Results after 8 years' modelling.*

The activity of Ra-226 in surface sediments is predicted to occur almost over all of Öregrundsgrepen, due to a relatively low partition coefficient and a higher fraction occurring in the water column. In contrast, the physical spread of Cs-135 from release areas (see Figure 6-1) is less extensive due to a higher partition coefficient.

Due to lower partition coefficients, a larger fraction of Ra-226 is released from sediments compared with Cs-135. The higher rate of release from sediments results in a higher level of activity in phytoplankton, see Figure 6-4.

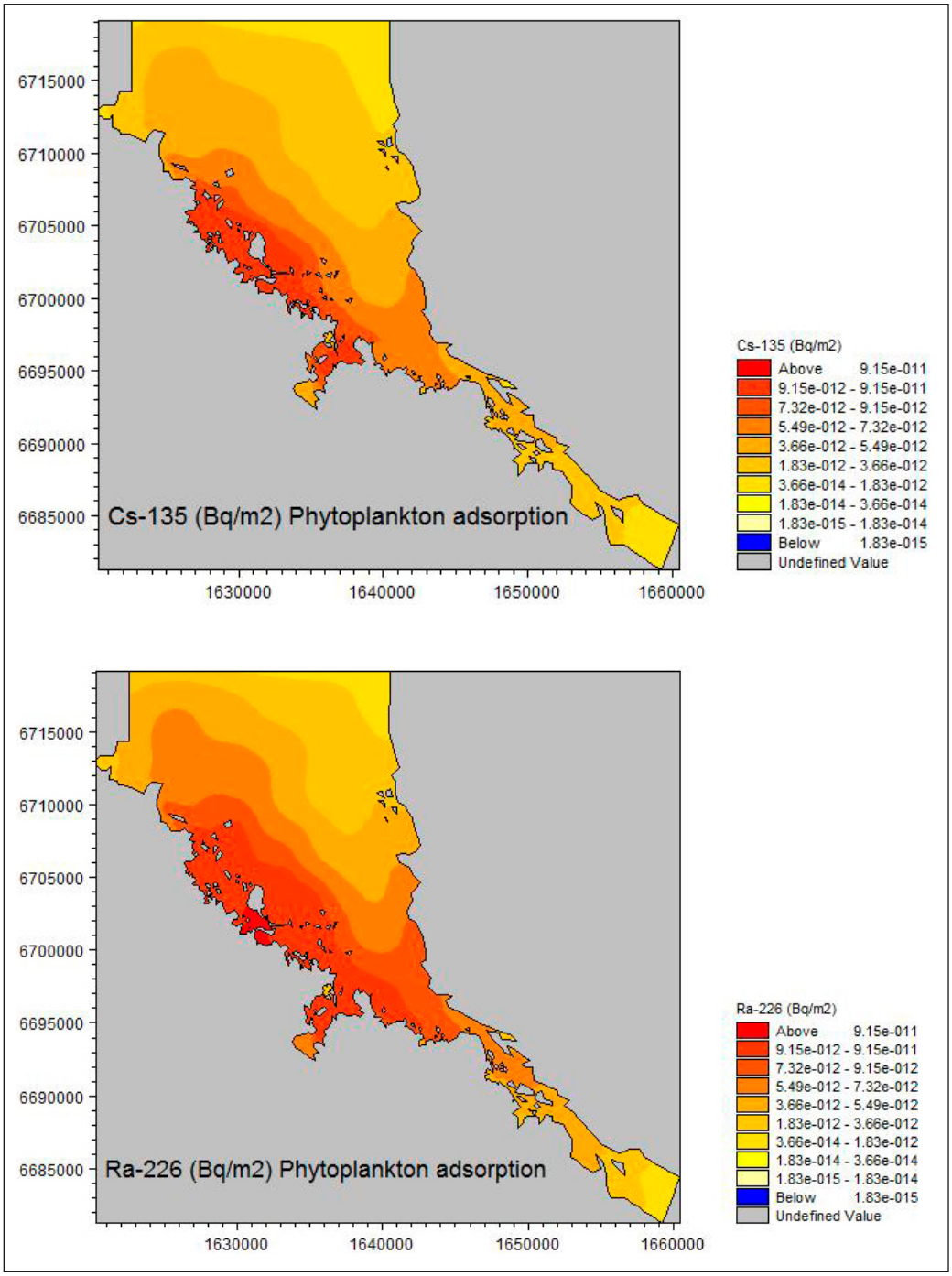


***Figure 6-4.*** *Modelled activity of Cs-135 (upper) and Ra-226 (lower) adsorbed to phytoplankton. Results after 8 years' modelling.*

The modelled radium activity in sediments is also reflected in deposit feeders, which exhibit a larger area with Ra-226 activity compared with Cs-135, and the difference in activity is cascaded to benthic predators, which also exhibit a wider spread of Ra-226 compared with Cs-135 (Figures 6-5 and 6-6).

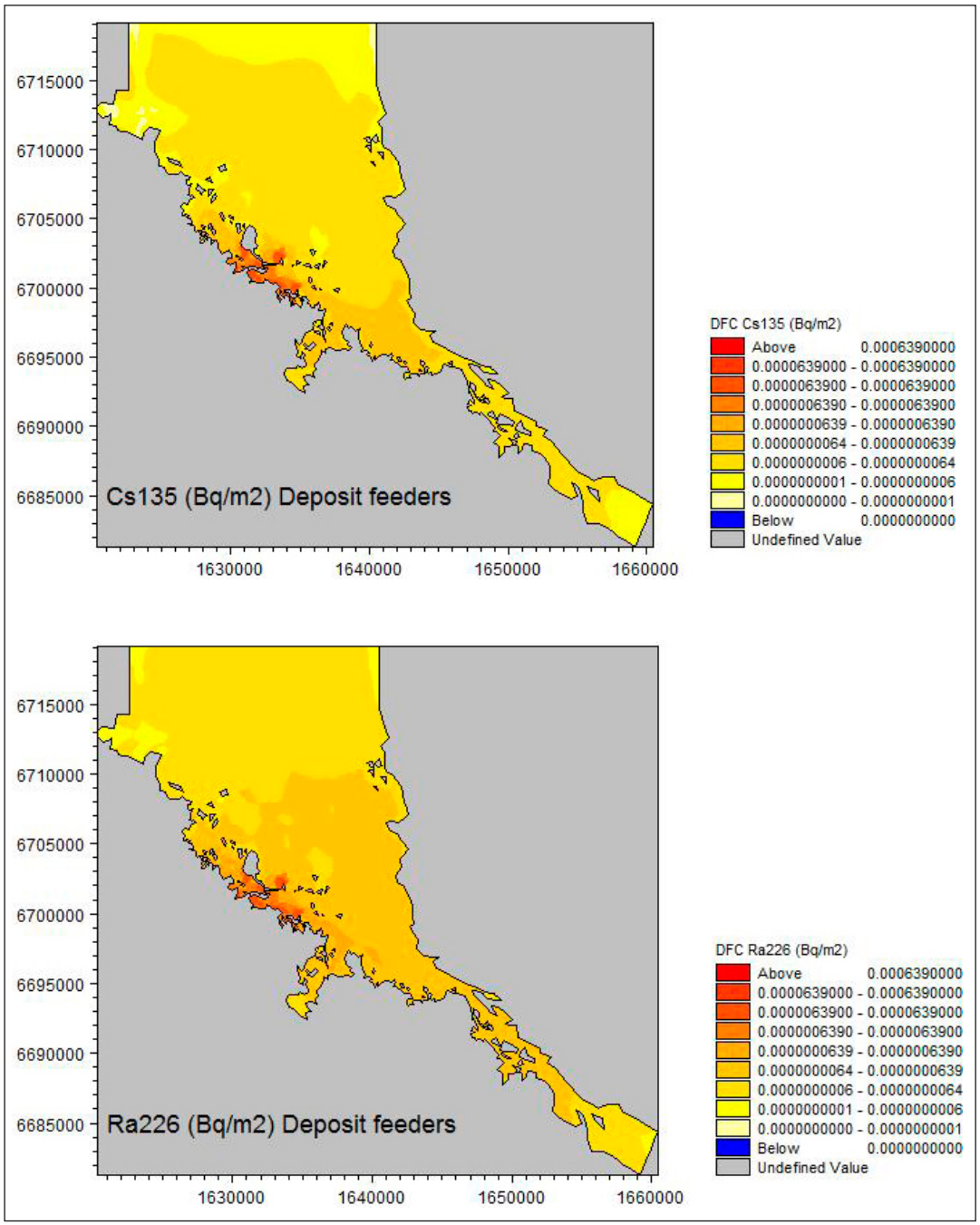


***Figure 6-5.*** *Modelled activity of Cs-135 (upper) and Ra-226 (lower) accumulated in deposit feeders. Results after 8 years' modelling.*

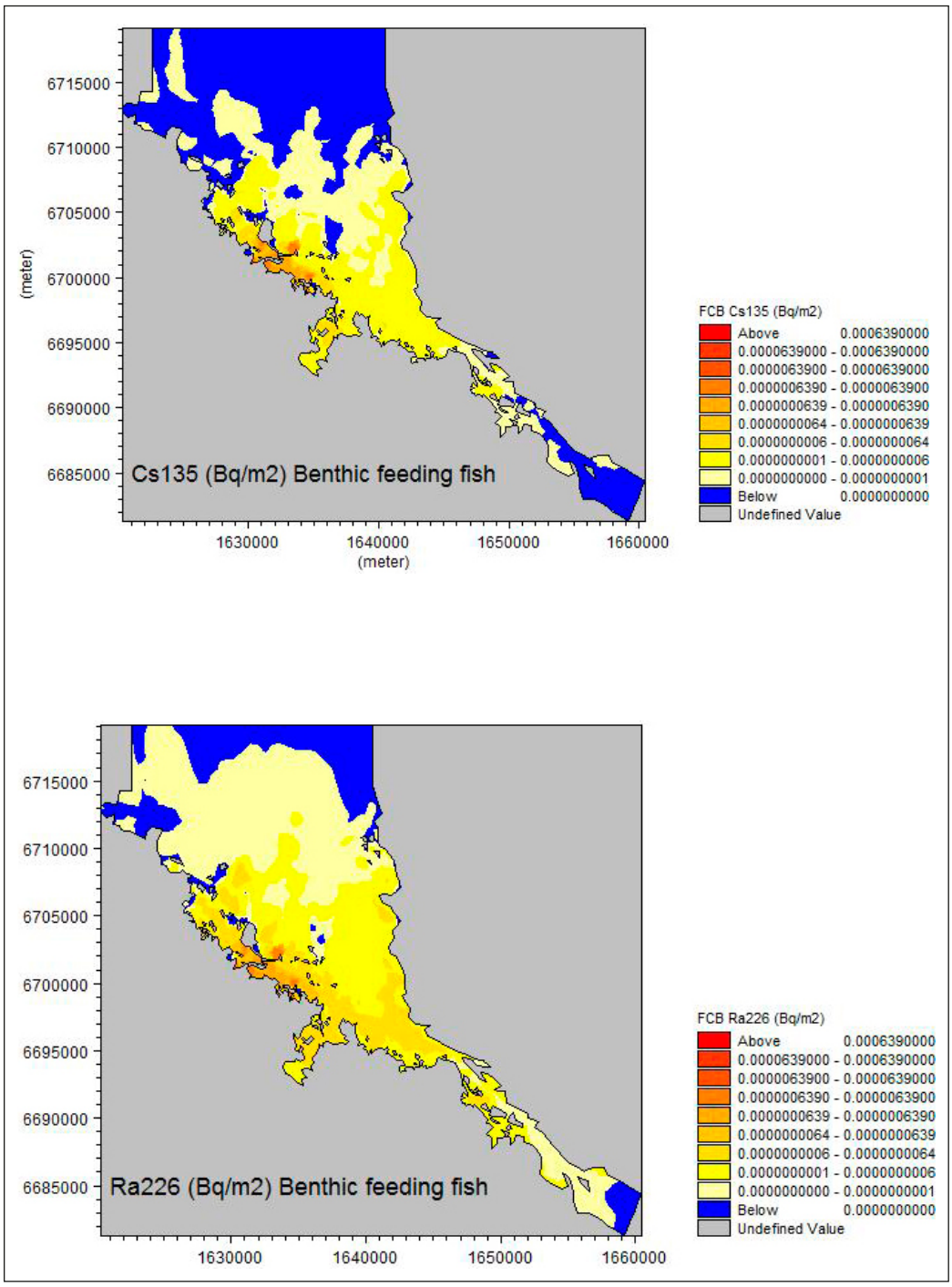


***Figure 6-6.*** *Modelled activity of Cs-135 (upper) and Ra-226 (lower) accumulated in benthic predators. Results after 8 years' modelling.*

### 6.2.3 Temporal and spatial variation in BCF

#### *Temporal characteristics – Ra-226*

To illustrate the variation in BCF, a time series for Ra-226 was sampled (from model results covering the 8th year of modelling from 1 January to 31 December) in 4 grid cells (Figure 6-7; Points 1–4). Almost independently of the distance from release point of Ra-226 (Point 1, see also Figure 6-1, where the area of groundwater release of radionuclides is presented), the temporal variation in BCF for phytoplankton shows similar patterns for all positions, i.e. a peak in January, stable values from April through September followed by a gradual increase through the autumn (Figure 6-8). The temporal variation in BCF is dependent on both variations in water concentration (especially near release from sediments, e.g. Point 1) and variations in algal biomass, with a dominance of the latter influence at increasing distance from radionuclide release.

Using a log-normal function, 75% of the variation in BCF could be explained by variation in algal biomass at Point 4 (Figure 6-9). The function indicates that radionuclide adsorption to phytoplankton is an important process in regulating the proportion between dissolved and particle-bound radionuclides, but also calls into question the concept of applying a fixed BFC value of a particular radionuclide to any environment.

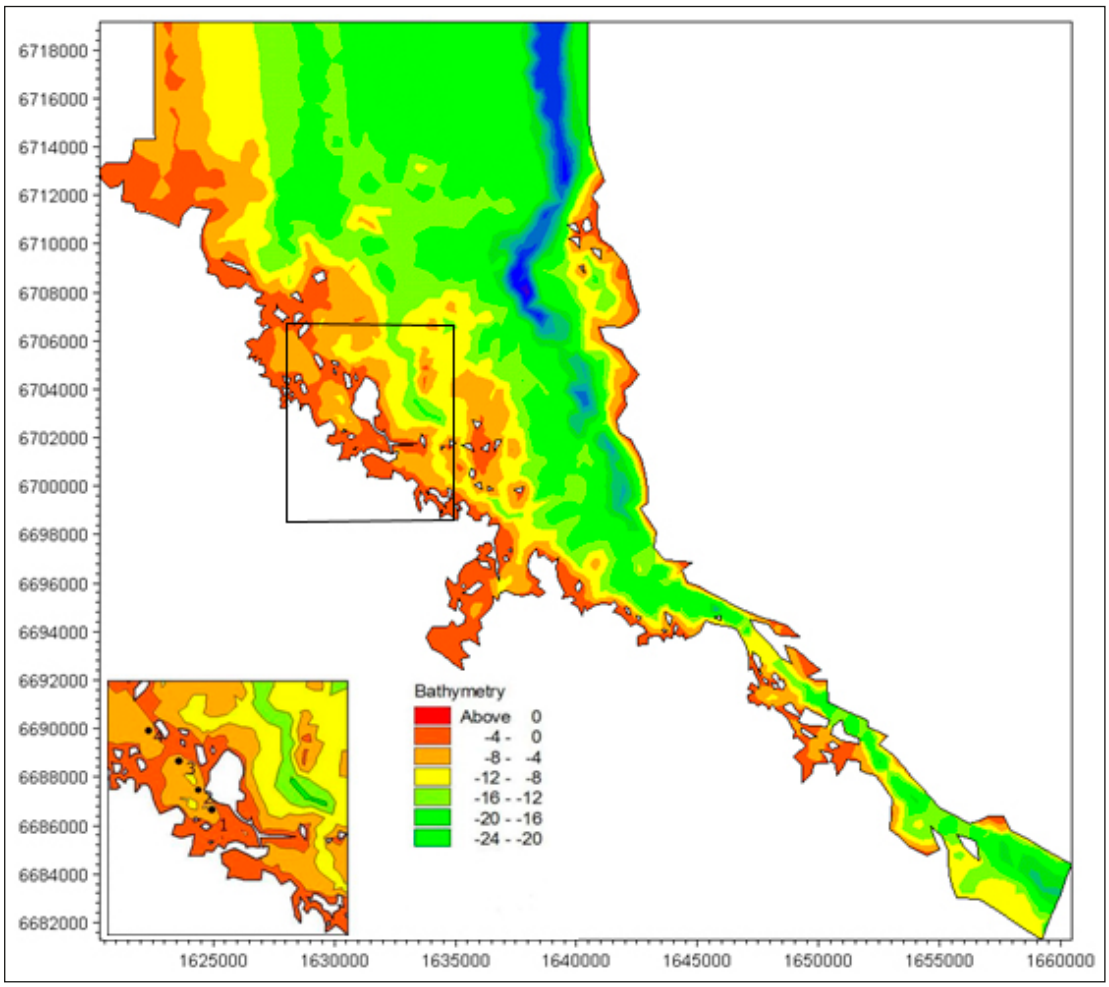


***Figure 6-7.*** *Location of model sampling points (1–4) where temporal data on BCF in phytoplankton were sampled in model results. Point 1 represents a grid cell where radionuclides are released into sediment Layer 2.*

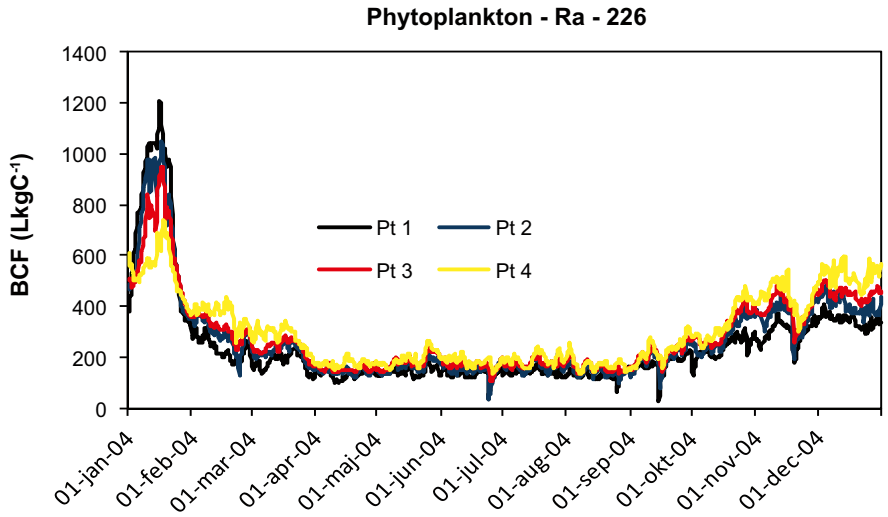


***Figure 6-8.*** *Modelled BCF (biological concentration factor) for Ra-226 during a year. Points 1 to 4 represent sites with an increasing distance from a radionuclide release point (Point 1). BCF values from each grid cell represent the average BCF over the water column.*

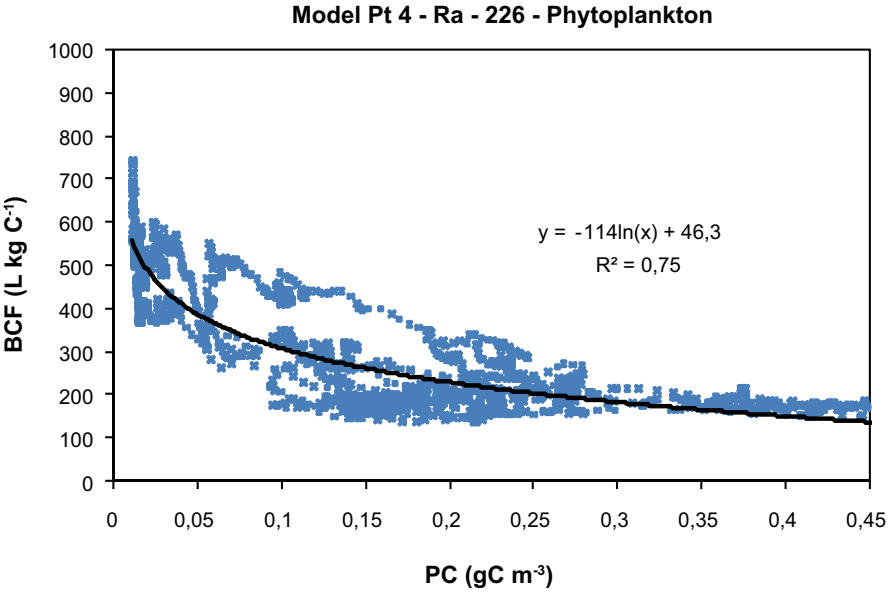


***Figure 6-9.*** *Scatter plot between phytoplankton concentration and bioconcentration factor (BCF) for Ra-226 in phytoplankton. Individual value points represent 6-hourly values averaged over the entire water column. A log-normal function applied to data explains 75% of the observed variation.*

### *BCF in grazers and predators*

For zooplankton and fish, the variation in BCF is unrelated to the biomass of the different biological components, but is related to the BCF in the next lower trophic level, underlining the fact that food-chain transfer of radionuclides is of greater importance than adsorption from water directly (see Figure 6-10). Correlations based on time series of BCFs (phytoplankton – zooplankton) from one grid point were most significant at the greatest distance from the release point (Point 1), underlining the fact that short-term variation in water concentration, which is most pronounced at the release point, does influence BCF through adsorption-desorption processes but food-chain transfer is the most important factor. If plots are based on temporally and spatially averaged BCF values, highly significant relationships that are best described by a power function indicate that "biomagnification" becomes more pronounced at higher BCFs in food (Figure 6-10 lower panel).

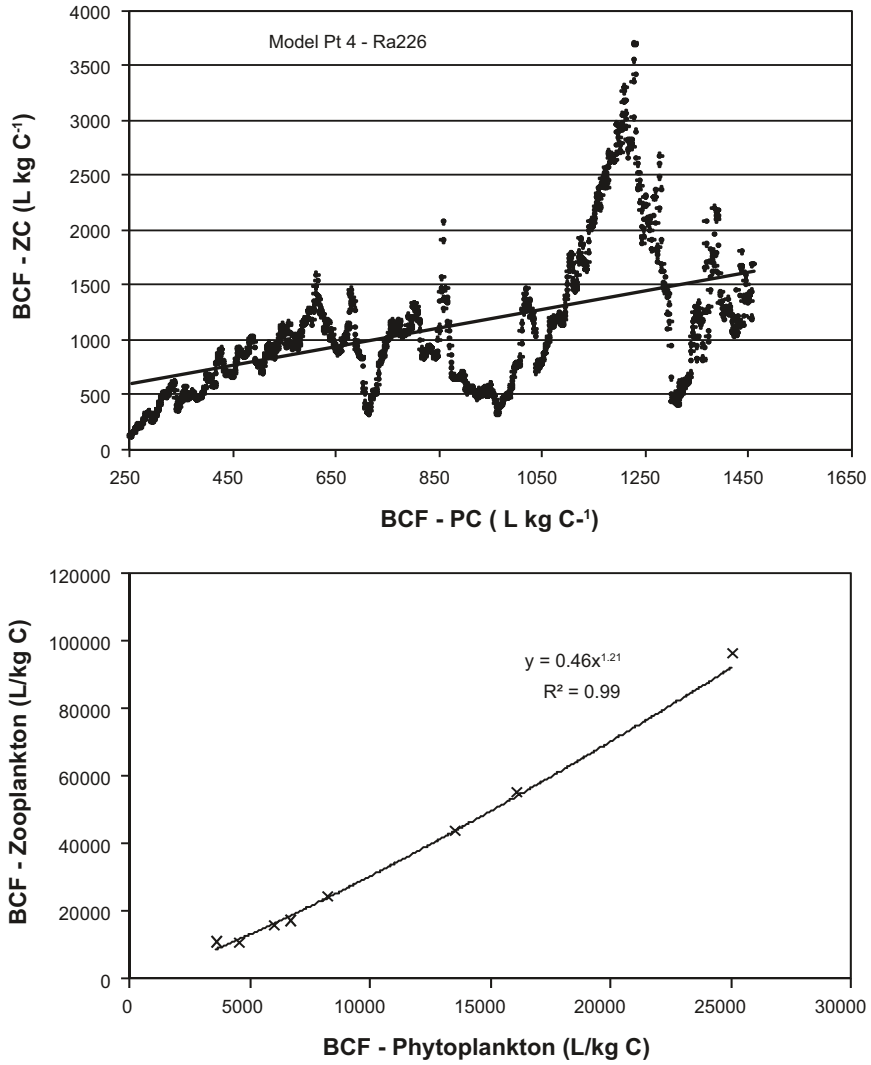


***Figure 6-10.*** *Upper panel: Scatter plot between bioconcentration factor for phytoplankton (BCF-PC) and bioconcentration factor for zooplankton (BCF-ZC) for Ra-226. Individual value points represent depth-averaged 6-hourly values in model Point 4. Lower panel: Scatter plot between BCF for phyto- and zooplankton based on temporally (one year) and spatially (all depth and grid points) averaged values from 8 basins.*

The mechanism behind "biomagnification" is a result of the model assumption that once assimilated the radionuclides are not lost by excretion or respiration as is carbon. Hence, concentrations of radionuclides in grazers and predators will continue to increase and attain higher values than in their prey because about 50–60% of assimilated carbon is lost to cover maintenance costs, while all radionuclide mass is retained in the predator. The increase in grazer BCF with increasing radionuclide concentration in phytoplankton is probably related to a varying distribution between adsorbed and absorbed radionuclides in phytoplankton, and the fact that only adsorbed radionuclides are completely assimilated.

### *Variation in BCFs between basins and functional groups in the pelagic system*

The spatial variations in BCFs for six radionuclides are presented in Figure 6-11, encompassing pelagic functional groups in the model (phytoplankton, zooplankton and planktivorous fish). A striking feature is an almost identical pattern in BCF variation across basins, although absolute values vary by almost 7 orders of magnitude depending on the particular radionuclide, i.e. the partition coefficient.

The highest BCFs were modelled in the deepest basins, i.e. 116, 123 and 126, while the lowest BCFs were modelled for the shallow basins, which received radionuclides through groundwater inflow. Depending on functional group and radionuclide, the relative range of BCFs (max/min) varied from

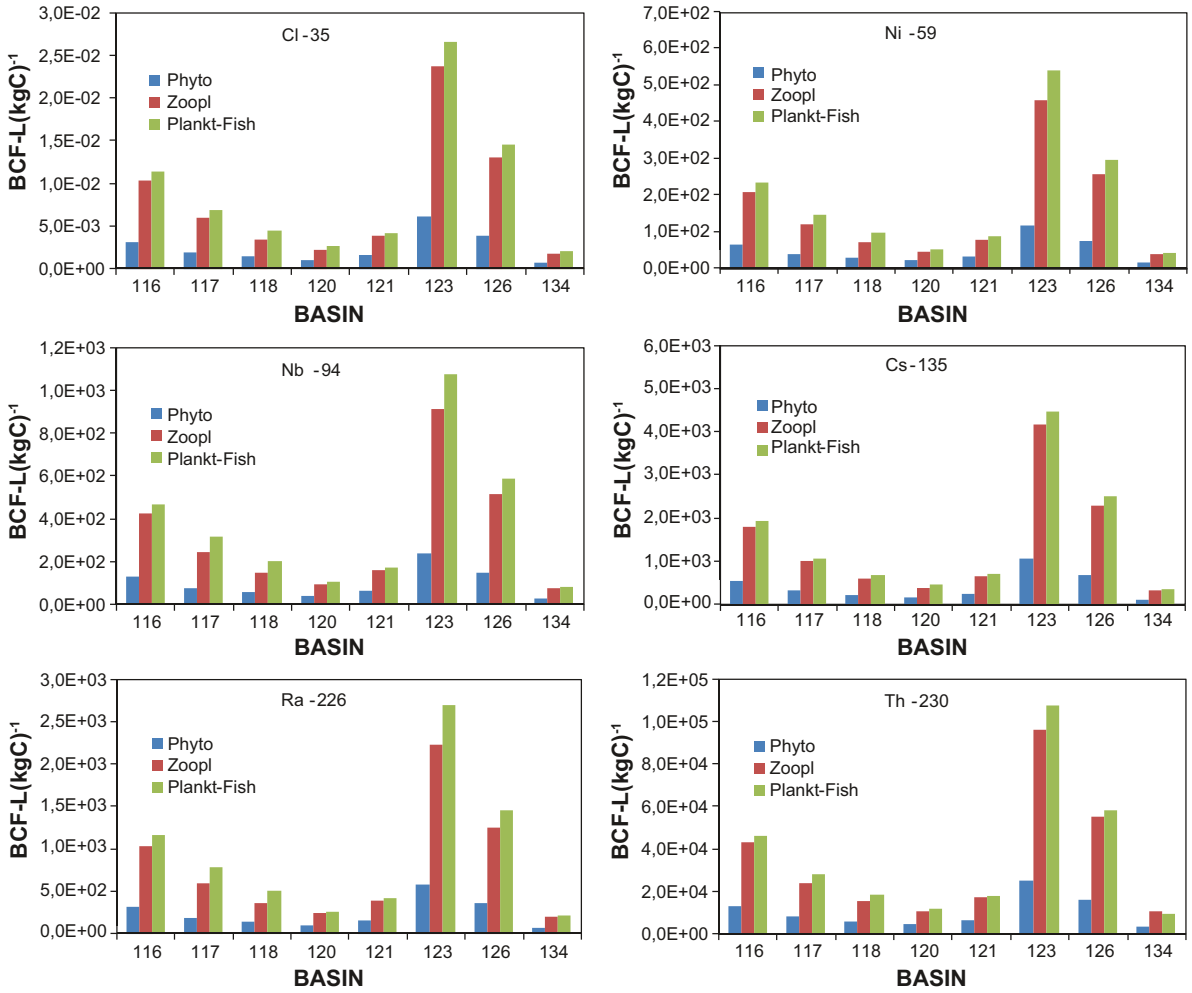


***Figure 6-11.*** *Bioconcentration factors (BCFs) for 6 radionuclides in 3 pelagic functional groups across 8 selected basins in Öregrundsgrepen. Values denote median values encompassing the entire basin volume and representing the whole (8th) model year.*

6.9 to 13.1. A less prominent but consistent feature for all basins and radionuclides was the increase in BCFs from phytoplankton through zooplankton to planktivorous fish.

The reason for the large variation in BCFs across basins was examined by comparing dissolved radionuclide concentrations in the water column (Figure 6-12). For Th-230, the dissolved concentration varied from a low $0.08\times10^{-7}$ Bq/l (basin 123, no groundwater input) to $1.3\times10^{-7}$ Bq/l (basin 120, with groundwater input of radionuclide). The relative range ($\approx 65$) was comparable to that of the other radionuclides. Hence, a large part of the variation in BCFs for phytoplankton can be explained by differences in concentrations of dissolved radionuclides. The plot showed that the BCF was more or less constant at concentrations greater than $10^{-8}$ Bq/l, followed a dramatic increase at lower concentrations when water concentrations approached zero (Figure 6-12 lower panel).

In summary, phytoplankton that constitutes the entry of radionuclides into the pelagic food chain accumulates radionuclides by adsorption (primarily); bioconcentration factors representing the ratio of the radionuclide concentration in phytoplankton to the radionuclide concentration in water show substantial variation driven primarily by the variation in phytoplankton concentration (i.e. the total surface area of potential binding sites) and water concentration. Based on the modelling exercises we may expect a variation by a factor of 10 in BCFs in plankton organisms for a specific radionuclide due to seasonal variation in biomass and spatial variation in radionuclide concentration.

The transfer of radionuclides to higher trophic levels in the pelagic food chain is mediated by adsorption and by intake of food containing radionuclides. Effects of varying dissolved concentrations on BCFs in phytoplankton may also be reflected in higher trophic levels.

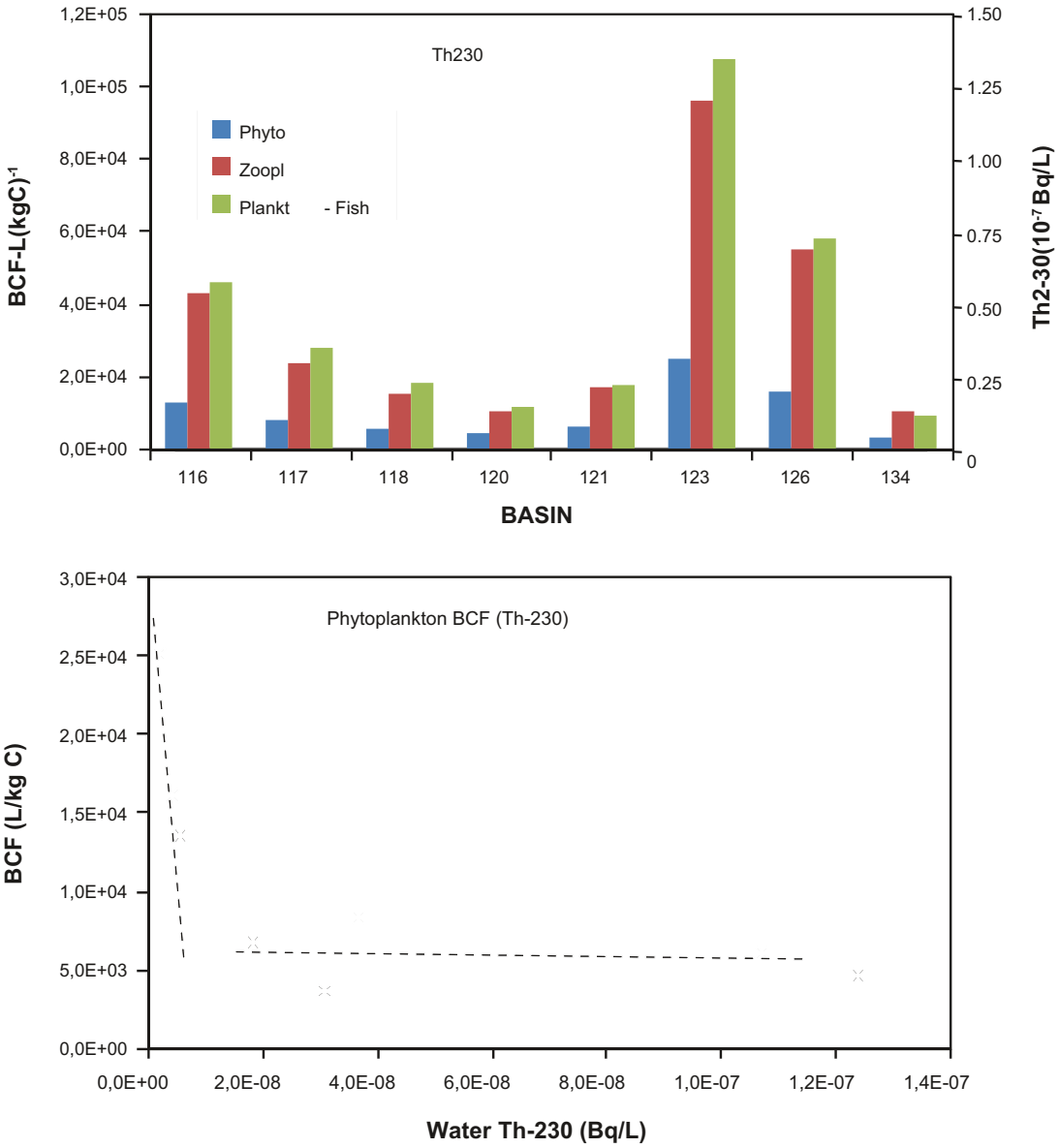


***Figure 6-12.*** *Bioconcentration factor for Th-230 in phytoplankton, zooplankton and planktivorous fish, and concentration of Th-230 in water across 8 Basins (upper). Bioconcentration factor for Th-230 in phytoplankton as a function of water concentration. All values represent median values for the 8 basins (across season, including spatial variation).*

### *Variation in BCFs between basins and functional groups in the benthic system*

The spatial variations in BCFs for benthic autotrophs and heterotrophs are shown in Figure 6-13. As in plankton and planktivorous fish, BCFs varied by 7–8 orders of magnitude between radionuclides, lowest for Cl-35 and highest for Th-230. This variation can be explained by the variation in partition coefficients.

In benthic autotrophs, where adsorption constitutes the most import accumulation process, the highest BCFs were predicted in the deep basins, e.g. basin 123 (without a release point for the radionuclide in the groundwater) and the lowest BCFs in the shallow basins. As for plankton, this pattern is a combination of low biomass in the deep basins caused by light limitation and a lower concentration of radionuclide than in the more shallow basins. In shallow basins, higher growth rates and biomass in benthic plants leads to “biomass dilution” of radionuclides.

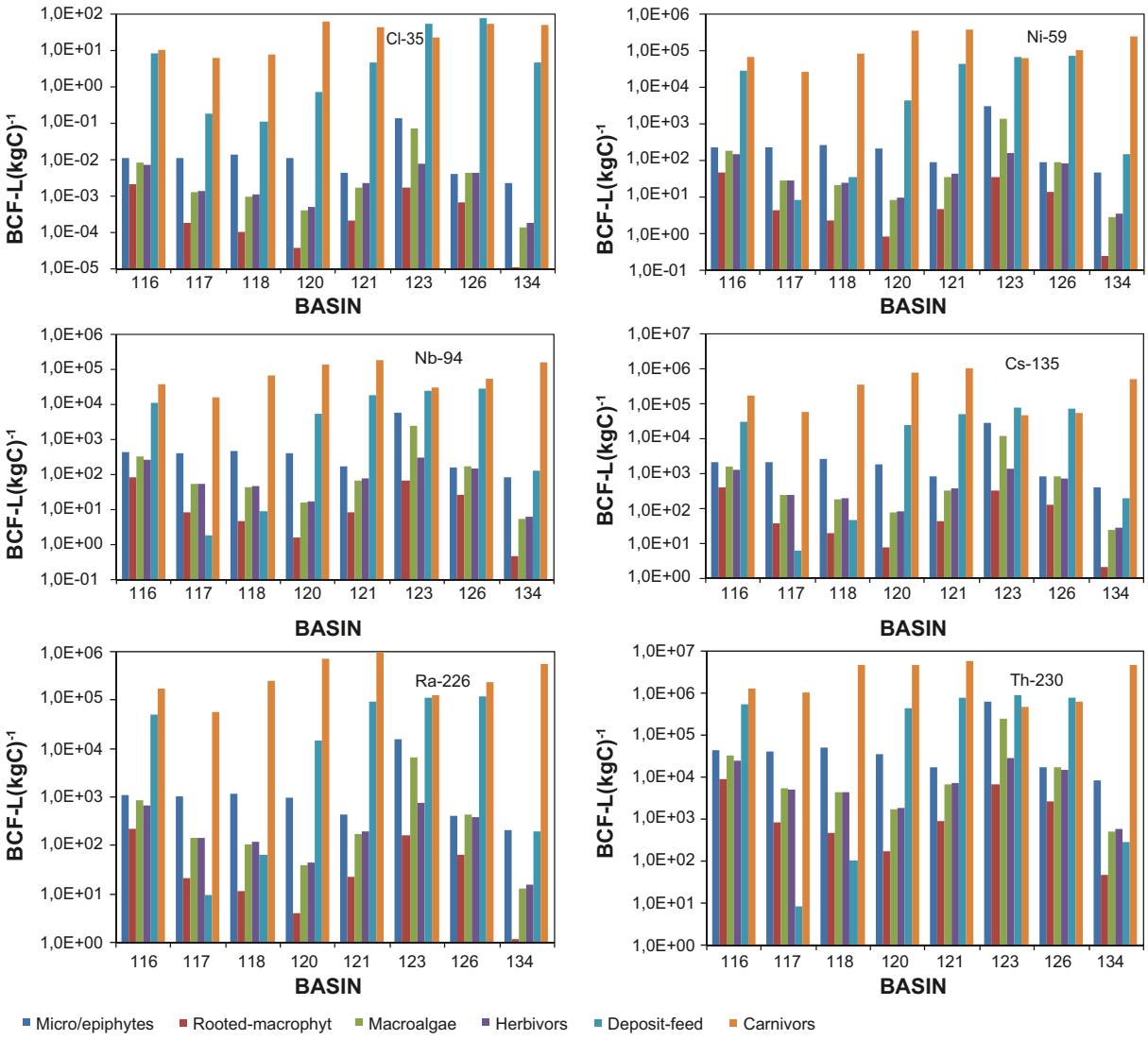


***Figure 6-13.*** *Bioconcentration factors for 6 radionuclides in 6 benthic functional groups across 8 selected basins in Öregrundsgrepen. Values denote median values encompassing the entire basin seabed area and representing the whole model year.*

In contrast, the spatial pattern of BCFs in benthic deposit feeders and carnivores was unrelated to depth. Instead, the BCF was scaled positively to accumulated positive growth in deposit feeders and carnivores over the season. Deposit feeders ingest detritus and inorganic material containing a mixture of adsorbed (inorganic and organic dead matter, sedimented algae) radionuclides. Hence, in areas with high organic content in sediments, deposit feeders will have higher rates of radionuclide ingestion than deposit feeders in low-organic sediments, because partition coefficients for organics are approximately one order of magnitude higher than for inorganic particles.

As radionuclides are not excreted in the RN model, deposit feeders will accumulate radionuclides continuously until part of the biomass is consumed by predators. In that way, basins with high detritus production will give rise to high BCFs in detritus feeders and, as detritus feeders constitute the main food for predators, this distribution of BCFs will also be reflected in the BCFs in predators.

### 6.2.4 Comparison with other studies

Given the important role of partition coefficients in distributing radionuclides between water, sediments and organisms, the actual choice of partition coefficients will have a profound influence on results, including in situations where modelling approaches differ. In Table 6-3, modelled BCF

**Table 6-3. Bioconcentration factors ($m^3$ $(kgC)^{-1}$) for phytoplankton, zooplankton, planktivorous fish and molluscs/benthos calculated for basin 116. BCF values from this study represent median values (over time and space) to facilitate comparison with the studies by /Kumblad and Kautsky 2004/ and /Nordén et al. 2010/ on basin 116. BCF data for fish for the Nordén study represent planktivorous and predatory fish. The benthos group was in this study exemplified by deposit feeders. Generic values from /IAEA 2004/ are also included for reference.**

| | Phytoplankton | | | | Zooplankton | | | Plank. Fish | | | | Benthos | | | |
|---|---|---|---|---|---|---|---|---|---|---|---|---|---|---|---|
| | IAEA | Kumblad and Kautsky | Nordén et al. 2010 | This study | IAEA | Kumblad and Kautsky | This study | IAEA | Kumblad and Kautsky | Nordén et al. 2010 | This study | IAEA | Kumblad and Kautsky | Nordén et al. 2010 | This study |
| Cl-35 | 0.0125 | 0.000048 | 0.13 | 0.003 | 0.013 | 0.000007 | 0.00001 | 0.0005 | 0.0003 | 0.001 | 0.00001 | 0.0006 | 0.0001 | 0.01 | 0.009 |
| Cs-135 | 0.250 | 0.113 | 64 | 0.64 | 0.375 | 0.025 | 2.02 | 0.952 | 0.105 | 2.1 | 2.16 | 0.33 | 0.066 | 2.1 | 31.8 |
| Nb-94 | 12.5 | 17.5 | 33 | 0.131 | 250 | 4 | 0.426 | 0.286 | 7.43 | 0.17 | 0.47 | 11.1 | 7.4 | 8.2 | 11.4 |
| Ni-59 | 37.5 | 3.88 | 35 | 0.069 | 12.5 | 0.875 | 0.225 | 9.52 | 4.38 | 0.12 | 0.25 | 22.2 | 2.4 | 9.2 | 28.9 |
| Ra-226 | 25 | 0.263 | 29 | 0.326 | 1.25 | 0.051 | 1.06 | 4.76 | 0.552 | 2.8 | 1.2 | 11.1 | 0.233 | 1.1 | 51.8 |
| Th-230 | 250 | 65 | 2895 | 13.51 | 125 | 15 | 43.7 | 5.71 | 14.29 | 1.1 | 46.6 | 11.1 | 24.4 | 70 | 54.7 |

results for phytoplankton, zooplankton, planktivorous fish and benthic deposit feeders are presented for this study and from the previous Kumblad modelling study, along with generic BCFs developed by the IAEA and site-specific BCFs for Forsmark /Nordén et al. 2010/.

For every radionuclide and organism group considered there was a substantial variation among the four sets of data, partly driven by the use of different partition coefficients, but also caused by different importance of food-chain transport of radionuclides. In the Nordén study BCF generally decreased from phytoplankton, through zooplankton to fish, while BCF consistently increased from phytoplankton, through zooplankton and fish to deposit-feeders in this study underlining the importance of food-chain transport of radionuclides (Table 6-3).

In this study and the previous study by /Kumblad et al. 2005/, the BCF for each radionuclide was linearly correlated with the $K_d/Kd_c$ for phytoplankton with identical slopes, because adsorption was the primary route of uptake and because the assumed surface-to-volume/biomass ratio in phytoplankton cells was identical in the two studies (Figure 6-14). By comparison, the slope 'BCF/Kd' in the Nordén study /Nordén et al. 2010/ was 10–50 times higher.

At higher trophic levels in the food chain, the slopes in linear regressions between $K_d$-$K_c$ and BCF for fish (planktivorous) were again comparable between this study and the Kumblad study, while the Kd and BCF values were unrelated in the Nordén study.

For benthos (e.g. deposit feeders), the ratio BCF:Kd was much higher in this model study compared with the Nordén study and the previous Kumblad study. This result stems from the model assumption that absorbed radionuclides from food were not excreted in the present radionuclide model. Consumers will therefore accumulate radionuclides as long as they ingest radionuclides in food until they die or are consumed by predators (Figure 6-14). By comparison, in the Kumblad model adsorption of radionuclides is the dominant uptake process, including in consumers and predators, because ingested radionuclides are excreted at a rate scaled to respiration.

For deposit feeders there was some scatter in the $Kd_c$-BCF relationship, compared with an almost perfect linear regression for BCFs for other organism groups. This scatter is apparently caused by a varying ratio (3–250) between $Kd_c$ and $Kd_{iss}$ for the different radionuclides. Hence, assuming a composition of 50% organics and 50% inorganics in ingested material for a deposit feeder, the accumulated radionuclide intake will vary according to the $Kd_c$: $Kd_{iss}$ ratios of the different radionuclides.

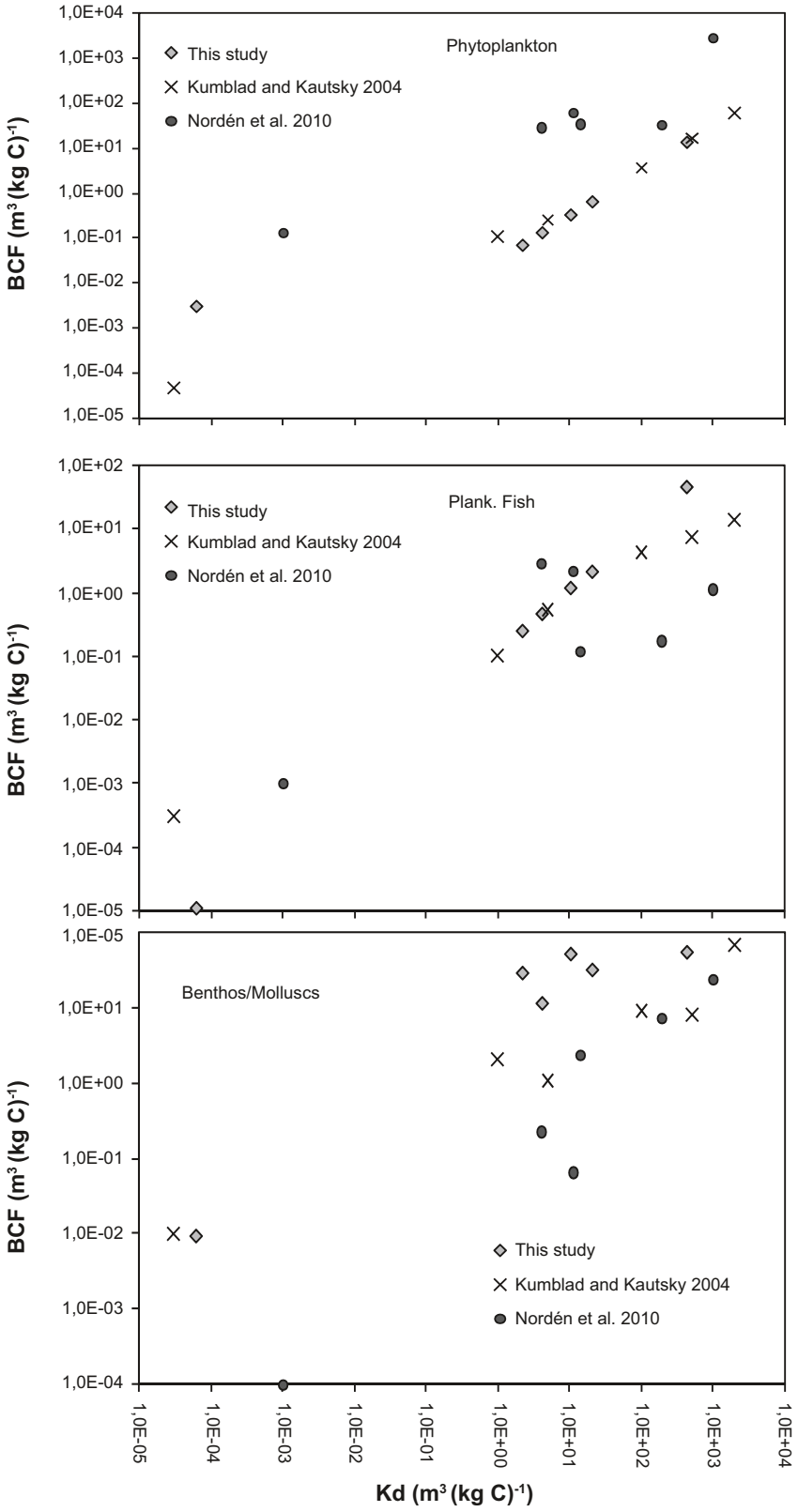


***Figure 6-14.*** *Linear regression between partition coefficients (this study: Kc; Kumblad and Kautsky: Kd) and bioconcentration factors (BCFs) for phytoplankton, planktivorous fish and benthos/deposit feeders. Based on data from basin 116.*

# 7 Conclusions

To our knowledge the work reported here represents the most extensive modelling efforts carried out where transports and dispersion, ecosystem processes and radionuclide spread are described dynamically in coupled models and with a high resolution. It is felt that flexible software such as MIKE-by-DHI with a range of built-in facilities such as a 'biomass-check' is a prerequisite to succeed in modelling on this scale.

During modelling work a number of issues emerged that should be mentioned:

- In Euleran ecosystem models state variables cannot move actively but are either fixed at bottom or move passively with currents. In effect, predators only rarely are included in high-resolution models because food production within a small grid cell (25×25 m) is so small that it cannot support a predatory fish. In the ECOLab model this was solved by fixing predators such as planktivorus fish in grid cells and run the model for several years to let the state variable come into 'equilibrium'. As a result planktivorus fish was eliminated in most of the Öregrundsgrepen model area but attained rather high biomasses in grid cells where currents – and fluxes of zooplankton – were high. Averaged over the entire model area the biomass was comparable results from on site sampling.
- As in every modelling study, the overall assumptions dictate the outcome of the modelling. In agreement with SKB it was decided that radionuclides accumulated through feeding in zooplankton, fish and benthic invertebrates were not excreted. Hence, in the model these organisms would continue to accumulate radionuclides throughout their life, and as a consequence the concentration of radionuclides will increase through the food chain. Based on this assumption the modelled accumulation of radionuclides in benthos and fish will constitute the absolute maximum, i.e. a worst-case scenario.
- Given the important role of partition coefficients (Kd) for the spread and accumulation of radionuclides and the diversity of Kd for individual radionuclides in the literature, selection of Kd's for modelling invariable will affect model results. But as shown in this report there was a close coupling between Kd-values and Biological Concentration Factors (BCF) in sediments, phyto- and zooplankton, and benthic plants. Hence, the spread and accumulation of other radionuclides with different partition coefficients can thus be inferred by comparison with relevant model results.
- The results for one of the basins in Öregrundsgrepen were compared with two other model studies, /Kumblad and Kautsky 2004, Nordén et al. 2010/. Modelled bioconcentration factors (BCFs) differed substantially between the three studies, but for phytoplankton and grazers the differences in BCF could largely be explained by different values for partition coefficients (Kds) used in the models. For detritus feeders and benthic predators, BCFs were consistently higher in this model study compared with the /Kumblad and Kautsky 2004/ and /Nordén et al. 2010/ studies, despite the fact that Kd values were lower. The higher modelled BCFs are a result of the model assumption that radionuclides are not excreted along with respired carbon (see above).

# 8 References

SKB's (Svensk Kärnbränslehantering AB) publications can be found at www.skb.se/publications.


**Arndt S, Regnier P, 2007.** A model for the benthic-pelagic coupling of silica in estuarine ecosystems: sensitivity analysis and system scale simulation. Biogeosciences, 4, pp 331–352.

**Azam F, Fenchel T, Field J G, Gray J S, Meyer-Reil L A, Thingstad F, 1983.** The ecological role of water-column microbes in the sea. Marine Ecology Progress Series, 10, pp 257–263.

**Bach H K, 1993.** A dynamic model describing the seasonal variations in growth and the distribution of eelgrass (Zostera marina L.). I. Model theory. Ecological Modelling, 65, pp 31–50.

**Banse K, 1982.** Cell volumes, maximal growth rates of unicellular algae and ciliates, and the role of ciliates in the marine pelagial. Limnology and Oceanography, 27, pp 1059–1071.

**BED, 2009.** Baltic Environmental Database. [Online]. Available at: http://nest.su.se/models/bed.htm.

**Borgiel M, 2005.** Forsmark site investigation. Benthic vegetation, plant associated macrofauna and benthic macrofauna in shallow bays and shores in the Grepen area, Bothnian Sea. Results from sampling 2004. SKB P-05-135, Svensk Kärnbränslehantering AB.

**Bosson E, Gustafsson L-G, Sassner M, 2008.** Numerical modelling of surface hydrology and near-surface hydrogeology at Forsmark. Site descriptive modelling, SDM-Site Forsmark. SKB R-08-09, Svensk Kärnbränslehantering AB.

**Buch K, 1945.** Kolsyrejämvikten i Baltiska Havet. Fennia, 68, pp 29–81.

**Bocci M, Coffaro G, Bendoricchio G, 1997.** Modelling biomass and nutrient dynamics in eelgrass (Zostera marina L.): applications to the Lagoon of Venice (Italy) and Øresund (Denmark). Ecological Modelling, 102, pp 67–80.

**Cammen L M, 1980.** Ingestion rate: an empirical model for aquatic deposit feeders and detritivores. Oecologia, 44, pp 303–310.

**Denman K L, 2003.** Modelling planktonic ecosystems: parameterizing complexity. Progress in Oceanography, 57, pp 429–452.

**DHI, 2007a.** MIKE21 & MIKE 3 Flow Model, Hydrodynamic and Transport Module, Scientific Documentation. DHI Water Environment Health, Hørsholm, Denmark.

**DHI, 2007b.** Eutrophication model 1 – ECO Lab template: a scientific description. MIKE by DHI. DHI Water Environment Health, Hørsholm, Denmark.

**DHI, 2008.** ECO Lab – Short scientific description. MIKE by DHI. DHI Water Environment Health, Hørsholm, Denmark.

**Dixon G K, Syrett P J, 1988.** The growth of dinoflagellates in laboratory cultures. New Phytologist 109, pp 297–302.

**Droop M R, 1983.** 25 years of algal growth kinetics: a personal view. Botanica Marina, 26, pp 99–112.

**Eriksson S, Sellei C, Wallström K, 1977.** The structure of the plankton community of the Öregrunds-grepen (southwest Bothian Sea). Helgoländer Wissenschaftliche Meeresuntersuchungen, 30, pp 582–597.

**Gray I E, 1954.** Comparative study of the gill area of marine fishes. Biological Bulletin, 107, pp 219–225.

**Haahtela I, 1990.** What do Baltic studies tell us about the isopod Saduria entomon (L.). Annales Zoologici Fennici, 27, pp 269–278.

**Hansen P J, Fenchel T, 2006.** The bloom-forming ciliate Mesodinium rubrum harbours a single permanent endosymbiont. Marine Biology Research, 2, pp 167–177.

**Hernández I, Andría J R, Christmas M, Whitton B A, 1999.** Testing the allometric scaling of alkaline phosphatase activity to surface/volume ratio in benthic marine macrophytes. Journal of Experimental Marine Biology and Ecology, 241, pp 1–14.

**Hernroth L (ed), 1976.** Recommendations on methods for marine biological studies in the Baltic Sea – mesozooplankton biomass assessment. Lysekil: Institute of marine research. (The Baltic Marine Biologists Publication 10)

**Huononen R, Borgiel M, 2005.** Forsmark site investigation. Sampling of phyto- and zooplankton in sea water. Abundances and carbon biomasses. SKB P-05-72, Svensk Kärnbränslehantering AB.

**IAEA, 2004.** Sediment distribution coefficients and concentration factors for biota in the marine environment. Vienna: International Atomic Energy Agency. (Technical reports series 422)

**Jansen J M, Koutstaal A, Wendelaar Bonga S, Hummel H, 2009.** Salinity-related growth rates in populations of the European clam Macoma balthica and in field transplant experiments along the Baltic Sea salinity gradient. Marine and Freshwater Behaviour and Physiology, 42, pp 157–166.

**Johansson M, Gorokhova E, Larsson U, 2004.** Annual variability in ciliate community structure, potential prey and predators in the open northern Baltic Sea proper. Journal of Plankton Research, 26, pp 67–80.

**Karlsson A, Eriksson C, Borell Lövstedt C, Liungman O, Engqvist A, 2010.** High-resolution hydrodynamic modelling of the marine environment at Forsmark between 6500 BC and 9000 AD. SKB R-10-09, Svensk Kärnbränslehantering AB.

**KiørboeT, Møhlenberg F, 1982.** Sletter havet sporene?: en biologisk undersøgelse af miljøpåvirkninger ved ral- og sandsugning. København: Miljøministeriet, Fredningsstyrelsen (in Danish).

**Kiørboe T, Møhlenberg F, Hamburger K, 1985.** Bioenergetics of the planktonic copepod Acartia tonsa: relation between feeding, egg production and respiration, and composition of specific dynamic action. Marine Ecology Progress Series, 26, pp 85–97.

**Kiørboe T, Møhlenberg F, Tiselius P, 1988.** Propagation of planktonic copepods: production and mortality of eggs. Hydrobiologia, 167-168, pp 219–225.

**Kotta J, Orav-Kotta H, Paalme T, Kotta I, Kukk H, 2006.** Seasonal changes in situ grazing of the mesoherbivores Idotea baltica and Gammarus oceanicus on the brown algae Fucus vesiculosus and Pylayella littoralis in the Central Gulf of Finland, Baltic Sea. Hydrobiologia, 554, pp 117–125.

**Kumblad L, Kautsky U, 2004.** Models for transport and fate of carbon, nutrients and point source released radionuclides to an aquatic ecosystem. SKB TR-04-13, Svensk Kärnbränslehantering AB.

**Kumblad L, Kautsky O, Naeslund B, 2005.** Transport and fate of radionuclides in aquatic environments – the use of ecosystem modelling for exposure assessments of nuclear facilities. Journal of Environmental Radioactinty, 87, pp 107–129.

**Kuparinen J, Leonardsson K, Mattila J, Wikner J, 1996.** Food web structure and function in the Gulf of Bothnia, Baltic Sea. Ambio Special Report 8, pp 13–21.

**Larsson U, Hajdu S, Walve J, Elmgren R, 2001.** Baltic Sea nitrogen fixation estimated from the summer increase in upper mixed layer total nitrogen. Limnology and Oceanography, 46, pp 811–820.

**Lessin G, Raudsepp U, 2006.** Water quality assessment using integrated modeling and monitoring in Narva Bay, Gulf of Finland. Environmental Modeling and Assessment, 11, pp 315–332.

**Lindahl G, Wallström K, 1980.** Växtplankton i Öregrundsgrepen, SV Bottenhavet. Meddelanden från Växtbiologiska institutionen, Uppsala, 1980:8.

**Lotze H K, Worm B, 2002.** Complex interactions of climatic and ecological controls on macroalgal recruitment. Limnology and Oceanography, 47, pp 1734–1741.

**Markager S, Sand-Jensen K, 1992.** Light requirements and depth zonation of marine macroalgae. Marine Ecology Progress Series, 88, pp 83–92.

**Middelboe A L, Sand-Jensen K, Binzer T, 2006.** Highly predictable photosynthetic production in natural macroalgal communities from incoming and absorbed light. Oecologia, 150, pp 464–476.

**Nordén S, Avila R, de la Cruz I, Stenberg K, Grolander S, 2010.** Element specific and constants parameters used for dose calculations in SR-Site. SKB TR-10-07, Svensk Kärnbränslehantering AB.

**Paalme T, Kukk H, 2003.** Comparison of net primary production rates of Pilayella littoralis (L.) Kjellm. and other dominating macroalgal species in Kõiguste Bay, northeastern Baltic Sea. Proceedings of the Estonian Academy of Sciences. Biology, Ecology, 52, pp 125–133.

**Paalme T, Kukk H, Kotta J, Orav H, 2002.** 'In vitro' and 'in situ' decomposition of nuisance macroalgae Cladophora glomerata and Pilayella littoralis. Hydrobiologia, 475-476, pp 469–476.

**Plus M, Chapelle A, Ménesguen A, Deslous-Paoli J-M, Auby I, 2003.** Modelling seasonal dynamics of biomasses and nitrogen contents in a seagrass meadow (Zostera noltii Hornem.): application to the Thau lagoon (French Mediterranean coast). Ecological Modelling, 161, pp 213–238.

**Rasmussen E K, Svenstrup Petersen O, Thompson J R, Flower J, Ahmed M H, 2009.** Hydrodynamic-ecological model analyses of the water quality of Lake Manzala (Nile Delta, Northern Egypt). Hydrobiologia, 622, pp 195–220.

**Samuelsson K, Andersson A, 2003.** Predation limitation in the pelagic microbial food web in an oligotrophic aquatic system. Aquatic Microbial Ecology, 30, pp 239–250.

**Sand-Jensen K, Borum J, 1991.** Interactions among phytoplankton, periphyton, and macrophytes in temperate freshwaters and estuaries. Aquatic Botany, 41, pp 137–175.

**Sarthou G, Timmenmans K R, Blain S, Tréguer P, 2005.** Growth physiology and fate of diatoms in the ocean: a review. Journal of Sea Research, 53, pp 25–42.

**Skovgaard A, Menden-Deuer S, 2003.** Long-term exposure of dinoflagellates to $^{14}$carbon: effects on growth rate and measurements of carbon content. Journal of Plankton Research, 25, pp 1005–1009.

**SLU, 2008.** Station vattenkemi: Forsmarksån Johannisfors. [Online]. Available at: http://info1.ma.slu.se/ma/www_ma.acgi$Station?ID=Intro&S=475. [25 April 2008].

**Smayda T J, Boleyn B J, 1965.** Experimental observations on the flotation of marine diatoms. I. Thalassiosira cf. Nana, Thalassiosira rotula and Nitzschia seriata. Limnology and Oceanography, 10, pp 499–509.

**Smayda T J, Boleyn B J, 1966a.** Experimental observations on the flotation of marine diatoms. II. Skeletonema costatum and Rhizosolenia setigera. Limnology and Oceanography, 11, pp 18–34.

**Smayda, T J, Boleyn B J, 1966b.** Experimental observations on the flotation of marine diatoms. III. Bacteriastrum hyalinum and Chaetoceros lauderi. Limnology and Oceanography, 11, pp 35–43.

**Steele J H, 1998.** Incorporating the microbial loop in a simple plankton model. Proceedings of the Royal Society of London, Series B, 265, pp 1771–1777.

**Vanderborght J-P, Folmer I M, Aguilera D R, Uhrenholdt T, Regnier P, 2007.** Reactive-transport modelling of C, N and O2 in a river–estuarine–coastal zone system: application to the Scheldt estuary. Marine Chemistry, 106, pp 92–110.

**Verhagen J H G, Nienhuis P H, 1983.** A simulation model of production, seasonal changes in biomass and distribution of eelgrass (Zostera marina) in Lake Grevelingen. Marine Ecology Progress Series, 10, pp 187–195.

**Vermeer C P, Escher M, Portielje R, de Klein J J M, 2003.** Nitrogen uptake and translocation by Chara. Aquatic Botany, 76, pp 245–258.

**Wallentinus I, 1978.** Productivity studies of Baltic macroalgae. Botanica Marina, 21, pp 365–380.

**Walve J, Larsson U, 2007.** Vattenundersökningar vid Norra randen i Ålands hav 2006. Systemekologiska institutionen, Stockholms Universitet (in Swedish).

**Wijnbladh E, Aquilonius K, Floderus S, 2008.** The marine ecosystems at Forsmark and Laxemar-Simpevarp. Site descriptive modelling, SDM-Site. SKB R-08-03, Svensk Kärnbränslehantering AB.

**Zimmerman R, Smith R D, Alberte R S, 1987.** Is growth of eelgrass nitrogen – limited? A modelling analysis of the effects of light and nitrogen on the growth dynamics of zostera marina. Marine Ecology Progress Series, 41, pp 167–176.